DIFFUSION OF VIOLOGENS ACROSS LIPID BILAYER MEMBRANES

Eberhardt R. Kuhn
B.S., University of Tubingen, West-Germany, 1981
M.S., University of Oregon, 1984

A dissertation submitted to the faculty of the

Oregon Graduate Institute
of
Science and Technology

in partial fulfillment of the
requirements for the degree
Doctor of Philosophy
in
Physical Chemistry

December, 1989

The dissertation "Diffusion of Viologens across Lipid bilayer membranes" by Eberhardt R. Kuhn has been examined and approved by the following Examination Committee:

James K. Hurst, Thesis Advisor

Professor

Thomas M. Loehr

Professor

William L. Pengelly

Associate Professor

David R. Boone

Associate Professor

TABLE OF CONTENTS

LIST of FIGURES

LIST of TABLES

Abbreviations

pc.....phosphatidylcholine

DHP.....dihexadecylphosphate

DMPC.....dimyristoylphosphatidylcholine

DPPC.....dipalmitoylphosphatidylcholine

SDS.....sodium dodecyl sulfate

viologen.....1,1'-dialkyl-4,4'-bipyridine

$(C_n)_2V^{2+}$..... N,N'-dialkyl viologen

C_nMV^{2+}.....N-alkyl-N-methyl viologen

PVS.....N,N'-bis(sulfonate-n-propyl)-4,4'-bipyridine

$Ru(bpy)_3^{2+}$.....tris(2,2'bipyridyl)ruthenium(II)

EDTA.....ethenediaminetetraacetate

$ZnTPPS^{4-}$.....5,10,15,20-(4'-sulfonatophenyl)
-porphinatozinc(II)

$ZnTMPyP^{4+}$.....5,10,15,20-(4'-N-methylpyridyl)
-porphinatozinc(II)

ABSTRACT

Diffusion of Viologens across Lipid Bilayer Membranes

Eberhardt R. Kuhn, Ph.D.

Oregon Graduate Institute, 1989

Supervising Professor: James K. Hurst

Transmembrane reduction of viologens in artificial vesicle systems was studied. It was determined that photostimulated diffusion, i.e. diffusion due to photoexcitation effects, does not occur in the investigated systems. It was discovered that viologens entrapped inside pc vesicles could be reduced by reductants in the external bulk phase. Both photochemical ($Ru(bpy)_3^{2+}$, EDTA) and chemical reductants (dithionite) were investigated. The results suggest that transmembrane electron transfer is accomplished by diffusion of viologen. The diffusion is driven by electrochemical gradients. The similarities between the photochemical systems and the chemical systems suggest that the mechanism are similar. The overall rate was zero order with respect to viologen and reductant. The rate was dependent on temperature (in an Arrhenius-type fashion), the identity of anions (Hofmeister series) in solution, and proportional to the concentration of entrapped viologen. This implies that the rate-limiting step is the electrophoretic migration of other ions to compensate the electrochemical potential that

develops upon viologen ion diffusion. This step could be accelerated by adding ionophores to the liposomes, but rate saturation could not be accomplished. In the presence of ionophores the overall rate had an autocatalytic appearance. The autocatalytic acceleration of the rate is likely to be due to direct electron transfer between viologens juxtaposed on opposite bilayer surfaces after initial outward migration of entrapped viologen. Based upon these observations a mechanism was proposed that could accurately reproduce the kinetic waveforms. Rate constants for several of the individual steps were determined independently. Because viologen diffusion is very rapid in pc vesicles, only a lower limit for the diffusion rates of the viologen dication and its radical cation could be determined.

Binding studies of viologen adsorption to pc vesicles showed that the maximum number of viologen that could be bound was considerably lower than the theoretical calculations of available binding sites. The data could not be fitted to a Langmuir plot, indicating that the binding sites are not independent of each other, but the shapes of the curves indicate apparent cooperative binding interactions.

CHAPTER 1

INTRODUCTION

Long-range electron transfer is an essential part of all living organisms[1-3]. Nature has devised complex redox chains to transport electrons over large distances across membranes[2]. One of the major electron transport chains in plants is the photosynthetic chain, where sunlight is converted to chemical energy. The end result is transmembrane charge separation that is utilized for driving endergonic reactions, e.g., the reduction of $NADP^+$ to NADPH. This phenomenon has spurred great interest among researchers trying to mimic Nature's photosynthetic energy conversion scheme[4-6]. One of the goals of these efforts is to use solar energy to split water into hydrogen and oxygen and then use the H_2 as a fuel[4]. But, just as in biological systems, the transfer of electrons over large distances and through potential energy barriers, e.g., membranes, is required to achieve charge separation. The exact mechanism of long-range electron transfer has been under investigation for many years[9,10] but the mechanistic details remain obscure.

1.1 Solar energy conversion schemes

The general strategy for solar energy conversion has been the same for many research groups worldwide[7,11]. The assemblies typically include a photosensitizer, a sacrificial electron donor, an electron acceptor and some means of maintaining charge separation. This can be accomplished with micellar systems[8b], where the reduced acceptor (e.g. viologen) becomes more solubilized in the micelle and thus back reaction with the oxidized sensitizer, which is in the aqueous phase, is retarded. Other systems use lipid bilayer membranes to separate the photoredox components[7,8a,11a]. Scheme 1 depicts a functional system of the latter type.

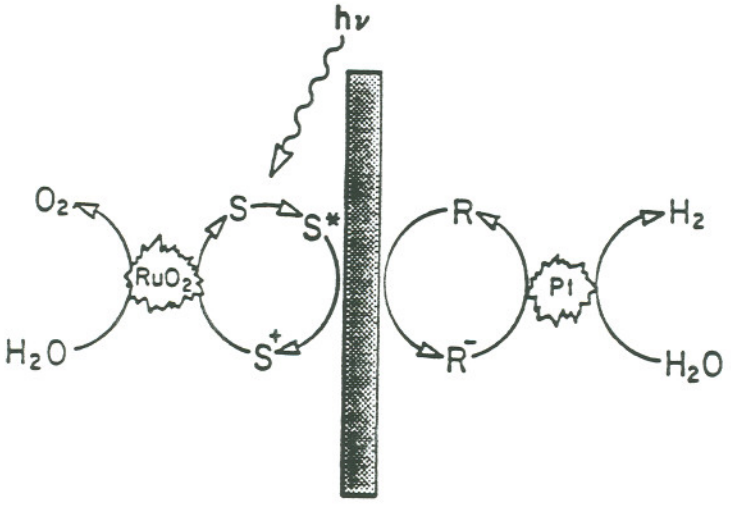

Scheme 1: Solar Water Photolysis System (from reference 6)

In this scheme the photosensitizer and the electron acceptor are separated by a semipermeable membrane that allows for electron transfer but prevents recombination of the reduced and oxidized redox species produced in following reactions. The exact topography of all components, including the membrane, can be varied greatly, however, by manipulation of such important parameters as membrane composition, and acceptor electrical charge and relative hydrophobicity. Additional important factors in controlling reactivity include sensitizer and acceptor redox potentials, membrane surface charge, and sensitizer photophysics. In pioneering studies of this type Calvin and coworkers[7] used as their sensitizer a derivatized $Ru(bpy)_3^{2+}$ with two long alkyl chains to anchor it into the membrane (scheme 2). Their vesicle membranes were comprised of phosphatidylcholine (pc) with this sensitizer and contained EDTA on the inside and N,N'-diheptyl-4,4'-bipyridine (diheptylviologen) on the outside. Upon illumination they observed the formation of the viologen radical after a pronounced lag period. Since sacrificial donor and electron acceptor were located on opposite sides of the bilayer this observation was interpreted in terms of electron exchange between Ru(II) and Ru(III) ions bound to opposite vesicle surfaces. To account for the measured overall redox rates the first order rate constant for transmembrane electron transfer has to be around 10^5 s^{-1}. The lag period was explained by the presence of adventitious oxygen in the sample.

A rate constant of similar magnitude was found by Tollin and coworkers[8a] for a system utilizing chlorophyll _a_ as a photosensitizer that was located on both sides of pc vesicle membranes. Methyl-viologen was entrapped in the interior and EDTA added to the continuous aqueous phase. Again, upon illumination the blue viologen radical accumulated. The researchers concluded from their results that transmembrane reduction had occurred by electron exchange between chlorophyll _a_ and a chlorophyll _a_ cation radical on opposite sides of the bilayer.

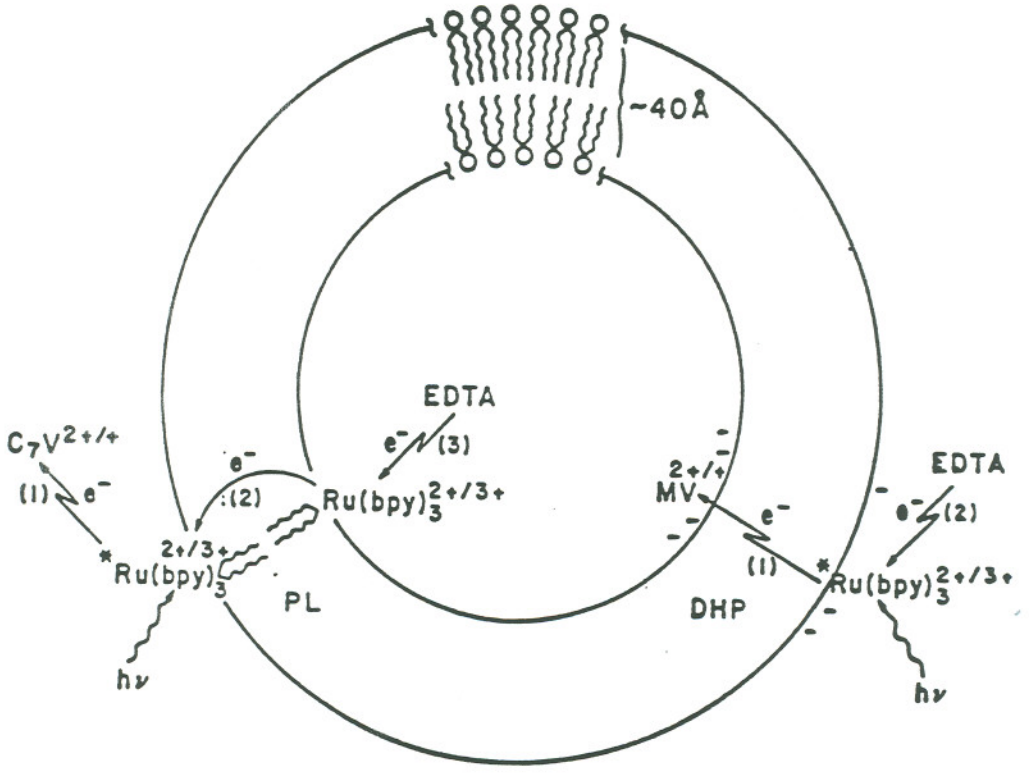

Scheme 2: Proposed Photochemical Transmembrane Electron Transfer Pathways

(from James K. Hurst, unpublished)

Fendler and coworkers[11a] also obtained similar results using DHP vesicles with entrapped methylviologen (MV^{2+}), but with sensitizer and sacrificial donor initially confined to the external bulk phase (Scheme 2). Their interpretation of the observed viologen radical formation was direct transmembrane electron transfer from photoexcited $Ru(bpy)_3^{2+}$ to MV^{2+}.

Theoretical calculations[9,10a] for electron tunneling through a barrier of the dimensions of a bilayer (ca. 40 A) predict rate constants from 10^{-2}-10^{-5} s^{-1}, many orders of magnitude slower than those reported above. This presents a conceptual problem with the interpretation of the above results. If the electron was indeed tunneling through the entire bilayer, the rates should be much slower. This implies that transmembrane electron transfer proceeds by a different mechanism, e.g., diffusion of redox partners.

When Lee et al.[11b] reinvestigated the Fendler system, they too found the build-up of viologen radical upon illumination. Their measured rates were of the same order of magnitude as those reported above. However, they further noted that the viologen had leaked out of the vesicle during the course of the experiment so that the redox reaction may have occurred on a single vesicle surface. Viologen leakage only occurred in systems where the chromophore was membrane bound. In unilluminated samples, no viologen leakage was observed. This opened up a new way of thinking about these kinds of apparent

transmembrane redox reactions. Now diffusion of any of the components involved had to be considered as a possible part of the overall mechanism. The importance of viologen diffusion in these systems was also realized by Tabushi and coworkers[42]. One of their systems contained $ZnTPPS^{4-}$ and flavin mononucleotide (FMN) separated by a pc bilayer, with dialkylviologens with different alkyl chain lengths added to both sides. Upon illumination the reduction of the FMN was observed. The observed quantum yield was dependent on the length of the alkyl tail of the viologen for alkyl chains from C_2 to C_8, with butyl chains giving the highest yields. This observation was explained in terms of relative lipophilicity and binding of the viologen. It was concluded that "overall charge separation was aided remarkably by phase transfer of the electron carrier viologen".

Scheme 3 depicts two conceptual models that could account for the scrambling of redox components. Both involve the thermal deactivation of the excited chromophore. In one case localized heating results in a transient micellerization within the membrane that can exchange sensitizer and acceptor. In the other case transient pore formation allows diffusion of the redox species. In either case photosensitized reduction would subsequently take place on a single vesicle surface.

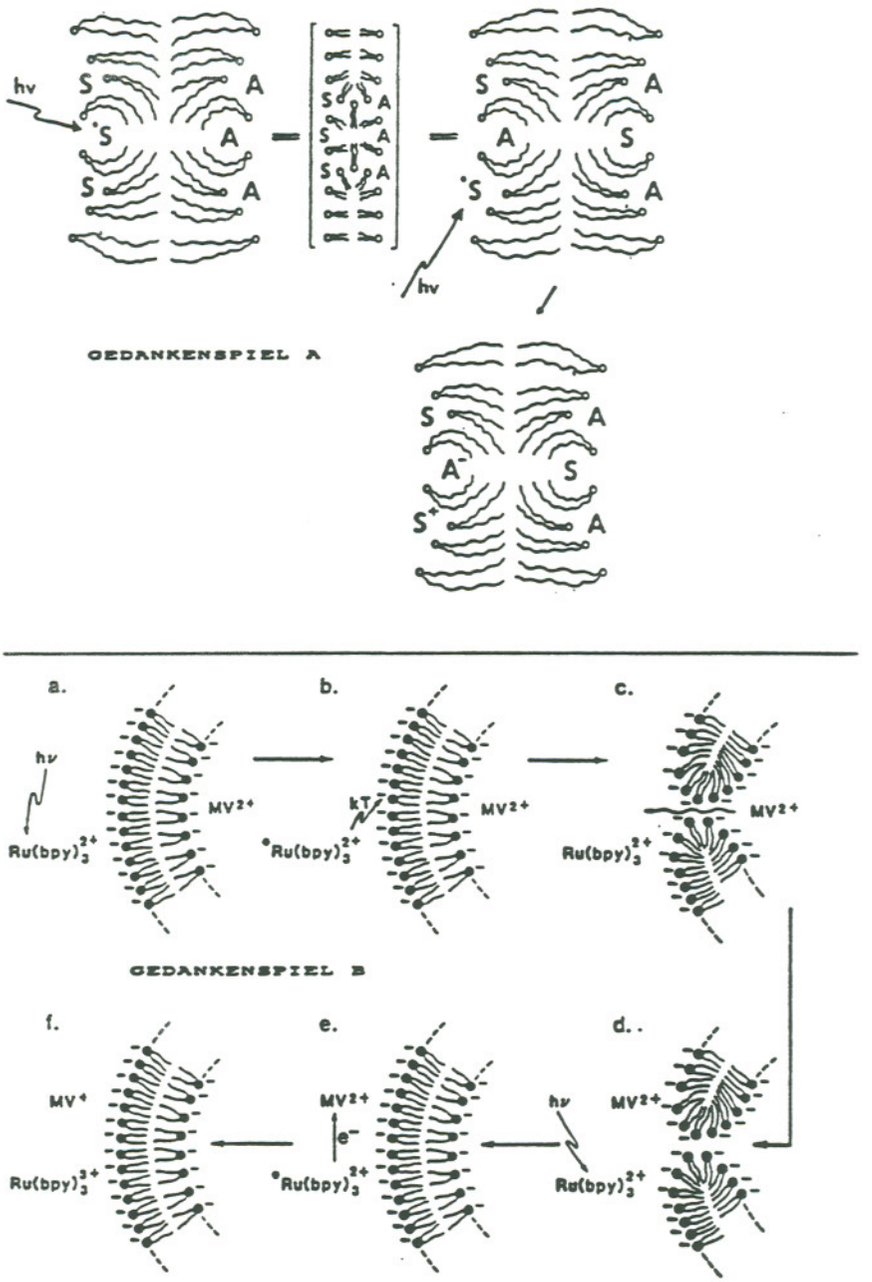

Scheme 3: Possible Scrambling Mechanisms (from reference 48)

Taking into account all the results from the early studies discussed above, the following mechanism for transmembrane reduction of viologens in vesicle systems is proposed:

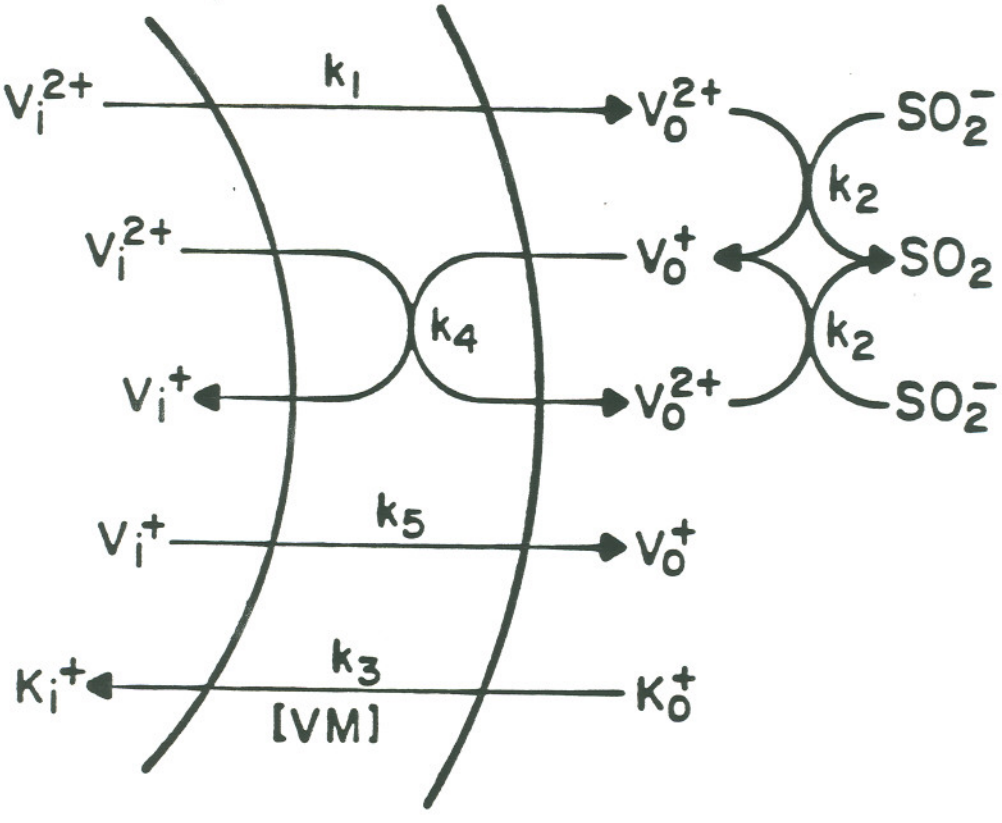

Scheme 4: Proposed mechanism for transmembrane reduction of viologen

The aspiration of this dissertation was to validate the proposed reaction scheme and to determine the contribution of each individual step to the observed overall reduction kinetics.

1.2 Ion diffusion across membranes

The diffusional behavior of small ions has been of great interest for many years[12-14]. Nature often generates an electrochemical gradient through ion pumping from one side of a membrane to the other to provide a driving force for biosynthesis or to perform other useful work[15]. In most cases these ions are small and univalent, such as Na^+, K^+, H^+, or OH^-. All of these ions have very small intrinsic permeabilities for biological membranes which allows maintenance of a concentration gradient. To shuttle these ions across the membrane Nature has devised protein ion pumps, which can operate against a gradient, and ionophores that either form channels through the membrane, or in a carrier-mediated fashion that actively transport ions from one side to the other. Many of these reagents show a remarkable selectivity for a certain ion[16], e.g., the carrier valinomycin shows a preference for K^+ over Na^+ of 10,000 to 1.

Over the past years many studies[12-14,17] have been done to better understand and characterize the diffusional behavior of these ions. Again, synthetic vesicles have often been chosen to mimic biological membranes. They are easy to prepare, relatively stable, provide a large surface area per volume, and are readily available. Transmembrane diffusion across of Cl^- pc liposome membranes is

several orders of magnitude faster than either Na^+ and K^+, although the absolute magnitudes of the rates are still uncertain. Typical values of intrinsic permeabilities for Na^+ and K^+ are 10^{-13}–10^{-15} cm s^{-1} and 10^{-11}–10^{-12} cm s^{-1} for chloride. Recent reports[17] indicate an even higher permeability for H^+/OH^- (their respective diffusion rates are kinetically indistinguishable) with intrinsic permeabilities up to 10^{-4} cm s^{-1}. All of these permeability coefficients depend on temperature, pH, and presence of other ions in solution, so only comparisons of rates under identical conditions are valid. Another complication in these measurements which may account for the different rates reported in various studies arises from the fact that the diffusion is so slow that other effects may distort the results. Vesicle fusion is known to occur upon aging[18], leading to partial release of the vesicle content to the bulk solution. Also vesicles can rupture under the influence of external stimuli, again releasing their content. Either one of these artifacts will result in an apparent increase in the observed diffusion rates.

One other very important aspect of ion diffusion across membranes is the build-up of an electrical potential. Biological membranes are known to withstand transmembrane potentials of up to 200 mV[16]. This potential is equivalent to an electric field of 300,000 V/cm, underscoring the suitability of bilayer membranes as charge-storing capacitors. Higher potentials will lead to membrane rupture. The same holds true for vesicle bilayers. Diffusion of a

mobile ion across the membrane rapidly develops a transmembrane potential. In the absence of charge compensation the potential that develops may become rate limiting and ultimately completely retard any further ion movement of the mobile ion. The effect of transmembrane electrical potentials has been demonstrated with the use of valinomycin in the study of H^+ diffusion[17]. In the presence of K^+ and valinomycin the observed diffusion rate was dramatically enhanced over that measured in their absence.

Recently, there have been reports of diffusion of viologens across vesicle bilayers[19-21]. One group observed the transmembrane reduction of dihexadecylviologen entrapped inside pc vesicles when dihexadecylviologen bound to the outer membrane surface was reduced by dithionite. They interpreted their results in terms of part tunneling, part diffusion-jump contribution to the observed transmembrane electron transfer. Research in our laboratory has utilized DHP vesicles and dithionite as the external reductant. Our results of transmembrane redox suggest rate-limiting electron transfer across the membrane (whose exact mechanism is still under investigation) followed by the comigration of a viologen radical to dissipate the developing charge gradient. Despite this clear evidence for transmembrane diffusion of viologen, the controversy over the mechanism of transmembrane redox remains.

1.3 Experimental strategy

In view of the apparent discrepancy between theory and experiment in many of the reported systems and the contradictory and still uncertain interpretations of similar results, a thorough study of the diffusional properties of viologens was undertaken and the results of this research are presented in this dissertation. The general strategy was to determine the influence of as many system parameters as possible. This included the use of a variety of different lipids to form vesicles with different phase transition temperatures. The vesicles were formed by different methods allowing for varying sizes and narrow size distributions. The alkyl chain length of the viologen was varied, as was the temperature, pH, ionic strength and identity of the buffer. Both photochemical and chemical reductants were employed, and various ionophores were utilized to determine potential gradient effects. The synthesis of radiolabeled viologens allowed the determination of viologen exchange at equilibrium across the bilayer membrane. Binding of viologens to vesicles was determined by equilibrium dialysis and ion-exchange chromatography.

CHAPTER 2

EXPERIMENTAL

2.1 Materials

2.1.1 Extraction of egg lecithin

Phosphatidylcholine was extracted from fresh hen egg yolk by a modified literature procedure[22]. Yolks from 24 eggs (525 g) were homogenized in 1.1 l acetone and allowed to settle for one hour. The suspension was filtered and the yellow acetone solution was discarded. The solids were washed 3 times with 200 ml each of cold acetone. The solids were then suspended in 1.1 l ethanol for one hour. After filtration the solids were resuspended in 500 ml ethanol and, after filtration, the combined ethanol extracts were evaporated to dryness on a rotary evaporator. The slightly oily solids were dissolved in 200 ml pentane to form a homogeneous yellow solution. The volume of the solution was reduced to approximately 70 ml on a rotary evaporator. The remaining hazy solution was poured into 500 ml cold acetone with rapid stirring. The white precipitate was allowed to settle in the freezer. After filtration the solids were washed 3 times with cold acetone (200 ml each). The solids were dried and dissolved in chloroform.

700 g alumina in 1 l chloroform were poured into a 5x50 cm column.

The chloroform solution of phosphatidylcholine was loaded onto the column and eluted with a 1:9 mixture of methanol:chloroform. After the void volume of about 1 l a yellow band came off the column, and 40 fractions of 25 ml each were collected thereafter. The fractions were analyzed by TLC (solvent system chloroform:methanol:acetic acid: water 25:15:4:2). Fractions 14-28 contained chromatographically pure lecithin and were combined. The solvent was removed by rotary evaporation and the solids dissolved in chloroform and divided into 10 ml aliquots for individual storage at -17^0 C until use. Typically, 24 egg yolks (500-550 g) yielded 13-15 g of chromatographically pure phosphatidylcholine.

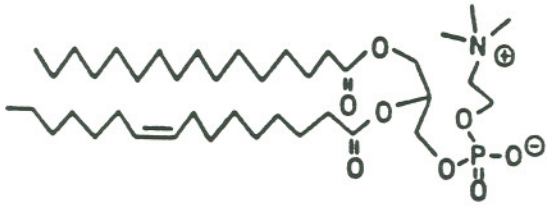

PC

2.1.2 Viologens

Several N,N'-dialkyl-4,4'-bipyridine (viologens) are commercially available (see 2.1.4 Other Reagents). To examine the influence of the alkyl tail, however, it was necessary to synthesize other viologens with the desired alkyl chains. A series of asymmetrically substituted

bipyridines (N-alkyl-N'-methylviologen, C_nMV^{2+}) with n = 4-20 had been synthesized in our laboratory by Dr. David H. Thompson. Symmetric dialkylviologens were prepared as follows:

Dialkylviologens[26], $(C_n)_2V^{2+}$, (C_n=hexyl, octyl, decyl, and octadecyl): 1.00 g (6.4 mmoles) 4,4'-bipyridine and a four-fold molar excess of n-alkyl bromide were refluxed in 30 ml DMF for 20 hours. The brownish-yellow precipitate was filtered and washed with 50 ml ether. The solid was dried and twice recrystallized from methanol/acetone to give the bright yellow product. TLC analysis in methanol:water:ethylammonium hydrochloride 6:6:2 on silica plates showed a single spot. The proton nmr spectra were recorded on a General Electric QE-300 instrument at 300 MHz and the following assignments were made:

dihexylviologen $C_{22}H_{34}N_2$ (D_2O): (ppm) 0.66 (t, 6H, J = 7 Hz), 1.15 (m, 12H), 1.92 (t, 4H, J = 9 Hz), 4.54 (t, 4H, J = 8 Hz), 8.36 (d, 4H, J = 8Hz) 8.95 (d,4H, J = 8 Hz).

dioctylviologen $C_{26}H_{42}N_2$ (D_2O): (ppm) 0.67 (t, 6H, J = 8 Hz), 1.16 (dd, 20H, J_1 = 7 Hz, J_2 = 7 Hz), 1.89 (t, 4H, J = 9 Hz), 4.54 (t, 4H, J = 9 Hz), 8.50 (d, 4H, J = 8 Hz), 9.08 (d, 4H, J = 8 Hz).

didecylviologen $C_{30}H_{50}N_2$ (MeOD): (ppm) 0.64 (t, 6H, J = 8 Hz), 1.06 (dd, 28H, J_1 = 10 Hz, J_2 = 10 Hz), 1.86 (t,4H, J = 8 Hz), 4.50 (t,

4H, J = 9 Hz), 8.45 (d, 4H, J = 8 Hz), 9.05 (d,4H, J = 8 Hz).

dioctadecylviologen $C_{46}H_{82}N_2$ (MeOD): (ppm) 0.66 (t, 6H, J = 8 Hz), 1.04 (s, 68H), 1.84 (t, 4H, J = 7 Hz), 4.50 (t, 4H, J = 9 Hz), 8.45 (d, 4H, J = 8 Hz), 9.05 (d, 4H, J = 8 Hz).

Propylviologen sulfonate (PVS) was synthesized according to literature methods[27] as follows: 2.00 g 4,4'-bipyridine (12.8 mmoles) were slowly added to 13.0 g (106.6 mmoles) 1,3-propane sultone at 40°C. The white precipitate was filtered, washed with acetone, and dried. The white solid was dissolved in water and precipitated again with acetone to further purify the product. TLC as above showed a single spot. Nmr data: $C_{16}H_{14}N_2O_6S_2$ (D_2O) (ppm) 2.32 (t, 4H, J = 10 Hz), 2.87 (t, 4H, J = 9 Hz), 4.75 (t, 4H, J = 9 Hz), 8.44 (d, 4H, J = 8 Hz), 9.01 (d, 4H, J = 8 Hz).

^{14}C-Labeled alkylmethylviologens[28]: 3.3 ml of $^{14}CH_3I$ in nitromethane (0.033 mmoles, 10.7 mCi/mmole) was added to a ten-fold molar excess monoalkylbipyridine[a] in a thick-walled glass ampule. The ampule was placed in liquid N_2 until the sample solidified and then sealed under a vacuum with a torch. The sealed ampule was placed in an oven at 105° for 24 hours. After allowing it to cool to room temperature the ampule was scored and the seal was broken to allow

---

[a]The momoalkylbipyridines were synthesized and kindly provided by Dr. David H. Thompson.

addition of 470 mg (3.3 mmoles) methyl iodide. The ampule was resealed as before and placed back in the oven for another 24 hours. After breaking the seal at room temperature the dark orange solution was transferred to a round-bottom flask. The ampule was rinsed several times with methanol, which was added to the round-bottom flask as well. The solvent was then removed by rotary evaporation, and the solid was washed with ether and recrystallized from methanol/acetone. TLC analysis on silica with the same solvent system showed a single spot identical to non-labeled sample.

^{14}C-labeled diheptylviologen: 0.85 mg $^{14}C_1$-heptanol and 7.7 mg heptanol (0.07 mmoles) were dissolved in 2 ml ether and 6.5 mg PBr_3 (0.025 mmoles) in 0.5 ml ether were added 50 ul at a time over 1 hour. The solution was stirred and maintained at 0^0 C with an ice bath during this addition. After equilibration to room temperature 0.1 ml NaOH (0.1 M) was added to neutralize the phosphoric acid produced and convert any unreacted PBr_3 to HBr. The solvent was then evaporated under a stream of nitrogen. 10.9 mg bipyridine (0.07 mmoles) and 2 ml DMF were added to the oily residue and the mixture was refluxed for 15 hours. The solution was cooled to -17^0 C to complete precipitation of the product. TLC analysis showed a single spot identical to commercial $(C_7)_2V^{2+}$. The solvent was carefully decanted and the remaining solids were dried under a stream of nitrogen and used without further purification.

Halide exchange[29]: Diheptylviologen dibromide was converted to

the dichloride salt by precipitation from an aqueous solution of picric acid, then redissolving the isolated solid in acetone and precipitating the chloride salt by passing gaseous HCl through the solution. The solid was filtered and recrystallized from acetone/methanol. The dibromide was converted to the dinitrate by precipitating Br^- as AgBr by adding 50% stoichiometric excess $AgNO_3$, and then removing excess Ag^+ by precipitation as the phosphate salt in 0.1 M phosphate buffer, pH 8.0.

2.1.3 [N,N,-di(hexadecyl)-2,2'-bipyridine-4,4'-dicarboxamide]-bis(2,2'-bipyridine)ruthenium: $Ru(bpy)_2L^{2+}$

The derivatized bipyridine ligand was synthesized by modified literature methods[23-25] as follows: 1.00 g 4,4' dimethyl-2,2'-bipyridine (5.4 mmoles) was dissolved in 60 ml 25% H_2SO_4. The solution was cooled to 5^0 and 2.0 g (12.7 mmoles) $KMnO_4$ were added while stirring for 30 minutes. The reaction mixture was allowed to warm to 30^0, then cooled again to 5^0 and another 2.0 g $KMnO_4$ were added. The mixture then was refluxed for 15 hours and a small amount of potassium metabisulfite was added to reduce any unreacted permanganate. Upon cooling a white solid precipitated from the solution and was subsequently filtered and dried. The acidity of the filtrate was lowered to pH 1.2 to ensure complete precipitation as the diacid. The solids were dissolved in aqueous $NaHCO_3$ and then precipitated with HCl to give white crystals of the 4,4' dicarboxylic acid-2,2' dipyridine. The diacid was converted to the acid

chloride by refluxing 450 mg (1.8 mmoles) diacid with 5 ml thionyl chloride for 3 hours. Excess $SOCl_2$ was removed under an aspirator vacuum attached to a liquid N_2 trap containing NaOH to neutralize any HCl gas. The product proved to be very moisture sensitive. Therefore it was immediately converted to the desired ligand by refluxing over pulverized 4 A molecular sieve for 17 hours in 10 ml dry benzene after adding 2.00g (8.3 mmoles) hexadecylamine. The product was extracted from the molecular sieve with butanol in a Soxhlet extractor. 90 mg (0.1 mmoles) derivatized bipyridine and 60 mg $Ru(bpy)_2Cl_2$ (0.1 mmoles) were refluxed in butanol for 4 hours under nitrogen. After cooling to room temperature an aqueous solution of $NaClO_4$ was added to initiate precipitation, which was then completed in the refrigerator (4^0). The brown solid was filtered, dissolved in acetone to remove any unreacted starting material, and then recrystallized from methanol. TLC analysis (solvent system chloroform:methanol:acetic acid:water 25:15:4:2) showed a single spot. The uv/vis spectrum was identical to published spectra[5b].

2.1.4 Other reagents

Diheptylviologen (Kodak), dimirystoylphosphatidylcholine, DMPC, and dipalmitoylphosphatidylcholine, DPPC, (Avanti), $Ru(bpy)_3^{2+}$ (Aldrich), $ZnTPPSCl_4$ (Midcentury), $Na_2S_2O_4$ (Amresco) were of the highest purity available and were used as received. $ZnTMPyP^{4+}$ (aqueous solution) was a gift from Dr. K. Kalyanasundaram, Ecole Polytechnique Federal de

Lausanne, Lausanne, Switzerland. Chromous ion was prepared by anaerobic reduction of $Cr(ClO_4)_3$ over Zn amalgam. Other materials were of reagent grade and were used as received.

2.2 Methods

2.2.1 Formation of egg-pc vesicles[b]

Vesicles were prepared either by ultrasonic dispersion or by high-pressure extrusion. In either case, a chloroform solution containing the egg pc (100 mg/ml) was first rotary evaporated to dryness in a round-bottomed flask, coating the glass surface with a film of the amphophil.

A: Sonication[30]:

After addition of buffer the lecithin was dispersed by two 10 minute sonications at 40 % power using the standard horn and tip of a Heat Systems Model W-225 Sonicator; the solution was cooled in an ice bath during sonication. The resulting translucent solutions were then filtered through 0.2 um pore size HAWP Millipore filters and centrifuged for 90 minutes at 100,000 g and 15^0 in a Beckman LS-65 ultracentrifuge using a TY65 fixed-angle rotor. The supernatant, which contained small

---

[b]Unless specified otherwise, the generic terms vesicle or liposome are taken to represent pc vesicles throughout this dissertation.

unilamellar vesicles of about 15 nm radius and was free of larger aggregates[30], was taken for experimentation. Viologens (and other ions) were entrapped inside the vesicle when desired by adding them to the buffer prior to sonication.

B: Extrusion[31]:

After adding buffer, the turbid suspensions were first subjected to five repetitive freeze-thaw cycles to completely hydrate the lipid. The mixture was then extruded 10-15 times through track-etched Nuclepore filters with a Lipex Biomembranes Inc. Extruder. The Extruder was pressurized to 600 psi with nitrogen at room temperature. By varying the filter pore size, unilamellar vesicles with narrow size distributions around various radii from 15-50 nm could be prepared.

Externally localized viologen was then removed by passing the vesicles down buffer-equilibrated Bio-Rad AG50-X8 cation-exchange or Bio-Rad Chelex 100 cation-exchange columns in their Na^+ or K^+ forms. Other ions were either also removed by ion-exchange chromatography or, if their binding affinity for the vesicles was low, by passing the suspension through Sephadex size-exclusion gel columns.

2.2.2 Other vesicles

DMPC, DPPC, and dihexadecylphosphate, DHP, vesicles were prepared by adding the appropriate amount of solid lipid to the buffer and either

sonicating without cooling or extruding at temperatures at least 10^0 above their respective liquid-crystalline to solid-crystalline phase-transition temperatures[c]. The extruder was equipped with a thermo-barrel to maintain a constant temperature throughout the extrusion. Other manipulations were the same as for egg-pc.

2.2.3 Equilibrium Dialysis

Equilibrium dialyses were carried out in Bel-Art Products dialysis cells, which have very favorable membrane surface to sample volume ratios. The two half-cells were separated by a # H40299 cellulose membrane with a nominal molecular weight cut-off of 6,000 daltons. This allowed free diffusion of the viologen (and other ions e.g. porphyrins)[d], yet completely prevented the vesicles from migrating. The binding affinity of the viologen to the vesicle can be simply determined by measuring the concentration of viologen on either side of the membrane following equilibration.

---

[c]In order to obtain homogeneous vesicles it is necessary to form them at temperatures above the liquid to solid crystalline phase transition temperature Tc of the lipid (see Results and Discussion). At temperatures below Tc lateral phase separation of the lipid during liposome formation can occur, resulting in inhomogeneous bilayers.

[d]It was found that a fraction of the porphyrins adsorbed to the membrane. The amount of adsorbed material could be estimated, however, by taking the optical spectrum of the membrane at the end of the dialysis. The membrane polymer only absorbs in the ultraviolet region and does not interfere with the visible bands of the porphyrin.

In a typical experiment vesicles were added to one half of the cell and buffer to the other. Control experiments showed that the same distribution was achieved whether the viologen was originally added to the compartment containing the vesicles or the one containing only buffer. Other control experiments showed that in systems with only buffer in one compartment and viologen added to the other the equilibrium distribution corresponded to equal amounts of viologen on both sides.

The cell was gently agitated to avoid developing concentration gradients within each compartment. Equal aliquots were taken from each side at various time intervals until no further changes in the viologen distribution were observed; the viologen concentration was determined by measuring the absorbance at 260 nm in the optical spectrum. At low viologen concentrations the optical interference of the vesicles was overcome by reducing the viologen to its blue radical form and measuring its concentration in the visible region of the spectrum.

For these experiments the concentration of lipid was typically 4 mM, and the concentration of viologen was varied from 10 uM to 1 mM. Most experiments were done in 0.1 M Na^{+} phosphate buffer at pH 8.0. This high ionic strength helped minimize any osmotic effects that would perturb the intercompartmental viologen dication distribution.

2.2.4 Photochemistry

Photochemical systems consisted of vesicles containing viologen in their inner aqueous phase and $Ru(bpy)_3^{2+}$ (or $ZnTPPS^{4-}$ or $ZnTMPyP^{4+}$) in the bulk medium. For systems where net viologen reduction was desired, the electron donor EDTA was added to the continuous aqueous phase. Two ml aliquots were deoxygenated in an optical cuvette with a long neck by bubbling with nitrogen. The samples were then immersed in a constant temperature bath and illuminated with filtered light from a 1600 W high-pressure xenon lamp (Oriel model # C-60-80). The incident light beam was passed through a 10 cm water cell, then Corning # 3-75 uv cutoff and # CS 4-70 blue-green filters before reaching the cuvette. This assured that the spectral irradiance was limited to 400-600 nm. The incident light intensity was 8.7 (+/- 1.3) x 10^{-7} einstein s^{-1}, determined independently either by Reinecke salt actinometry[35] or with a Coherent 210 Power Meter. In control runs the temperature inside the cuvette was monitored with a copper/constantan thermocouple. By this method it was determined that the temperature of the illuminated sample did not vary by more than 0.5^0 over the course of a one-hour experiment. The solution inside the cuvette was continuously stirred by means of a magnetic stir bar driven by a submersible hydrodynamic magnetic stirrer.

2.3 Ionophores

In systems where a rapid ion movement was desired, ionophores were added to preformed vesicles, either as aqueous or methanolic solutions. The following control experiments were performed to establish that addition of small amounts of methanol (1-5% v/v) did not affect membrane integrity:

A: Potassium ion was encapsulated within the vesicles by forming the vesicles in the presence of K^+ and then exchanging external K^+ with Na^+ using an ion-exchange column. The concentration of K^+ in the bulk phase was monitored with a potassium ion-specific electrode. Addition of small amounts of methanol did not change the observed voltage, while addition of a methanolic solution of valinomycin caused an increase in the external K^+ concentration. From the initial slope of the voltage vs. time curve the rate of K^+ transfer could be evaluated. These experiments also established the usefulness of valinomycin as a functional ionophore in pc vesicles.

B: Diheptylviologen (50 uM) was entrapped within the vesicles as described above, and, after addition of methanol (1-5% v/v), the continuous aqueous phase was probed for viologen by adding $S_2O_4^{2-}$ (see 2.4 Kinetic Methods). No increase in external viologen concentration following methanol addition was observed.

The purpose of the added ionophores is the rapid dissipation of charge gradients. However, since such gradients are necessary to maintain entrapment of membrane permeable ions within the vesicle, the ionophores were added just before the start of the kinetic measurements.

To test for loss of membrane integrity upon addition of valinomycin, radiolabeled sucrose was entrapped inside the vesicle and valinomycin was added at various concentrations to small aliquots of that vesicle suspension. At various time intervals the vesicle samples were passed through a Sephadex gel column to remove any escaped sucrose. By comparing the scintillation counts of the different samples the effect of valinomycin loading was determined.

2.4 Kinetic Measurements

Alkylviologen dications are colorless with a strong uv band around 260 nm, but can be reduced to a cation radical form, which is intensely blue[32a] in its monomeric form and purple in its aggregated form[32b]. All the reductants used in this series of experiments have been shown to be unable to diffuse across vesicle bilayers[19]; therefore they provide a convenient way to measure the concentration of viologen on the outside of the vesicles.

One of the goals of this dissertation research was to determine the rate of viologen diffusion across lipid bilayer membranes under a

variety of conditions, including the absence and presence of a driving force.

2.4.1 Passive diffusion

Suspensions containing vesicles with internally localized viologen were deoxygenated by bubbling with argon for 5 minutes, a procedure which was shown to be sufficient to remove more than 97% of the oxygen[33,e]. To prevent oxygen interference during the kinetic run argon was continuously blown over the top of the sample throughout the experiment. To measure the rate of viologen leakage small aliquots were transferred via a gas-tight syringe to a septa-stoppered, degassed optical cell at various time intervals and the amount of escaped viologen was determined by adding dithionite and measuring the optical spectrum.

The same procedure was used to determine leakage rates in the presence of valinomycin, which was added prior to degassing as a methanolic solution.

---

[e]Prolonged bubbling had to be avoided because it lead to slow destruction of the vesicles and thus increased the detectable amount of viologen (see Results and Discussion).

2.4.2 Redox-driven diffusion

The samples were deoxygenated in septa-stoppered optical cells and, after removal from the argon manifold, dithionite was added and the cells placed in a Hewlett-Packard 8452A diode array spectrophotometer to record changes in the viologen spectrum. Temperature controlled experiments at 5-45^0 C were done on a Perkin Elmer Lambda 9 spectrophotometer that was equipped with a thermostated cell holder. The accessible temperature ranged from 0^0 to 110^0 C and could be controlled very accurately to within 0.2^0 C. The viologen radical concentration was monitored at 604 nm. The same protocol was utilized when Cr^{2+} was used as the external reductant.

Rapid kinetic measurements were done with a stopped-flow instrument of conventional design[34a]. Data were collected with a Nicolet 4094B digital oscilloscope. This allowed direct transfer of the digitized data to a Digital Pro 350 computer. The computer was equipped with several kinetic curve fitting programs. Data could be quantitatively analyzed by a nonlinear method with a program adapted from Bevington[34b]. However, this program allowed the experimental traces to be fitted to a series of first order processes or simple second order processes only. The traces from transmembrane viologen reduction in the presence of valinomycin could not be fitted to first order kinetics. These curves were analyzed by simulating a postulated mechanism[36] through a series of iterations based on simple mass balance equations

(see Appendix A). The fits could then be compared to the actual data and the "goodness-of-fit" was judged from the residual of the graphic display.

2.4.3 Transmembrane viologen exchange

The exchange rate of ^{14}C-$(C_7)_2V^{2+}$ bound to opposite sides of the membrane was estimated with the use of radiolabeled viologens. The vesicles were formed in the presence of ^{14}C labeled viologen and external viologen was removed by ion-exchange chromatography as usual. The concentration of entrapped viologen was determined spectroscopically and an equivalent amount of unlabeled $(C_7)_2V^{2+}$ was added back to the sample. At various time intervals aliquots of this sample were taken and the external viologen was removed with Bio-Rad Chelex-100 resin. To minimize dilution effects and to increase speed[f] the dry resin was placed in a fritted funnel atop a bell jar. The sample was then pulled through the resin with an aspirator and the radioactivity was measured with a Beckman LS-3150 T scintillation counter using a Beckman Ready Solv GP scintillation cocktail. From the amount of retained radiolabel the exchange rate could be evaluated.

---

[f]Rapid removal of external viologen is important because the resulting concentration gradient will cause more viologen leakage out of the vesicle and thus distort the results from equilibrium exchange.

2.5 Photochemical Systems

2.5.1 Definitions

The following reactions account for the net reduction of viologen by photosensitizers (S):

$$S + h\nu = S^{*} \quad (1)$$

$$S^{*} + V^{2+} = S^{+} + V^{+} \quad (2)$$

$$S^{+} + D = S + D^{+} \quad (3)$$

$$S^{+} + V^{+} = S + V^{2+} \quad (4)$$

Following illumination of the sensitizer (1) viologen is reduced by the excited chromophore (2). The quenching of the oxidized sensitizer by the sacrificial donor (3) successfully competes with back electron transfer from the reduced viologen to the oxidized sensitizer (4) which leads to net accumulation of the viologen radical.

Reversible systems are defined as systems that do not have a sacrificial donor, e.g., EDTA, and thus, although electron exchange between sensitizer and viologen occurs, no net accumulation of reduced viologen is observed. Systems which allow for net reduction-oxidation will be called non-reversible.

2.5.2 Reversible systems

A system containing viologen on the inside and a photosensitizer on the outside of a vesicle was illuminated as described above. To measure the amount of viologen leakage, dithionite was added after a certain time period and the optical spectrum was recorded. Each time point was measured with a fresh aliquot from the same vesicle preparation batch. All manipulations were done anaerobically.

2.5.3 Non-reversible systems

The sacrificial electron donor EDTA was added to the exterior phase of the above system and illuminated as before. At various time intervals the optical cell was removed from the light beam and the optical spectrum was recorded. All time points were done on the same aliquot.

2.5.4 Photodamage

The following tests were performed to determine whether or not the vesicle membrane was photodamaged during the course of the photochemical experiment. Two identical samples consisting of vesicles containing entrapped viologen and external sensitizer with or without EDTA were illuminated for 30 minutes. One sample was then removed from the light beam and kept in the dark for another 30 minutes while the other sample

was irradiated for another 30 minutes. The amount of escaped viologen in each sample after 30 minutes and after 60 minutes was then compared to determine if leakage due to photodamage had occurred.

2.6 Other instrumentation

Fluorescence spectra were recorded on a Perkin-Elmer MPF-66 spectrophotometer. Fourier transform infrared spectra were obtained with a Perkin-Elmer 1800 FTIR instrument.

CHAPTER 3

RESULTS and DISCUSSION

3.1 Equilibrium Dialysis

Binding of viologens to vesicles may affect the rate of viologen reduction by dithionite because strong binding of viologen will increase its membrane surface concentration and thus may facilitate transmembrane diffusion.

A very convenient way to determine binding of small molecules to larger aggregates is by equilibrium dialysis. The small molecule or ion is freely diffusible through a semipermeable membrane that separates two half cells. The large aggregate, e.g. a vesicle, cannot diffuse to the other half cell if the molecular weight cut-off of the membrane is below the molecular weight of the aggregate. If there is no binding to the aggregate the small ion will distribute to give equal chemical potentials on both sides of the membrane. If binding does occur, then the concentration of the ion on the side opposite the aggregate will be lower at equilibrium than the concentration on the aggregate side because again, the free ions will distribute to equal the chemical potentials at equilibrium, and the

difference will be the amount of bound ion.

To determine binding of viologens to pc vesicles membranes with nominal molecular weight cut-offs at 6,000 daltons were used. This allowed for easy diffusion of all viologens measured (molecular weights up to 662 g/mol), but was too small for diffusion of vesicles (aggregated weight about 1,000,000 daltons). Free permeation and complete equilibration of the viologen was demonstrated by adding viologen in 0.1 M phosphate buffer to one half cell of the dialysis system and dialyzing it against the same buffer. After 24 hours the concentration of viologen in each half cell was identical (Table 1). However, the sum of the concentrations in each half cell did not account for 100 % of the original amount of viologen. The difference was shown to be adsorbed to the membrane. This was confirmed qualitatively by dropping dithionite solution onto the membrane and observing formation of the blue viologen radical. The amount of membrane bound viologen was very small for all measurements. It did not exceed 10 % (at low concentrations) and typically was 5 $\pm$ 2 %. Because only a small fraction of the viologen was adsorbed to the membrane this interference did not appreciably affect the binding of the viologen to the vesicle and was corrected for in subsequent calculations of binding constants. The fraction of viologen bound to the vesicles was calculated from the difference in viologen concentration in each half cell as follows:

Table 1: Viologen equilibration in the absence of vesicles.

	$[(C_7)_2V^{2+}]$ (uM)	
	before dialysis	after dialysis
half cell A	155	73
half cell B	0	72

4 mM pc, 0.1 M phosphate buffer, pH 8.0

$$[V^{2+}]_{bound} = [V^{2+}]_{pc} - [V^{2+}]_{buffer}$$

where V^{2+}_{pc} and V^{2+}_{buffer} represent the viologen concentrations in the half cell containing the pc vesicles and the half cell containing only buffer, respectively. The fraction of bound viologen can then be defined as

$$F = [V^{2+}]_{bound} / [V^{2+}]_{free}$$

where V^{2+}_{bound} is the fraction of viologen bound to the vesicles and V^{2+}_{free} is the fraction of viologen in bulk solution which is equal to the viologen concentration on the buffer-only side.

To assure correct results several other control experiments were performed. It is necessary to know the time required for the dialysis system to come to equilibrium. This was determined by periodically removing small aliquots from each half cell and determining the viologen concentration at that time. The results are plotted in Figure 1 and show that a minimum of 10 hours was required to reach equilibrium. Figure 1 also demonstrates that the same viologen distribution was reached at any given time whether the viologen was initially added to the vesicle or the buffer-only side. This indicates that bound viologens can freely exchange with bulk viologens and that possible osmotic effects do not influence the

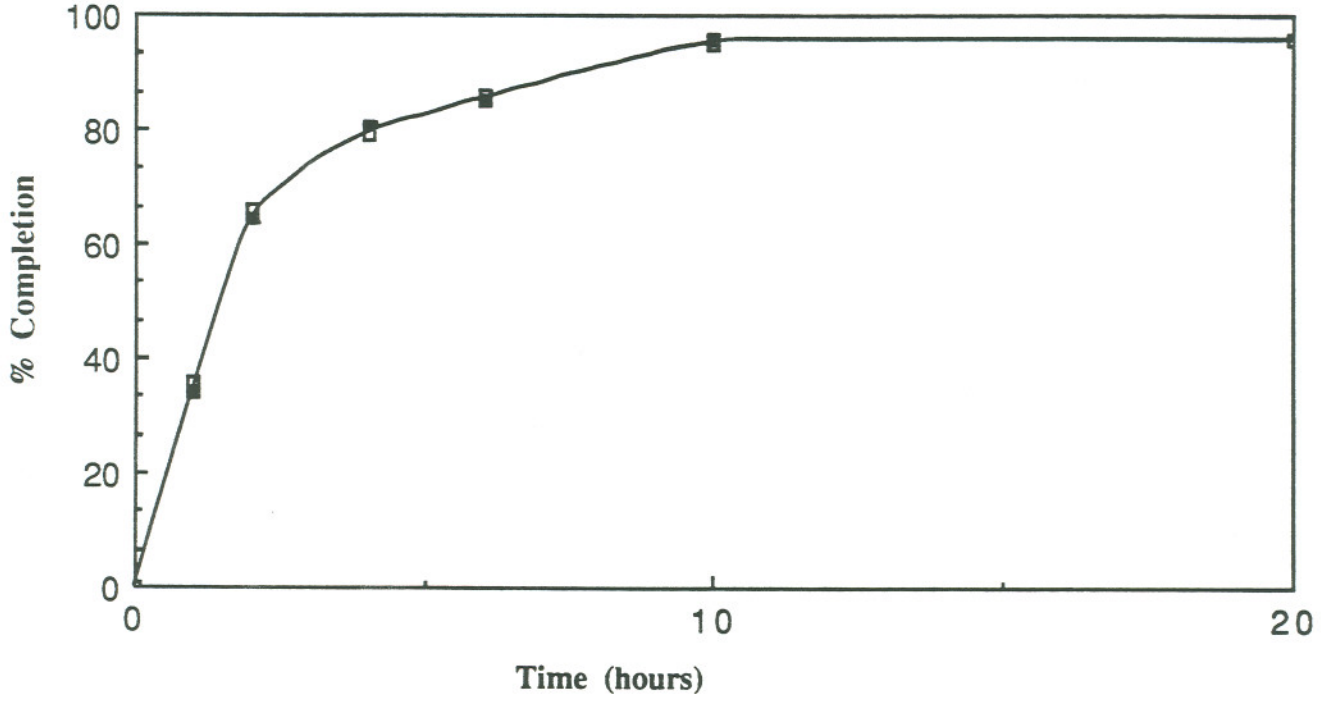

Figure 1: Time dependence of equilibration in binding studies of $(C_7)_2V^{2+}$ with pc vesicles
4 mM pc, 22° C, 150 uM $(C_7)_2V^{2+}$ to start on one side, 0.1 M phosphate buffer, pH 7.5,
open squares: $(C_7)_2V^{2+}$ initially on buffer side
dark squares: $(C_7)_2V^{2+}$ initially on pc side

viologen distribution[a].

The results from the equilibrium dialysis with diheptyl-viologen and pc vesicles are presented in Figure 2. It shows that the fraction of bound viologen is dependent on the total viologen concentration. The relatively large data scatter is due to uncertainties in the spectrophotometric $(C_7)_2V^{2+}$ concentration determination because of the light scattering of the vesicles. This scattering varies from sample to sample, especially after dialysis, and is therefore difficult to correct for properly. At lower concentrations the fraction of vesicle-bound viologen is greater than at higher concentrations. This result indicated that the binding sites are not independent.

It can be estimated that complete surface coverage of a 4 mM pc vesicle solution requires about 600 uM viologen[b]. This represents an upper limit for viologen binding, and actual binding is expected to be considerably lower. Figure 2 shows that the amount of bound $(C_7)_2V^{2+}$ never exceeds 100 uM. Binding interactions were further manifested by a Scatchard plot[54] (Figure 3). This plot is based on the Scatchard equation:

---

[a]The high ionic strength of the buffer (0.4 M) also helps minimize such osmotic effects that may be expected due to the pc concentration gradient.

[b]This calculation is based on vesicles of 30 nm diameter and assuming a "surface area" for viologen of about 50 A^2.

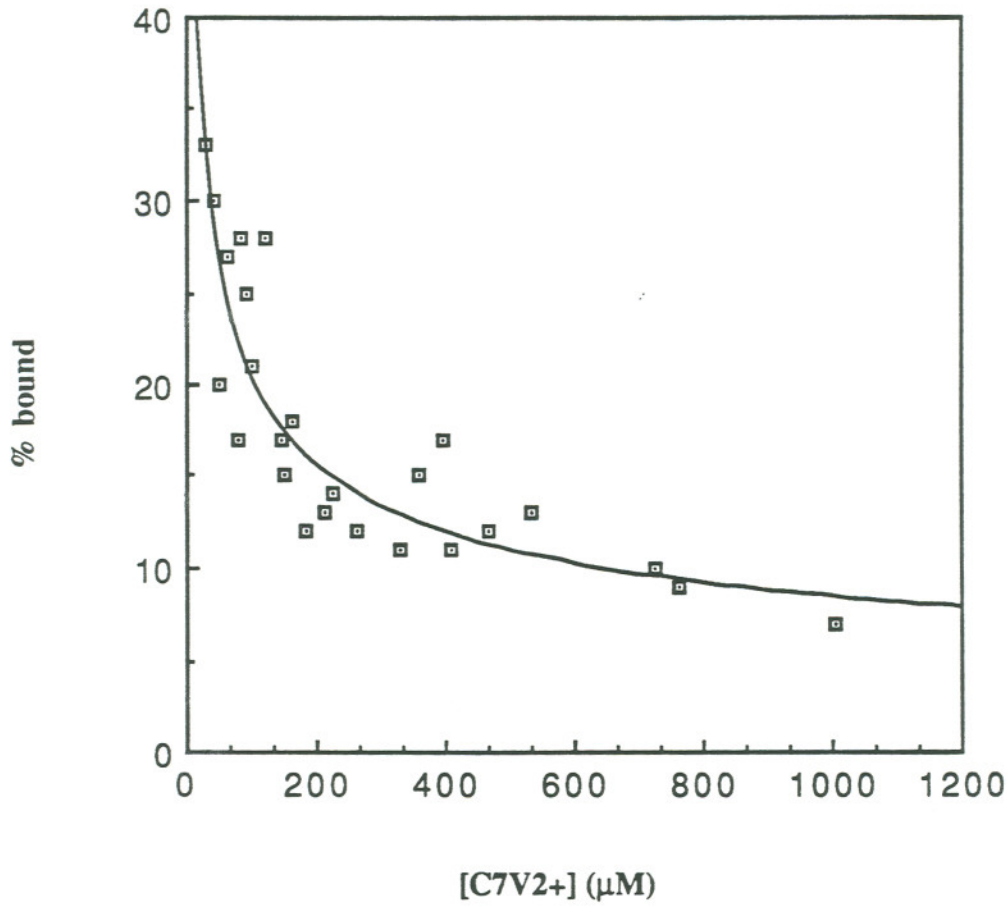

Figure 2: Binding of $(C_7)_2V^{2+}$ to pc vesicles

4 mM pc, 22^0 C

0.1 M phosphate buffer, pH 7.5

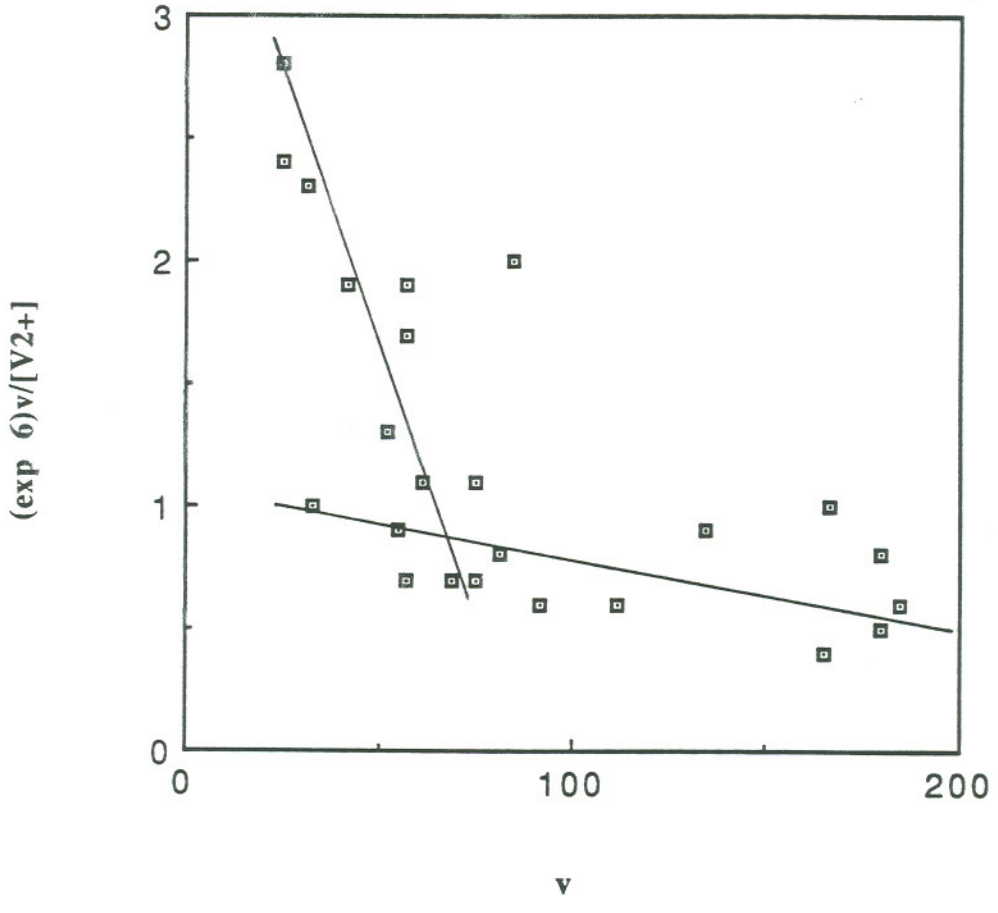

Figure 3: Scatchard plot of $(C_7)_2V^{2+}$ binding to pc vesicles

data from Figure 2

$$v/[A] = K\ (N-v)$$

where $v = [A]_{bound}/[M]$ is the number of small molecules (A) bound per vesicle (M), [A] is the bulk concentration of the adsorbing molecule, K is the equilibrium constant for binding, and N is the number of available binding sites. This model assumes that all binding sites are equal and binding of one adsorbent does not affect subsequent binding of other adsorbents. If this is correct then a plot of v/[A] vs. v should yield a straight line with a slope of -K, a y-intercept of NK, and x-intercept of N. Plotting the data of $(C_7)_2V^{2+}$ binding to pc vesicles in 0.1 M phosphate buffer, pH 8.0, according to this model does not yield a straight line (Figure 3). This implies that the binding sites on the vesicle surface are not independent of each other. Figure 3 could, however, be interpreted in terms of bimodal binding, with different binding constants at low and high viologen loading. At low loading an apparent binding constant $K = 4\ (\pm\ 1) \times 10^4\ M^{-1}$ could be estimated, while at high loading $K = 3\ (\pm\ 1) \times 10^3\ M^{-1}$. N, the number of available binding sites per vesicle, was 85 $\pm$ 15 and 240 $\pm$ 25, respectively.

Another way of analyzing binding of small molecules to large aggregates is by constructing a Langmuir adsorption isotherm[55]. Langmuir derived the following equation for the adsorption of a gas

on a solid surface:

$$p = (1 / K)(p^{max} - p)\,[A] \qquad (10)$$

where p is the number of adsorbed molecules per unit area of membrane, p^{max} is the maximum number of molecules adsorbed per unit area, K is the dissociation constant, and [A] is the surface concentration of the adsorbing molecule. Figure 4 shows the $(C_7)_2V^{2+}$ binding data plotted according to this equation. From this plot an apparent association constant Ka = 3×10^4 M^{-1} and a p^{max} value of 180 molecules/vesicle can be estimated. The value of p^{max} was estimated from the horizontal section of the plot in Figure 4 at high [A], i.e. the region where no further increase in binding is observed. Ka was estimated by rearranging the Langmuir equation as follows

$$p = (1/K)\,(p^{max} - p)\,[A]$$

$$K = \{(p^{max} - p)/p\}\,[A]$$

when $p = p^{max}/2$

$$K = [A]$$

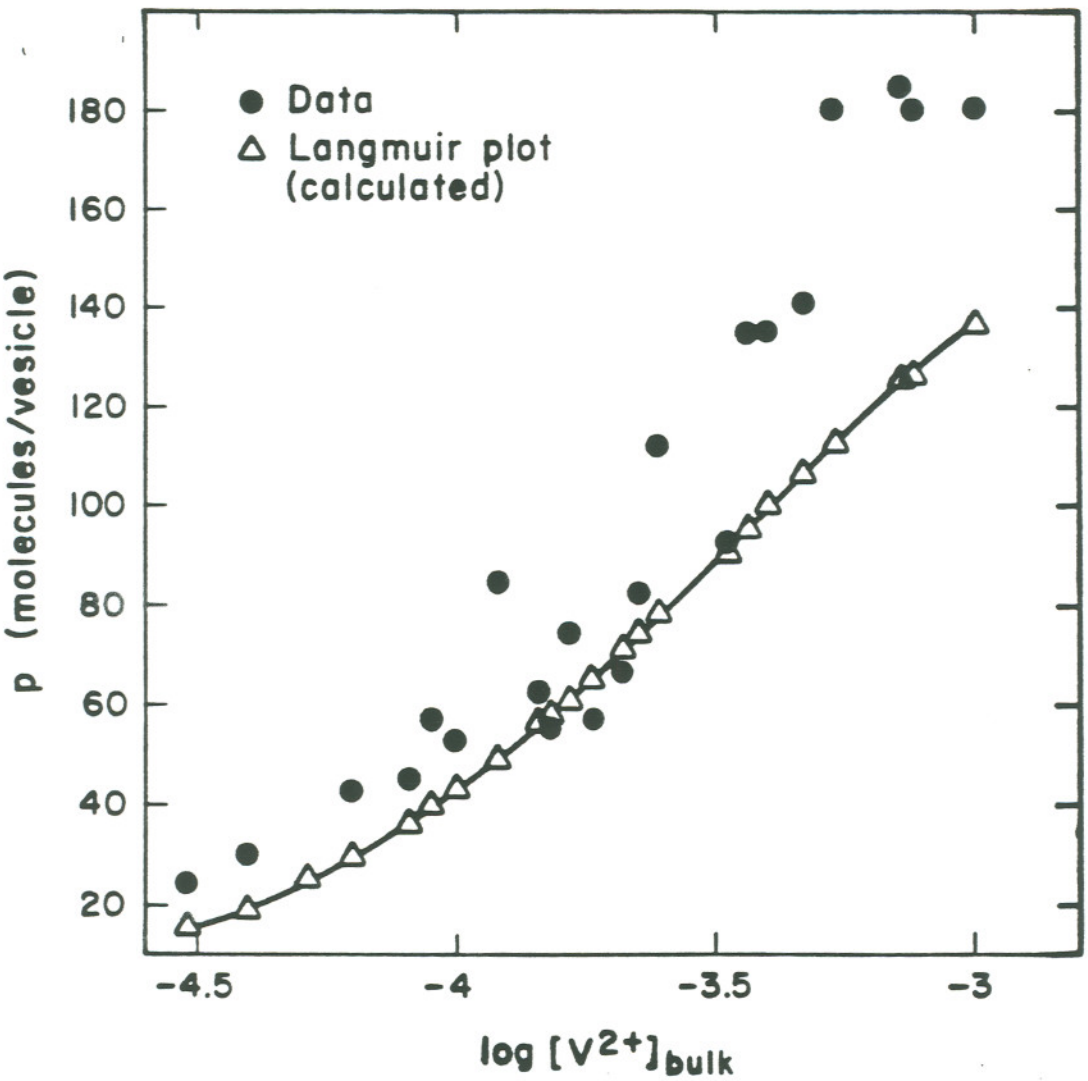

Figure 4: Langmuir plot of $(C_7)_2V^{2+}$ binding to pc vesicles

data from Figure 2

and then determining [A] at $p = p^{max}/2$. Using these approximate values for K and p^{max} one can calculate p at given $[A]^c$ from equation (10) and construct a Langmuir isotherm (Figure 4). The theoretical curve does not fit the data well. At low loading the experimental data are close to the calculated curve, but at higher loading there is significant deviation from the isotherm. The maximum number of $(C_7)_2V^{2+}$ per vesicle is reached at much lower loadings than the Langmuir plot would predict. This suggests that there are cooperative binding effects at higher loadings, consistent with the bimodal binding observed in the Scatchard plot. Both plots indicate that at higher loadings binding of additional viologen is facilitated by already bound viologen. Although the exact origin of this phenomenon was not fully understood it might involve lateral phase separation , where the viologen forms micro-domains within the bilayer at higher loadings. Subsequent binding of additional viologens might then be facilitated by these micro-domains. Both plots give about the same maximum number of $(C_7)_2V^{2+}$ that can be bound, 200 molecules per vesicle. This corresponds to a lipid:$(C_7)_2V^{2+}$ ratio of about 50.

The poor fits of both the Scatchard and Langmuir plots and the observation that viologen binding never exceeds 100 uM could also

---

[c] [A] at the surface is assumed to be the same as the bulk concentration of A because of the lack of electrostatic attraction at the surface.

result from binding of viologens to anionic impurities in the phosphatidylcholine, e.g., phosphatidylserine. If viologens bind with a 1:1 stoichiometry of lipid:viologen, then 2 mole percent phosphatidylserine would be sufficient to bind all viologens, even at the highest loadings. Because phosphatidylcholine is extracted from natural sources (egg yolk) containing a variety of lipids it is conceivable that the lipid used for the these experiments contains minute amount of lipids other than phosphatidylcholine, since the technique used for purity control (TLC) cannot easily detect impurities of 1-2%. If that impurity would be anionic, such as phosphatidylserine, which is also found in egg yolk, then it would be integrated in the vesicle membrane and the cationic viologen would preferentially bind to it. And, as mentioned above, phosphatidylserine contamination as little as 1.5-2% could account for even the highest viologen binding. This hypothesis could be tested by using synthetic lipids, such as DMPC and DPPC, to form the vesicles for the binding studies. These synthetic lipids contain no impurities, so true binding to phosphatidylcholine headgroups can be determined. There is, however, one strong argument against the involvement of phosphatidylserine in viologen binding to pc vesicles. If electrostatic attraction between anionic lipid molecules and viologens were primarily responsible for binding, then short chain viologen analogs, such as methylviologen, should exhibit some degree of binding. Short tail viologens, however, show no appreciable amount of vesicle binding (vide infra), thus arguing against lipid

impurity as the origin of viologen binding to pc vesicles.

It is expected that the chain length of the viologen alkyl tail will affect binding to vesicle membranes. The longer chains can penetrate deeper into the hydrocarbon core of the bilayer and the stronger hydrophobic forces will account for higher binding. Although the zwitterionic nature of the headgroup predicts that the membrane surface bears no net charge the following observations suggest that the vesicle surface consists of two distinct electrical layers, an outer, positive layer formed by the choline group and an inner, negative layer formed by the phosphate group. This charge layer model is supported by the anion binding described later (see Section 3.4 and reference 46). Thus the viologen dication would be electrostatically repelled from the membrane surface and binding is a result of hydrophobic interactions of the alkyl tails with the bilayer hydrocarbon region. The results from binding studies of a number of viologens with varying alkyl tails are shown in Table 2. To allow for a valid comparison all measurements were done at the same viologen concentrations since binding is dependent upon loading. It shows that binding is a function of alkyl chain length. The complete lack of binding of methyl viologen supports the idea that electrostatic forces are opposing viologen binding. It is worth noting that there is a large increase in binding for the dialkyl viologens in going from diheptyl to dioctyl. If one assumes that the bipyridine core of the viologen lies parallel to the vesicle surface

Table 2: Pc vesicle binding fractions (F) for various viologens under constant conditions.

Viologen	F
$(M)_2V^{2+}$	0.005
C_6MV^{2+}	0.075
C_8MV^{2+}	0.235
$C_{12}MV^{2+}$	0.563
$C_{14}MV^{2+}$	2.15
$C_{16}MV^{2+}$	19.0
$(C_6)_2V^{2+}$	0.111
$(C_7)_2V^{2+}$	0.205
$(C_8)_2V^{2+}$	2.33
$(C_{10})_2V^{2+}$	5.67
$(C_{18})_2V^{2+}$	49.0
PVS	0.010
MDV*	0.053

[viologen] = 200-250 uM, 22° C,

0.1 M phosphate buffer, pH 8.0

* MDV = methyl diviologen

(so that the quaternary nitrogens may ion pair with the anionic oxygen of the phosphate group) then the distance from the surface to the pure hydrocarbon region of the bilayer is about six methylene groups. Thus, only the terminal methyl group of the alkyl tail of diheptyl viologen reaches into that core. And, although dioctyl viologen has only one more methylene group than diheptyl viologen, the hydrophobic interaction (and hence the degree of binding) has increased. The free energy gained by removing an alkyl chain from water and placing it inside a micelle is about 2.1 kcal/mol for terminal CH_3 groups and about 0.7 kcal/mol per CH_2 group[56]. Thus, by adding one more methylene to $(C_7)_2V^{2+}$ the gain in free energy is raised by at least 33 % at 23^0, i.e. from 4.2 kcal/mol to 5.6 kcal/mol.

There is further evidence for electrostatic attraction and repulsion at pc vesicle interfaces. As mentioned earlier one of the premises for photostimulated transmembrane electron transfer was that the redox mediators are bound to the membrane surface. Therefore it was necessary to determine the degree of binding to pc vesicles of the various sensitizers used. Those sensitizers were $ZnTPPS^{4-}$, $ZnTMPyP^{4+}$, and $Ru(bpy)_3^{2+}$. The two porphyrins are structurally almost identical (Figure 5) and the primary difference is their overall charge. Thus, in the absence of electrostatic effects, their binding should be very similar. This is not the case, however. While $ZnTPPS^{4-}$ shows considerable binding to pc vesicles (Table 3),

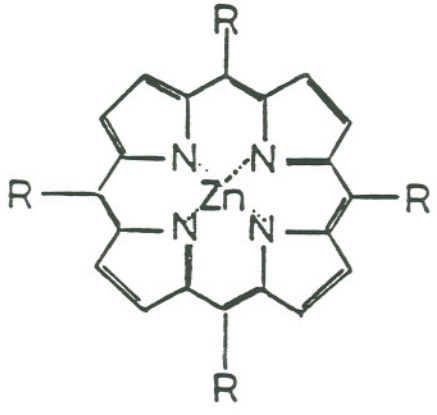

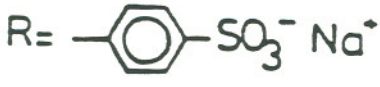

1

2

Figure 5: Molecular structures of $ZnTPPS^{4-}$ (1) and $ZnTMPyP^{4+}$ (2)

Table 3: $ZnTPPS^{4-}$ binding to pc vesicles

$[ZnTPPS^{4-}]$ (uM)	F
2.8	0.67
12.7	0.53
22.4	0.27

4 mM pc, 22° C, pH 8.0

0.1 M phosphate buffer

$ZnTMPyP^{4+}$ does not bind at all. This implies that binding is controlled by electrostatic effects. Since anions are adsorbed and cations appear to be repelled the vesicle surface bears an effective positive charge. This is expected if the pc headgroup is not oriented parallel to the membrane surface. Because of the headgroup configuration[d] the positive layer would be closest to the water interface, so that any ion approaching the vesicle would first experience a positive electrical field. This, of course, repels cations and attracts anions. Consistent with this hypothesis is the complete lack of binding of $Ru(bpy)_3^{2+}$ and MV^{2+} that was also observed.

---

[d]The literature generally describes the pc headgroup orientation with the choline group ion-pairing with the phosphate group, i.e. the headgroup lying parallel to the vesicle surface. However, this orientation is expected to be sensitive to salt effects.

3.2 Photochemical Systems

The initial reports of photostimulated transmembrane electron transfer[7,8,11a] generated much interest in these systems because of their potential usefulness in solar energy conversion[4]. Because of the apparent discrepancy between theoretical predictions and experimental findings of photoinduced transmembrane redox reactions, one of the systems[11a] was reinvestigated[11b]. It was concluded that the viologen had leaked out of the vesicle, but the exact mechanism of the viologen diffusion was not fully understood at the time. Localized membrane heating arising from nonradiative deactivation of the photosensitizer was thought to be one possible explanation because the viologen diffusion showed a strong temperature dependence. This phenomenon could be general, so we investigated other systems for this effect. The focus of our study was on the contribution of diffusion of the electron acceptor (viologen) across the membrane in systems comprised of pc vesicles, entrapped viologens, and various sensitizers in the external medium. As mentioned above it is conceivable that photostimulated diffusion occurs by a local "melting" of the membrane. Nonradiative deactivation of the excited state of the photosensitizer can create "hot spots" in the vicinity of the chromophore leading to fluidization of the membrane. Although energy dissipation through the vibronic modes of the lipid is expected to occur rapidly the

transitory changes in the bilayer structure may be sufficient to allow transmembrane diffusion of components bound to either surface. This postulate requires that the redox mediators be bound to the membrane.

3.1.1 Reversible systems

The first system to be studied consisted of pc vesicles with entrapped $(C_7)_2V^{2+}$. Typical concentrations were 4 mM pc and 50-150 uM viologen in 0.1M phosphate buffer, pH 8.0. A photosensitizer was then added to the external phase at a concentration sufficient to give an absorbance of no less than unity in order to capture at least 90 % of the photons. Three different sensitizers, $ZnTPPS^{4-}$, $ZnTMPyP^{4+}$, and $Ru(bpy)_3^{2+}$, were employed. Equilibrium dialysis showed (vide infra) that the anionic sensitizer binds much more strongly to the surface of the vesicle than cationic ones. Thus $ZnTPPS^{4-}$ will be predominantly surface bound while $ZnTMPyP^{4+}$ was predominantly in bulk solution. Hence, comparison of their behavior provided an ideal test of the above postulate. Scheme A shows the typical topography of the photochemical systems. Both the Soret and Q-bands of the porphyrins and the visible charge-transfer band of the Ru-complex were illuminated using the filtered light from the high intensity source. The results of illuminating these systems using any of the sensitizers clearly showed that no photostimulated viologen diffusion occurs.

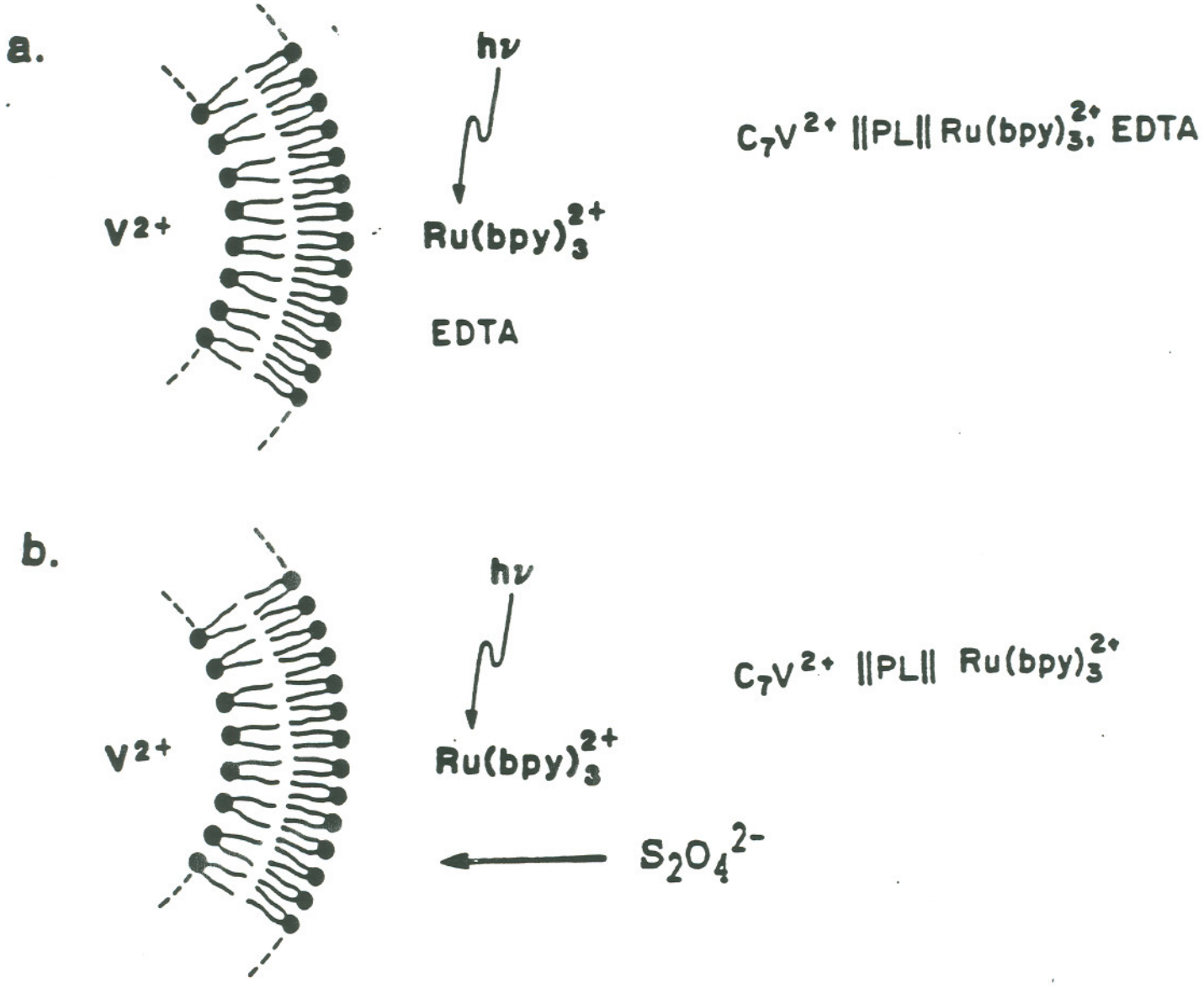

Scheme A: Topography of photochemical systems

a: Non-reversible system

b: Reversible system

Indications of photostimulated diffusion in early experiments were obtained, but were shown to be due to an experimental artifact, as discussed below. Since the viologen radical is readily reoxidized by air, all experiments were done anaerobically. This was accomplished by bubbling dry nitrogen or argon through the solution prior to adding dithionite. In the initial photochemical experiments N_2 was bubbled through the sample during the illumination. This not only deoxygenated the sample but also served as a convenient way of stirring it. Stirring is necessary to minimize concentration gradients that might arise over the course of time. A flow meter was placed in the nitrogen feeding line to measure the rate of N_2 flow through the cuvette. Variations in the flow rate from 20 ml/min to 500 ml/min produced increasing amounts of viologen leakage, proportional to the degree of bubbling (Table 4). This unexpected result indicated a physical disruption of the membrane. The possible cause for the disruption is that the bubbling increases the liquid-gas interface. Lipids are known to form monolayers at such interfaces[38], with their polar headgroups in the more polar liquid (e.g., water) and the hydrocarbon tails in the less polar gas (e.g., N_2). It can then be expected that individual lipid molecules will exchange between the bilayer that constitutes the vesicle wall and the solution-nitrogen bubble interface causing a temporary discontinuity in the membrane that can result in the release of entrapped solutes. Increasing the solution-gas interfacial area by increasing the number of bubbles should then cause an increase in

Table 4: Gas-flow dependence of viologen leakage

N_2 flow (ml/min)	$[(C_7)_2V^{2+}]_{escaped}$ ♯ (uM)
0	2
50	13
200	25

4 mM pc, 65 uM $(C_7)_2V^{2+}$, 22°C,

20 mM phosphate buffer, pH 7.8

5-10 fold excess dithionite

♯ after 15 min bubbling

released viologen, which is consistent with the observations. To avoid that artifact the sample was only degassed briefly (3-5 minutes) and then stirred by means of a magnetic stir bar. With this precaution none of the experiments below showed any photostimulated diffusion.

The system $(C_7)_2V^{2+}//pc//Ru(bpy)_3^{2+}$ was illuminated for various time intervals and then tested for diffused viologen by adding dithionite to the bulk aqueous phase. Dithionite is unable to penetrate the bilayer on the timescale of these experiments[20]. This was shown by entrapping a highly charged redox active ion that itself does not penetrate the membrane, such as $Fe(CN)_6^{3-}$, inside the vesicle and then adding $S_2O_4^{2-}$ to the outside. The reaction can be monitored by measuring the absorbance of ferricyanide at 420 nm, because the reduced form, $Fe(CN)_6^{4-}$, does not absorb in the visible region. When dithionite was added to vesicles that contained entrapped ferricyanide, no reduction was observed. An identical sample was kept in the dark for the same time interval and its viologen leakage was measured in the same manner. "Photostimulated" diffusion was then determined as the difference between the dark and the light experiments. It was found that the amount of dithionite-reducible viologen at a given time in the illuminated sample was equal to that of the sample kept in the dark. The dark diffusion rate was estimated to be 2×10^{-9} M s^{-1} from the initial rate of leakage of

$(C_7)_2V^{2+}$,[a] at 22° C (Table 5).

Comparable results were obtained with $ZnTPPS^{4-}$ and $ZnTMPyP^{4+}$ (Table 6). Thus, binding of the chromophore seems to be irrelevant for diffusion. The effect of sensitizer binding was further probed by comparing $Ru(bpy)_3^{2+}$ with its derivatized version, $Ru(bpy)_2L^{2+}$, where L is a bipyridine that had been modified by attaching two long hexadecyl carbon chains to the aromatic ring. These alkyl tails now bind the sensitizer to the vesicle membrane. The rate of $(C_7)_2V^{2+}$ leakage upon illumination of a system containing this sensitizer was identical to that for the underivatized $Ru(bpy)_3^{2+}$ and equal to the dark diffusion (Table 6). This confirms that sensitizer binding has little or no effect on transmembrane viologen diffusion. When the light intensity was reduced to 50% and even 10% by placing neutral density filters in front of the sample, no change in the amount of diffusing viologen was observed. Furthermore, the amount of viologen leakage was the same when vesicles were illuminated without added sensitizer (Table 6). This independence of viologen leakage on the chromophore was further confirmed by the use of other dyes, such as bromothymol blue, Eriochrome Black T, and Neutral Red, and by illumination at different, discrete wavelengths corresponding to absorption maxima and minima. In all cases the viologen diffusion

---

[a]Leakage continues until an equilibrium is established, but upon aging other factors such as vesicle fusion contribute to the amount of escaped viologen and thus increase the observed rate of leakage.

Table 5: Dark diffusion of $(C_7)_2V^{2+}$

time (min)	$[(C_7)_2V^{2+}]_{reducible}$ (uM)
30	4
60	9
90	14
120	18

4 mM pc, 22° C, 65 uM $(C_7)_2V^{2+}$

20 mM phosphate buffer, pH 7.5

dithionite in 5-7 fold excess

Table 6: Viologen Leakage in Photochemical Systems

system	$[(C_7)_2V^{2+}]$ (uM)
$(C_7)_2V^{2+}$//pl//$ZnTPPS^{4-}$	10
$(C_7)_2V^{2+}$//pl//$ZnTMPyP^{4+}$	12
$(C_7)_2V^{2+}$//pl//Neutral Red	9
$(C_7)_2V^{2+}$//pl//Bromothymol Blue	10
$(C_7)_2V^{2+}$//pl//Eriochromeblack T	11
$(C_7)_2V^{2+}$//pl//$Ru(bpy)_3^{2+}$	11
$(C_7)_2V^{2+}$//pl//$Ru(bpy)_2L^{2+}$	12
$(C_7)_2V^{2+}$//pl//	9

4 mM pc, 22 C, 70 uM $(C_7)_2V^{2+}$

20 mM phosphate bufffer, pH 7.5

dithionite in 5-7 fold excess

after 60 minutes illumination

was very similar to the dark diffusion (Table 6).

Additional experiments were done where the system was symmetric with respect to the sensitizer, i.e. the chromophore was on either side of the membrane. Again, no increase in escaped $(C_7)_2V^{2+}$ was found. Thus, in all systems described, diffusion of viologen due to photostimulation did not occur.

Temperature is potentially a very important factor. Lipid bilayer membranes have phase transitions at very characteristic temperatures Tc[37]. The membrane fluidity above and below this temperature is considerably different. Below Tc, the bilayer is in its solid crystalline state, implying a high degree of order of the alkyl chains. Thus, the hydrocarbon portion of the membrane is quite rigid and the permeability to other molecules is very low. Above Tc, the bilayer is in its liquid crystalline state with increased motion of the alkyl tails, which allows for easier penetration of other species into the bilayer. The fluidity of the bilayer and thus its permeability increases with increasing temperature. Therefore any diffusional process across the membrane should exhibit a pronounced temperature dependence.

Although all illuminations were done in a constant temperature bath whose temperature was easily controlled and monitored, it is conceivable that the temperature inside the irradiated optical cell

increased due to the light absorption of the photosensitizer. Upon physical deactivation of the excited state the absorbed photonic energy is converted into excitation of translational and vibrational modes, constituting an increase in solution temperature. In control experiments the actual temperature inside the cell was therefore monitored with a copper/constantan thermocouple. All vesicle systems were checked in this way, and the position of the thermocouple within the cell and relative to the light beam was varied to determine possible temperature gradients[b] within the cell. The temperature for all control runs did not increase by more than 0.5^0 during a one hour illumination. Therefore thermal effects due to bulk heating of the dye-containing solution are insignificant in these systems.

3.1.2 Non-reversible systems

The most thoroughly studied system was $(C_7)_2V^{2+}//pc//Ru(bpy)_3^{2+}$,EDTA[c]. When this system was irradiated the blue viologen radical appeared. To quantitate the amount of radical formed the cuvette was periodically removed from the light beam, the

---

[b]Such a temperature gradient may be expected because the majority of photons will be absorbed at the front face of the cuvette.

[c]The notation $(C_7)_2V^{2+}//pc//Ru(bpy)_3^{2+}$, EDTA is representative of a system containing $(C_7)_2V^{2+}$ entrapped inside a pc vesicle and $Ru(bpy)_3^{2+}$ and EDTA added to the external phase. The vertical bars represent the bilayer.

optical spectrum was recorded, and the cell was placed back in the photolysis apparatus. Because the diode array spectrometer can measure a complete spectrum in less than one second the sample had to be removed from the light beam and nitrogen line for only a very short period of time, thus minimizing artifacts such as air contamination of the sample. From the optical spectrum the concentration of viologen radical was determined by measuring its absorbance at 604 nm. A plot of the radical concentration versus time showed a short induction period followed by a rapid linear rise until all viologen was reduced (Figure 6). The concentration of entrapped $(C_7)_2V^{2+}$ was determined by measuring its absorbance at 260 nm or, in experiments where interference from light scattering by the vesicles was too high, SDS was added to solubilize the vesicles and release their content. The amount of viologen was then determined by adding dithionite and measuring the absorbance of the radical cation.

The overall reaction showed a pronounced temperature dependence (Figure 7), increasing at higher temperatures. The shape of these curves implies a complex mechanism that could not be fitted to a simple rate law. From the nearly linear, steep portion of those curves a maximal rate of reduction was estimated. Although this rate is not strictly representative of the entire reaction it does constitute a significant portion of the reaction. If this maximum rate fits the Arrhenius form it is possible that a single step is rate-limiting. The Arrhenius equation ,

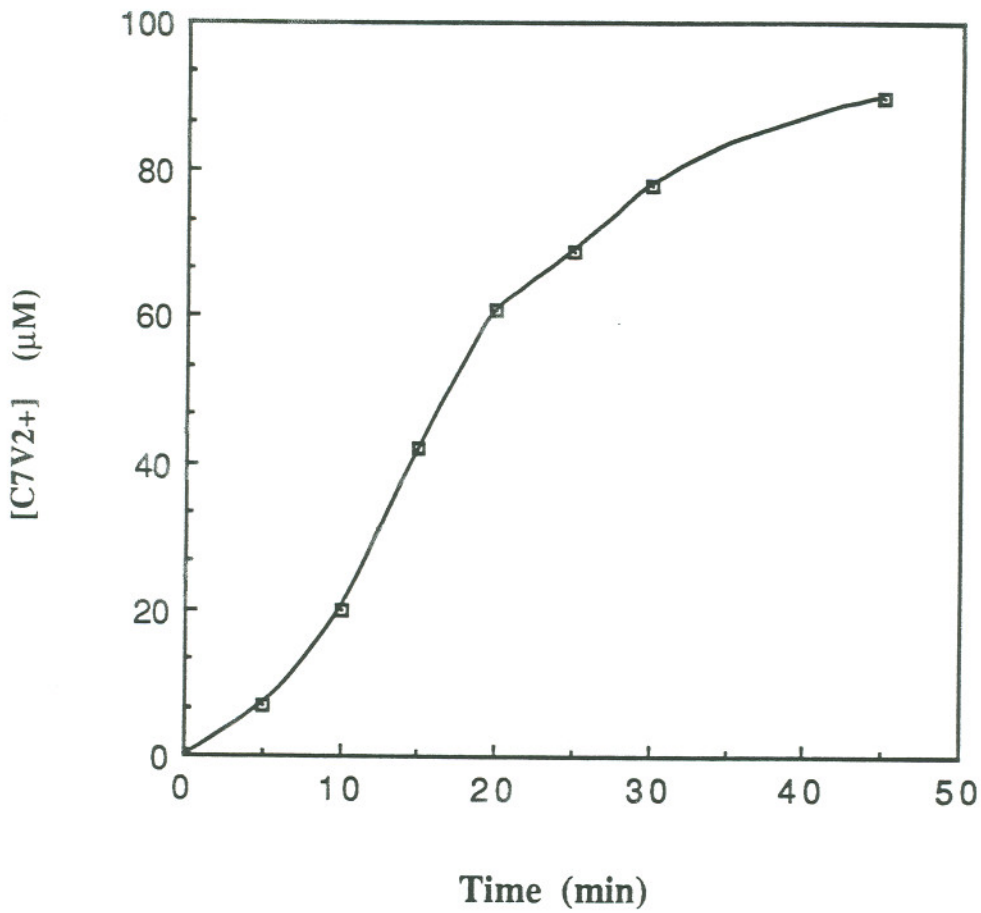

Figure 6: Photochemical reduction of $(C_7)_2V^{2+}$

4 mM pc, 22° C, 95 uM $(C_7)_2V^{2+}$

85 uM $Ru(bpy)_3^{2+}$, 1 mM EDTA

0.1 M phosphate buffer, pH 8.0,

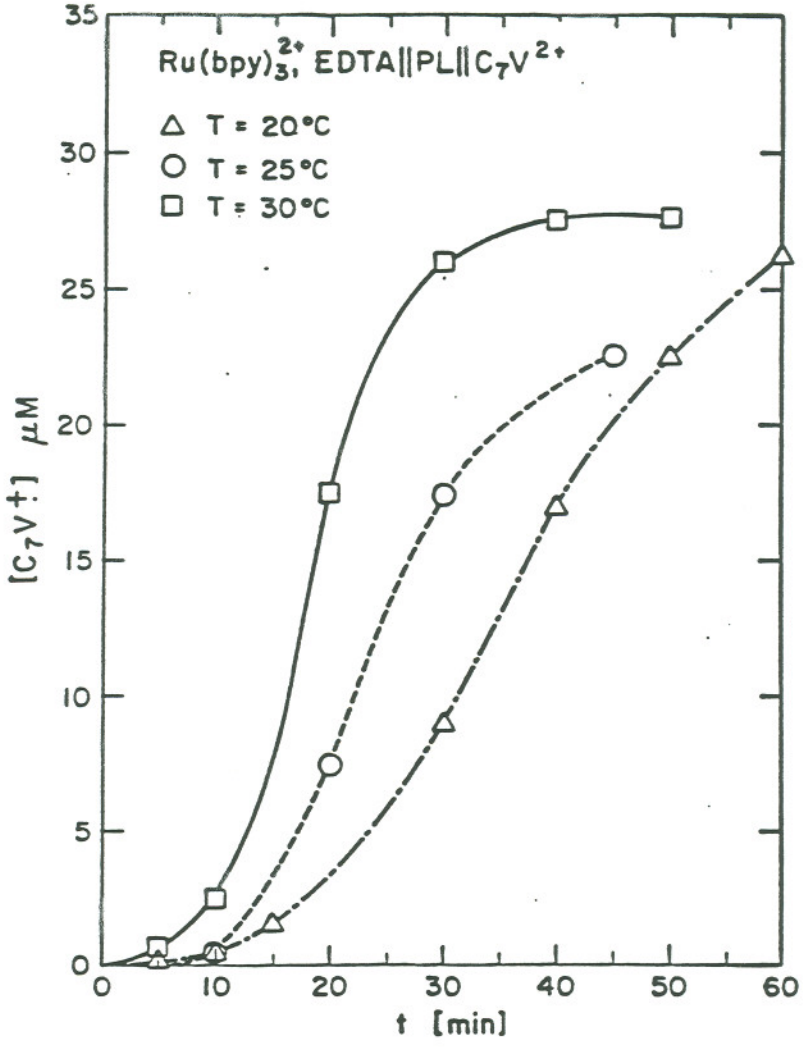

Figure 7: Temperature dependence of the photochemical reduction of $(C_7)_2V^{2+}$

4 mM pc, 28 uM $(C_7)_2V^{2+}$, 85 uM $Ru(bpy)_3^{2+}$,

1 mM EDTA, 0.1 M phosphate buffer, pH 8.0

$$\ln(k/T) = \ln(k/h) + \Delta S^{\ddagger}/R - \Delta H^{\ddagger}/RT$$

predicts that a plot of ln(k/T) versus 1/T should be linear, with a slope of $-\Delta H^{\ddagger}/T$ and a y-intercept equal to $\ln(k/h)+\Delta S^{\ddagger}/R$. The plot (Figure 8) indeed yields a straight line from which an activation enthalpy $\Delta H^{\ddagger}$ of 20 $\pm$ 4 kcal/mol and an entropy $\Delta S^{\ddagger}$ of -32 $\pm$ 8 e.u. was calculated.

The membrane bound derivative of $Ru(bpy)_3^{2+}$ gave essentially the same results (Table 7), again confirming the notion that sensitizer binding is not essential to transmembrane viologen reduction.

Qualitatively, $ZnTPPS^{4-}$ and $ZnTMPyP^{4+}$ gave the same results but, because "bleaching" of the porphyrins was extensive, it was impossible to obtain good quantitative data. The substantial decrease in the intensity of the absorption bands significantly lowered the amount of absorbed light and is presumably due to formation of dihydro- and tetrahydroporphyrin derivatives.

As expected, the system symmetric with respect to the sensitizer, $(C_7)_2V^{2+}$, $Ru(bpy)_3^{2+}//pc//Ru(bpy)_3^{2+}$, EDTA, gave the same results, i.e. formation of the viologen radical cation at the same rate. The quantum yield for reduction was calculated as the ratio of radical produced to photons absorbed by the chromophore over

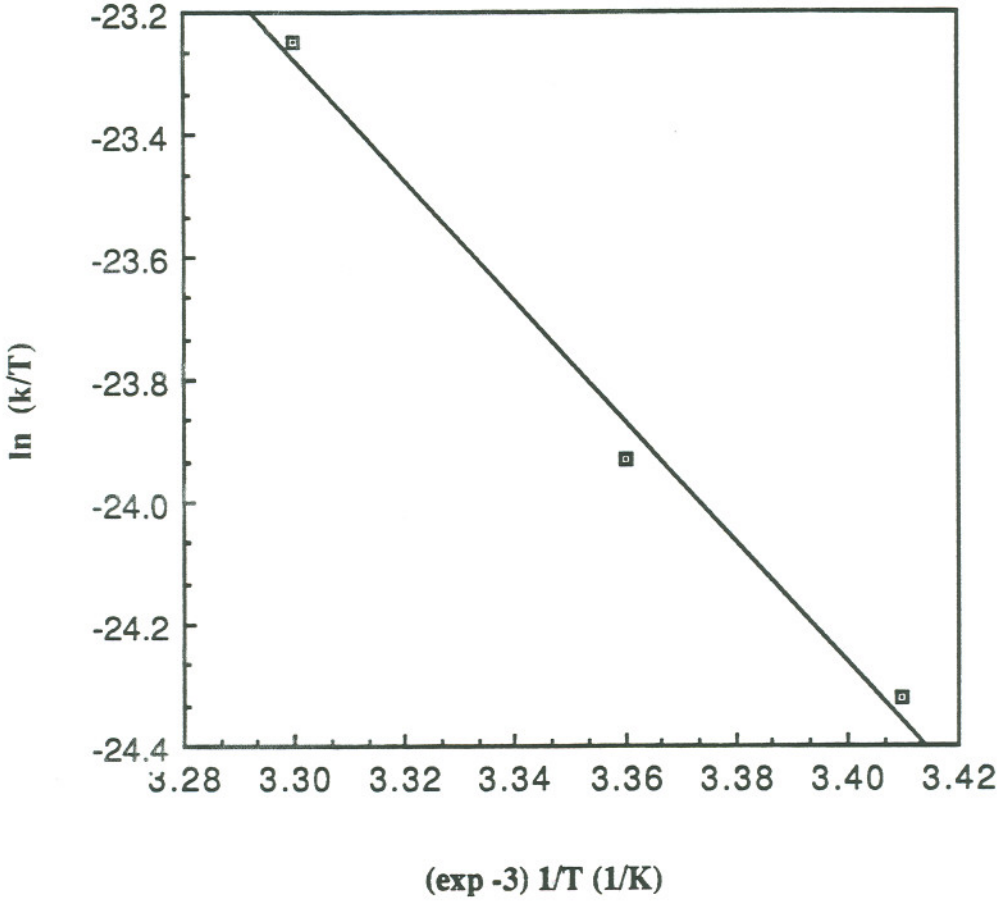

Figure 8: Arrhenius plot of the photochemical reduction of $(C_7)_2V^{2+}$

same conditions as in Figure 6

Table 7: Maximal rates of viologen reduction by $Ru(bpy)_3^{2+}$ complexes

Ru-complex	rate ($x10^{-8}$ M s^{-1})
$Ru(bpy)_3^{2+}$	1.17
$Ru(bpy)_2L^{2+}$	1.33

4 mM pc, 30 uM $(C_7)_2V^{2+}$, 22° C,

75 uM Ru-complex, 1 mM EDTA

0.1 M phosphate buffer, pH 8.0

entire duration of the photolysis. For $Ru(bpy)_3^{2+}$, this quantum yield is shown Table 8.

Experiments designed to probe for possible photodamage to the vesicle walls showed that the amount of reducible viologen after 30 minutes of light exposure did not increase after 30 minutes in the dark. This establishes that the vesicles did not become leaky upon illumination. The sample that was kept in the light continued to produce viologen radical, but reduction could be stopped at any time by simply removing it from the light beam (Figure 9). Therefore, it can be concluded that no photodamage to the bilayer had occurred.

To determine the location of $(C_7)_2V^{2+}$ at the end of the experiment the sample was oxygenated[d], degassed again, and dithionite was added. It was found that no viologen was immediately reducible. This implies that all viologen is still within the vesicle. This finding appears to contradict the idea of viologen diffusion as the mechanism for transmembrane redox. Although the above results are consistent with those reported by Calvin[5] and Fendler[11a], the mechanisms proposed therein are unavailable to our system because binding of the sensitizer is essential for transmembrane electron exchange. The lack of binding of $Ru(bpy)_3^{2+}$ to the pc membrane

---

[d] O_2 is freely membrane permeable. Thus the oxidation of viologen radical by oxygen is not electrogenic and is not expected to disturb the relative distribution of viologen inside and outside.

Table 8: Quantum yields for $(C_7)_2V^{2+}$ reduction by $Ru(bpy)_3^{2+}$

temperature (^{0} C)	Quantum yield ($x10^{-5}$)
20	1.8
25	2.8
30	5.8

30 uM $(C_7)_2V^{2+}$, 80 uM $Ru(bpy)_3^{2+}$, 1 mM EDTA
4 mM pc, 0.1 M phosphate buffer, pH 8.0

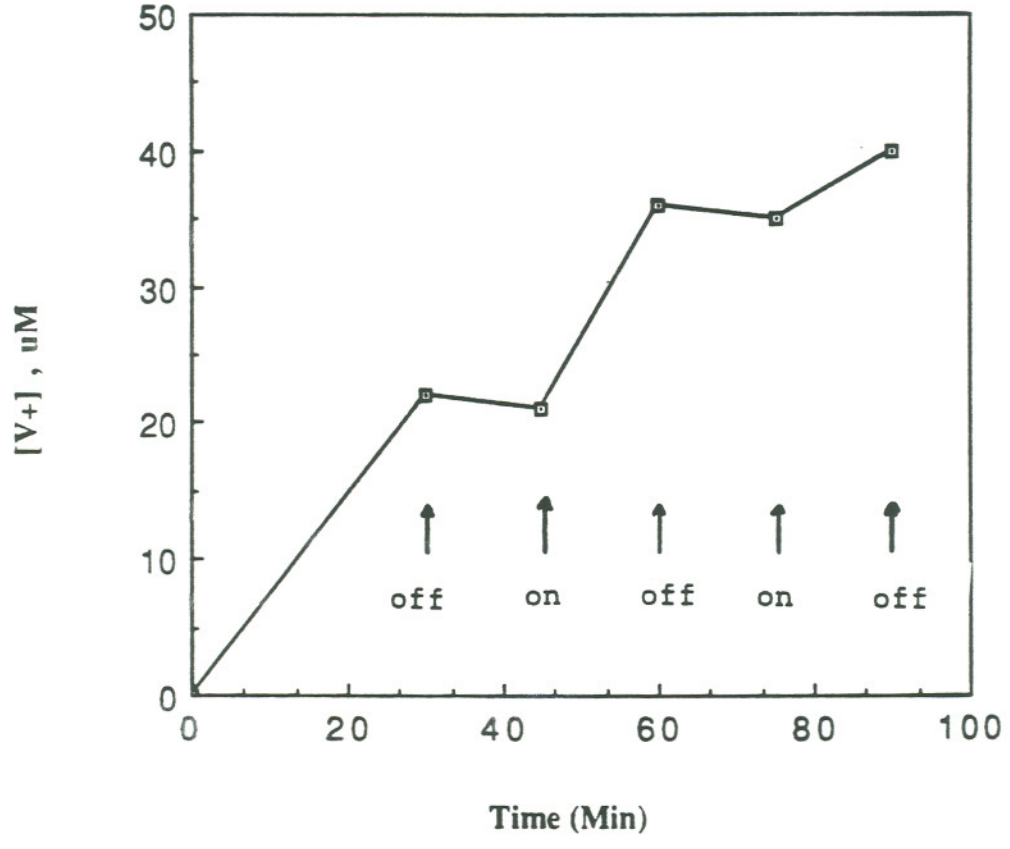

Figure 9: Test for membrane damage in photochemical systems

4 mM pc, 22° C, 40 uM $(C_7)_2V^{2+}$, 85 uM $Ru(bpy)_3^{2+}$, 1 mM EDTA

0.1 M phosphate buffer, pH 8.0

light was turned on and off where indicated

surface makes the distance between electron donor and acceptor far too great for any kind of transmembrane electron exchange, such as tunneling. Yet the viologens remained inside the vesicle, ruling against simple viologen leakage as a mean of transmembrane reduction.

How then did the electron cross the bilayer? This apparent paradox was finally resolved with the discovery of other transmembrane reduction systems involving chemical reductants where transitory or net translocation of viologen could be demonstrated unambiguously.

3.3 Dithionite Kinetics:

During the course of the photochemical experiments it was discovered that adding sodium dithionite to solutions containing vesicles with entrapped $(C_7)_2V^{2+}$ caused slow reduction of the viologen, similar to the photochemical reduction observed earlier. As shown in those studies, dithionite itself is not able to migrate across the membrane on the time scale of the observed transmembrane electron transfer. It was again suspected that the viologen may be leaking out of the vesicle.

Because of the zwitterionic nature of the pc headgroup the vesicle surface bears no net charge. Evidence from other experiments (see Equilibrium Dialysis) suggests though that the vesicles have an outer layer of positive charge. For example, $ZnTPPS^{4-}$ binds considerably while $ZnTMPyP^{4+}$ shows no binding (Section 3.1). It is conceivable that interactions of ions in solution with the "choline cation" of the pc headgroup may alter the bilayer packing. This change in structure may be accompanied by a change in membrane permeability. Hence the possibility exists that ionic interactions between dithionite ($S_2O_4^{2-}$) and the choline group may increase the permeability of the bilayer to viologen and thus lead to increased leakage. If this is the case, then other ions of similar structure and charge should have similar effects.

To test this hypothesis a series of ions similar to $S_2O_4^{2-}$ were added to vesicles containing $(C_7)_2V^{2+}$ in 0.1 M phosphate buffer, pH 8.0, and then incubated at room temperature for the same time period that was sufficient to allow complete reduction in the presence of dithionite. After that incubation dithionite was added to test for escaped viologen. The anions studied were $S_2O_5^{2-}$, SO_4^{2-}, and $C_2O_4^{2-}$ at a concentration of 1 mM, which is a typical dithionite concentration. None of these ions induced any noticeable $(C_7)_2V^{2+}$ leakage. This result suggests that any changes that might have occurred in the pc headgroup conformation did not alter the membrane permeability.

A detailed kinetic study of the transmembrane $(C_7)_2V^{2+}$ reduction by dithionite revealed that the formation of the viologen radical was a zero or pseudo-zero order process (Figure 10). This indicated that a step other than the transmembrane electron transfer was rate limiting because electron transfer reactions would exhibit first or second order kinetics[48].

The zero order rate was independent of the dithionite concentration and was unaffected by dithionite concentrations from a two-fold to a twenty-fold stoichiometric excess of electrons (Table 9). This confirms the observation that dithionite was not membrane permeable. It also argues against pore formation within the membrane, because pores would allow non-specific diffusion of all

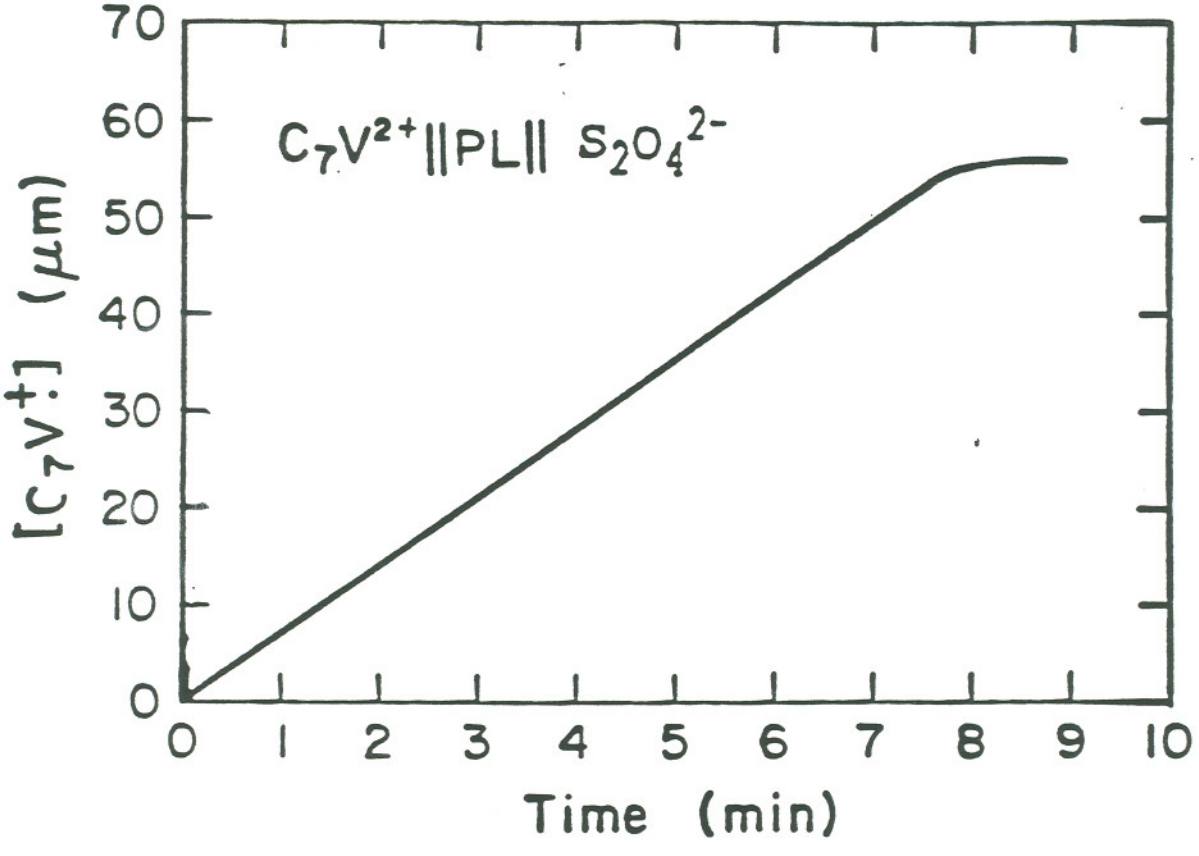

Figure 10: Transmembrane reduction of $(C_7)_2V^{2+}$ by dithionite

4 mM pc, 22° C, 60 uM $(C_7)_2V^{2+}$

0.1 M phosphate buffer, pH 8.0

330 uM dithionite

Table 9: Dithionite dependence of $(C_7)_2V^{2+}$ reduction rate

$[S_2O_4^{2-}]$ (uM)	rate ($x10^{-7}$ M s^{-1})
91	2.2
215	2.1
290	2.2
430	2.1
500	2.3
640	2.0
980	1.9

98 uM $(C_7)_2V^{2+}$, 4 mM pc, 22° C,

.1 M phosphate buffer, pH 8.0

species in solution. Dithionite could migrate into the vesicle to reduce the viologen, but this process is expected to show a rate dependence on the dithionite concentration according to Fick's law of diffusion.

The overall redox process is similar to the non-reversible photochemical system. Thus the possibility exists that the redox mechanisms are similar. Yet the molecular compositions for those systems are quite different, indicating that the nature of the reductant is not important. This was further confirmed by using Cr^{2+} as the external reductant. The light blue chromous ion was added in 5-7 fold excess via gas-tight syringe to a degassed optical cell containing vesicles (4 mM pc) with entrapped $(C_7)_2V^{2+}$ (60 uM) in 0.1 M phosphate buffer, pH 8.0. The observed rate of viologen reduction remained zero order. Furthermore rates for reduction by dithionite and Cr^{2+} were practically identical for the same preparation of vesicles (Table 10). This result demonstrates clearly that the identity of the reductant is irrelevant to the transmembrane redox step.

As discussed below a number of parameters that might be expected to influence the transmembrane viologen reduction process were investigated.

It was found that the rate was proportional to the

Table 10: Comparison of $(C_7)_2V^{2+}$ reduction rates by chromous and dithionite ions

reductant	rate ($x10^{-7}$ M s^{-1})
$S_2O_4^{2-}$	1.6
Cr^{2+}	1.4

102 uM $(C_7)_2V^{2+}$, 4 mM pc, 22° C

phosphate buffer, pH 8.0

reductant in 5-7 fold excess

concentration of entrapped viologen over the range 15-200 uM (Figure 11). This proportionality seems in conflict with the zero order nature of the reaction. However, the consideration of other factors discussed below (see 3.4 Electrochemical Principles) will show that this can be understood in terms of a simple model.

It is known that the alkyl chain length of the viologen has a significant effect on transmembrane redox in other systems[48]. Typically the rate of transmembrane redox was inversely proportional to the chain length. The majority of the research described in this dissertation was done with the commercially available diheptyl viologen dibromide. To test the influence of the alkyl chain length a series of dialkyl viologens were synthesized (see Experimental Section), including dihexyl-, dioctyl-, didecyl-, and dioctadecylviologen. Other viologens that were investigated were the commercially available dibenzyl- and the asymmetric hexadecylmethylviologen[a]. All of these viologens (except dioctadecyl viologen) could be entrapped inside a vesicle and removed from the outside by ion-exchange chromatography. The results from the dithionite reduction are presented in Table 11. The rate remained zero order and essentially independent of the alkyl chain length. The different measured rates listed in Table 11 were a consequence of differing concentrations of the various viologens entrapped within

---

[a]This and other alkylmethyl viologens were synthesized and kindly provided by Dr. David H. Thompson.

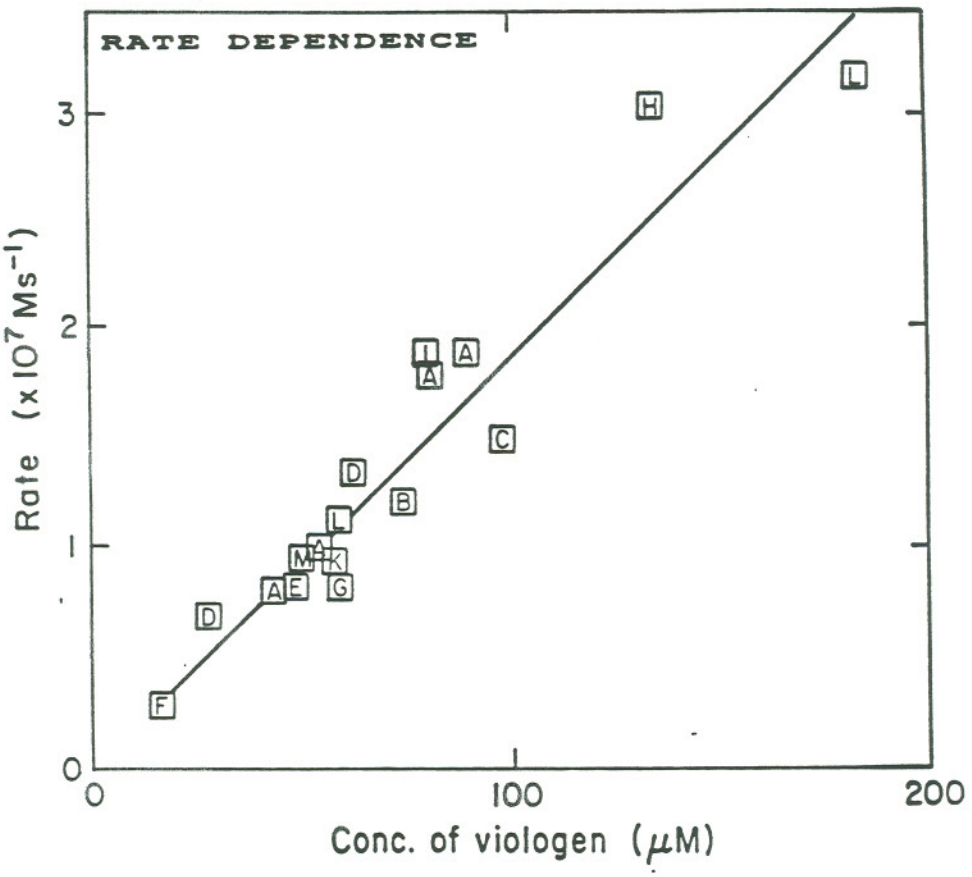

Figure 11: Reduction rate dependence om concentration of entrapped viologen

Figure 6: Dependence of transmembrane reduction rate on concentration of viologen

4 mM pc, 22° C, 5-7 fold excess dithionite

A: $(C_7)_2VBr_2$, 100 mM phosphate buffer, pH 8.0

B: $(C_7)_2VBr_2$, 100 mM phosphate buffer, pH 6.0

C: $(C_7)_2VBr_2$, 20 mM phosphate buffer, pH 8.0

D: $(C_7)_2VCl_2$, 100 mM phosphate buffer, pH 8.0

E: $(C_7)_2V(NO_3)_2$ ditto

F: $(B)_2VCl_2$ ditto

G: $(C_6)_2VBr_2$ ditto

H: $(C_8)_2VBr_2$ ditto

I: $(C_{10})_2VBr_2$ ditto

K: $(C_7)_2VBr_2$, 100 nm diameter vesicles

L: $(C_7)_2VBr_2$, 80 nm diameter vesicles

M: $(C_7)_2VBr_2$, 50 nm diameter vesicles

Table 11: Alkyl chain dependence of the viologen reduction rate

n	$[(C_n)_2V^{2+}]$ (uM)	rate ($x10^{-7}$ M s^{-1})	normalized rate*
6	62	0.9	0.9
7	60	1.1	1.1
8	150	3.3	1.4
10	117	2.4	1.3
benzyl	12	0.3	1.6

4 mM pc, 22° C, 0.1 M phosphate buffer, pH 8.0

dithionite in 5-7 fold excess

* rate was normalized by dividing the measured rate by the ratio of the viologen concentrations

the vesicle, which became apparent when normalized to the results for $(C_7)_2V^{2+}$ (Figure 11). Variations in entrapment correlated with differing binding affinities of the viologens (see section 3.5). As expected the longer alkyl chains bound more strongly than the shorter ones, allowing for higher entrapment.

There is an inherent asymmetry in the two monolayers that comprise the membrane bilayer. This is largely due to the different radii of curvature of the inner versus the outer surface, which results in a different packing of the lipid headgroups. The concave nature of the inner vesicle surface forces a very tight packing of the headgroups, while the convex outer surface allows for more surface area per headgroup. Any molecule or ion trying to penetrate the membrane will experience the influence of the headgroup density. This asymmetry is greatest for very small vesicles, and becomes less with increasing vesicle size. Thus, if this asymmetry is in any way limiting ion diffusion across the bilayer a change in vesicle size and hence a change in the degree of asymmetry should result in a different rate of transmembrane reduction.

The recently developed Extruder[31] allows for the rapid and easy formation of vesicles of different sizes. The size of the vesicles is controlled by the pore size of the filter through which the lipid suspensions are extruded. The available filters allow the formation

of vesicles with diameters of 30, 50, 80, 100, and 200 nm[b]. The experiments described above were done with vesicles of 30 nm diameter, produced either by sonication or extrusion. Formation of larger vesicles followed by kinetic measurements of transmembrane reduction showed that for vesicles with 30, 50, 80, and 100 nm diameter the rate of viologen reduction remained unchanged, i.e. zero order and only dependent on the amount of entrapped viologen (Table 12). Thus headgroup packing constraints had no impact on the rate of transmembrane viologen reduction.

The issue of membrane permeability of viologens has been controversial for some time[20,42]. One reason is the fact that viologen is a dication, and most ions have low permeabilities through hydrocarbons. Viologen salts have characteristic intense colors, that are dependent upon the counterion. The chloride salt is white, the bromide bright yellow and the iodide is dark orange. These colors are due to charge transfer bands between the halide and the bipyridine core. The fluorescence of viologen halides has been observed in solution and is attributed to tight ion pairing between the viologen and the halide counterion[51]. If this interpretation is correct then it is conceivable that it is the neutral viologen-halide ion pair that diffuses across the membrane. To test this hypothesis the counter ion of the diheptyl viologen was varied. The degree of

---

[b]For comparison, sonicated vesicles are small and unilamellar with a narrow size distribution around a diameter of 30 $\pm$ 5 nm[30].

Table 12: Vesicle size dependence of $(C_7)_2V^{2+}$ reduction rate

vesicle diameter (nm)	rate ($x10^{-7}$ M s^{-1})
30	2.8
50	2.8
80	2.8
100	2.4

95 uM $(C_7)_2V^{2+}$, 4 mM pc, 22° C,
0.1 M phosphate buffer, pH 8.0
dithionite in 5-7 fold excess

ion-pairing is likely to vary with these counterions. Repeating the kinetic experiments with these viologen salts showed no effect of the counter-ion (Table 13). The reaction remained zero order and proportional to the concentration of entrapped viologen. Thus ion pairing, if present at all, does not affect the kinetics of transmembrane redox.

These kinetic experiments clearly established that the viologen reduction rate is independent of any factors relating to the nature of the viologen, the size of the vesicles, and the concentration or identity of the reductant. However, solution parameters such as ionic strength and pH could influence the kinetics. All the above studies were performed in 0.1 M Na^+ phosphate buffer, pH 8.0. Thus the experiments were repeated in 0.1 M Na^+ phosphate buffer, pH 6.0, and then in 0.02 M Na^+ phosphate buffer at pH 8.0. But neither change in pH nor change in ionic strength caused a measurable change in the rate of reduction (Table 14). The kinetics remained zero order and only dependent on the concentration of entrapped viologen (Figure 11).

An additional variable that was examined was temperature. It can be expected that the system would show a strong temperature dependence, as was observed in the photochemical systems. The reduction kinetics were measured at various temperatures between 5^0 and 45^0 C. The rate remained zero order at all temperatures, but

Table 13: Counterion dependence of the $(C_7)_2V^{2+}$ reduction rate

counterion	$[(C_7)_2V^{2+}]$ (uM)	rate ($x10^{-7}$ M s^{-1})	normalized rate
Br^-	88	2.0	2.0
Cl^-	25	0.77	2.7
Cl^-	66	1.5	2.0
NO_3^-	49	0.91	1.6

4 mM pc, 22° C, 0.1 M phosphate buffer, pH 8.0, dithionite in 5-7 fold excess

Table 14: Ionic strength and pH dependence of the $(C_7)_2V^{2+}$ reduction rate

[phosphate buffer](mM)	pH	$[(C_7)_2V^{2+}]$(uM)	rate ($x10^{-7}$ M s^{-1})
100	8.0	56	1.1
20	8.0	102	1.6
100	6.0	80	1.3
20	6.0	43	0.89

4 mM pc, 22^0 C, dithionite in 5-7 fold excess

increased with increasing temperature (Figure 12). From the Arrhenius plot (Figure 13) of these rates an apparent activation enthalpy delta $H^{\ddagger}$ = 20 $\pm$ 7 kcal/mol and a delta $S^{\ddagger}$ = 32 $\pm$ 9 e.u. were calculated. These numbers are almost identical to those obtained in the photochemical system. However, direct comparison of these numbers is not strictly valid because for the dithionite Arrhenius plot the zero order rate constants were used while for the photochemical system the maximal rate was used. Nevertheless, the comparable strong temperature dependence of the photochemical and chemical redox systems suggest a possible common origin.

Figure 12 shows that viologen reduction almost ceases at lower temperatures. This is expected because the bilayer viscosity increases with decreasing temperatures until the bilayer is in its solid crystalline state below the phase transition temperature Tc. For natural pc this transition is broad and ranges from -10 to 0 ^{0} C. The reason for this broadness is that natural pc is a mixture of various lipids that differ slightly in their alkyl tails. Below Tc the bilayer is more ordered and rigid and thus less permeable to impurities. To test for the effects of phase transition synthetic lipids with the same headgroup as pc but well defined tails and narrow phase transitions, e.g. DMPC and DPPC, can be used. The phase transition temperatures are 19.7^{0} C for DMPC and 37.8^{0} C for DPPC[37]. This conveniently allows for experimentation above and below Tc for both lipids. The results from the temperature controlled

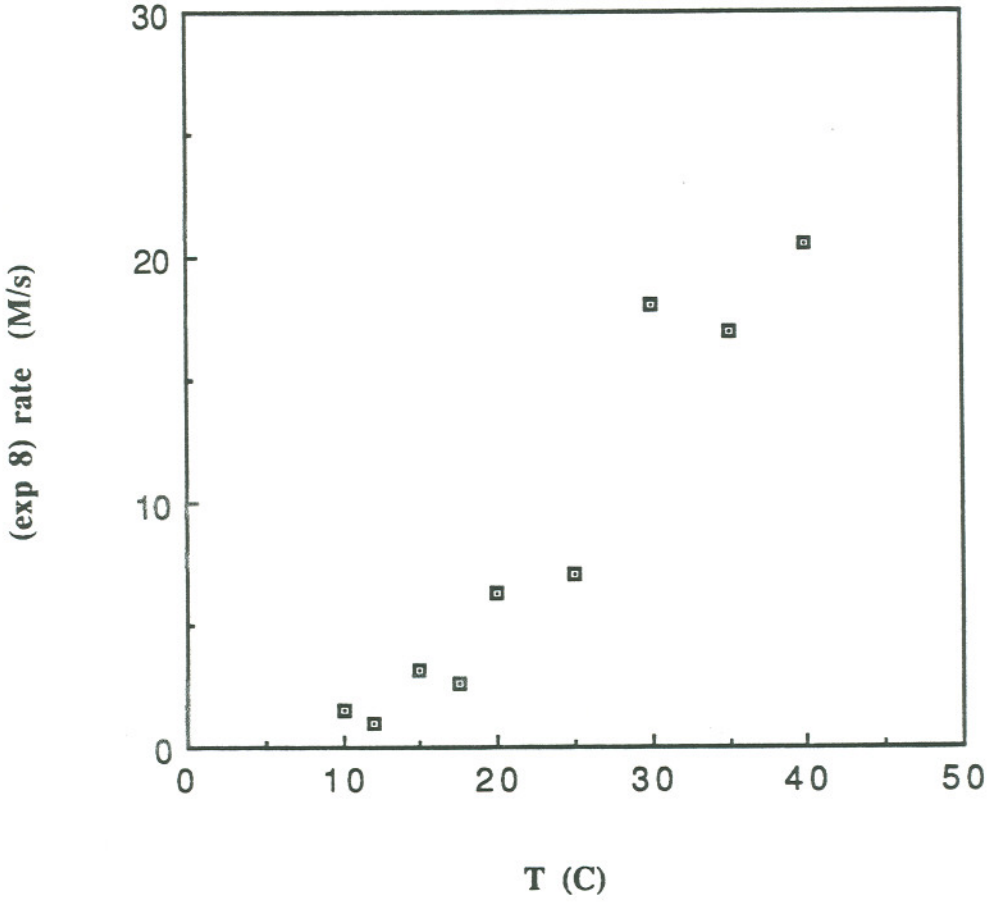

Figure 12: Temperature dependence of the transmembrane reduction of $(C_7)_2V^{2+}$ by dithionite
4 mM pc, 45 uM $(C_7)_2V^{2+}$, 280 uM dithionite
0.1 M phosphate buffer, pH 8.0

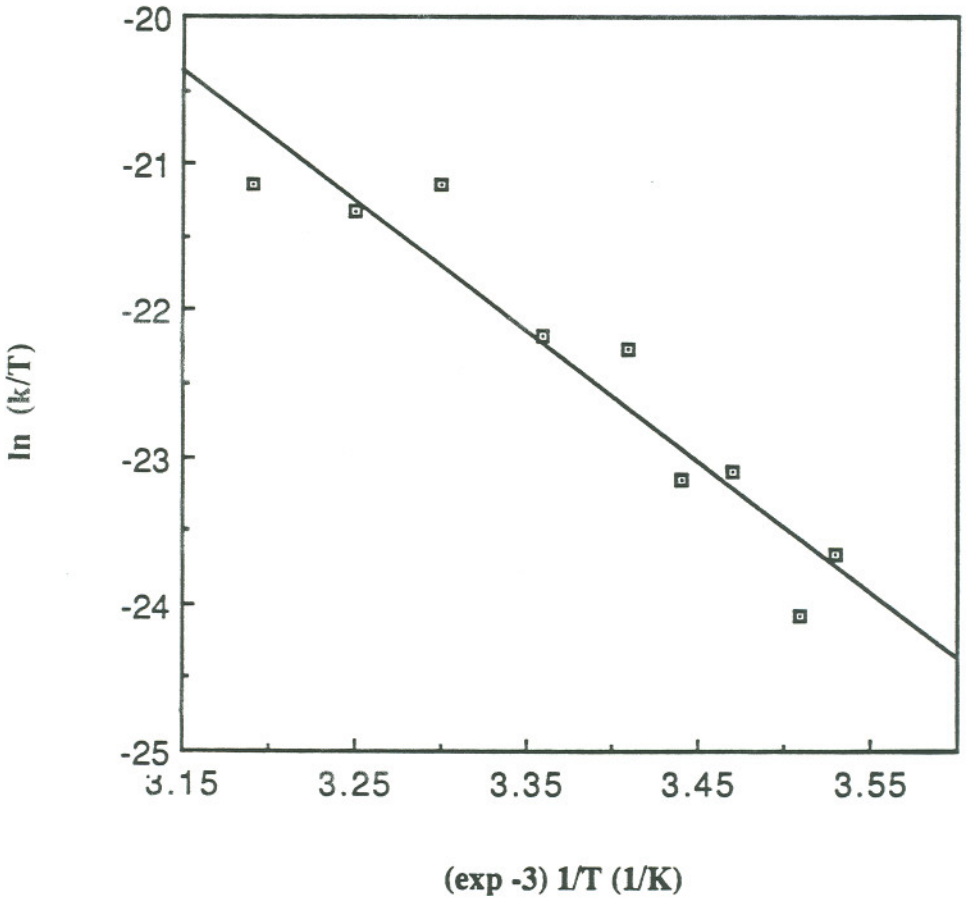

Figure 13: Arrhenius plot of the transmembrane reduction of $(C_7)_2V^{2+}$ by dithionite
same conditions as in Figure 12

reduction kinetics are shown in Tables 15 and 16. The DMPC system shows the expected temperature dependence with rates increasing at higher temperatures (also, at temperatures above 40^0 the viologen is converted predominantly, i.e. > 80 %, to its fully reduced form, V^0; vide infra). The Arrhenius plot (Figure 14) yields a straight line from which an activation energy E_a of 21.9 kcal/mol can be calculated. For DPPC there is a discontinuity in the Arrhenius plot (Figure 15). At lower temperatures the calculated activation energy is 31.8 kcal/mol, while at higher temperatures E_a is only 16.3 kcal/mol. The break point of the plot coincides very closely with the phase transition temperature of DPPC. This observation supports the idea that reactivity in this vesicle system is a function of membrane hydrocarbon fluidity. The difference of the activation energies above and below Tc is due to the additional energy requirements below Tc to overcome the lower membrane fluidity.

Some complications arose from the observation that at higher temperatures the $(C_7)_2V^+$ converted to $(C_7)_2V^0$, the doubly reduced, neutral form of viologen. When $(C_7)_2V^{2+}$ bound to the external surface of DMPC vesicles was reduced at room temperature to the radical cation and the temperature was then raised by 15-20^0 the radical was further reduced to the yellowish viologen zero, whose optical spectrum is quite different from that of both the dication and the radical (Figure 16). Upon cooling the V^0 converted back to the radical. This heat conversion cycle could be repeated several times

Table 15: Temperature dependence of $(C_7)_2V^{2+}$ reduction in DMPC vesicles

T (^{0} C)	rate ($x10^{-8}$ M s^{-1})
10	1.7
15	3.3
20	7.1
30	24

4 mM PMPC, 25 uM $(C_7)_2V^{2+}$

0.1 M phosphate buffer, pH 8.0

dithionite in 5-7 fold excess

Table 16: Temperature dependence of $(C_7)_2V^{2+}$ reduction in DPPC vesicles

T (^{0} C)	rate ($x10^{-7}$ M s^{-1})
20	0.17
25	0.32
35	2.1
40	4.3
45	5.8
50	8.4
55	12
60	20

4 mM DPPC, 92 uM $(C_7)_2V^{2+}$

0.1 M phosphate buffer, pH 8.0

dithionite in 5-7 fold excess

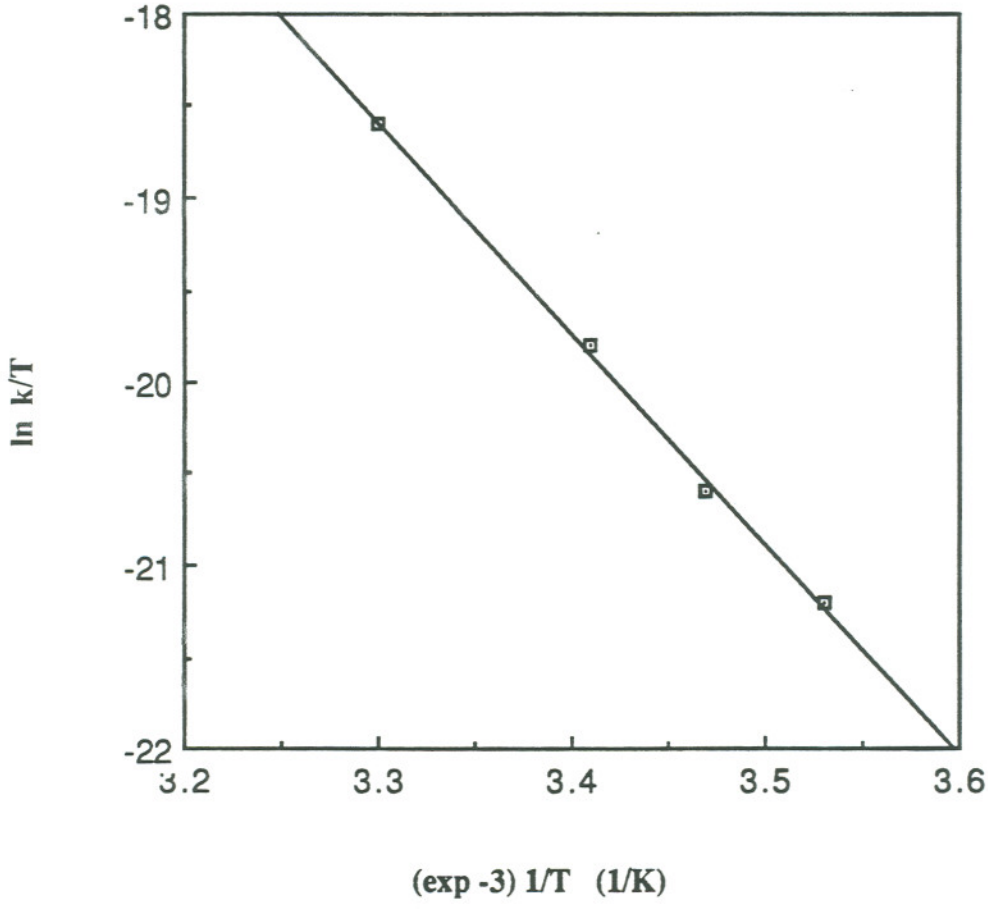

Figure 14: Arrhenius plot for transmembrane reduction of $(C_7)_2V^{2+}$ by dithionite in DMPC vesicles same conditions as in Table 15

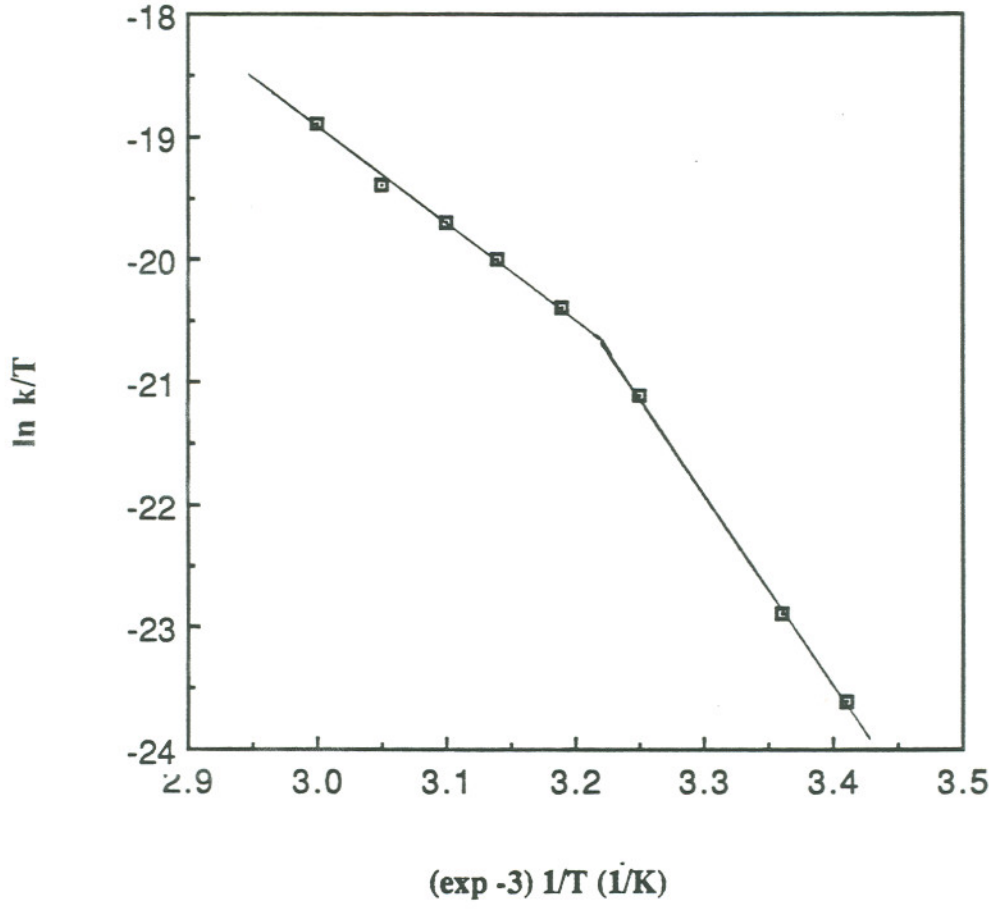

Figure 15: Arrhenius plot for transmembrane reduction of $(C_7)_2V^{2+}$ by dithionite in DPPC vesicles same conditions as in Table 16

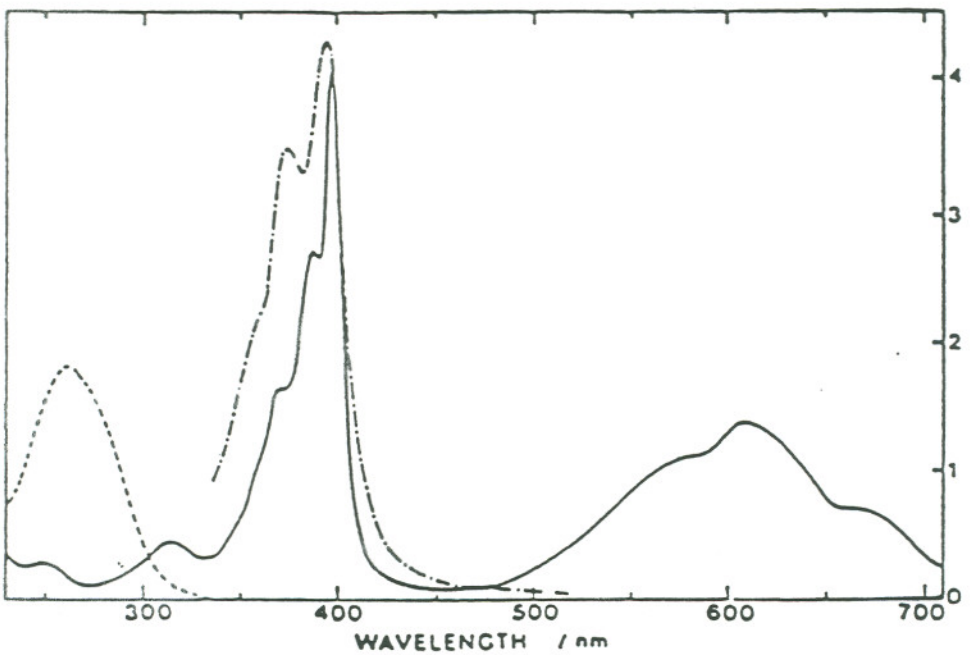

Figure 16: Optical spectra of viologen

dashed line = V^{2+}

solid line = V^{+}

dot-dashed line = V^{0}

with nearly quantitative conversion in either direction. Originally, heating the sample after reduction was aimed at facilitating viologen penetration into the membrane as a result of increased bilayer fluidity. However, independent experiments where dithionite is added to 50 uM $(C_7)_2V^{2+}$ in 0.1 M phosphate buffer, pH 8.0, at room temperature showed that $(C_7)_2V^{2+}$ is reduced to $(C_7)_2V^0$ in aqueous solution within a minute[c], while vesicle-bound viologen is reduced only to the radical cation. The results from the DPPC experiments the viologen could be interpreted in such a fashion, i.e. the radical dissociates from the vesicle upon heating and is then further reduced in bulk solution. This dissociation may well affect the rate of transmembrane viologen reduction and, although the V^+ and V^0 forms are nearly isosbestic at 400 nm, the wavelength used to monitor transmembrane reduction, the influence of the reduction to V^0 following the transmembrane reduction is not fully known and is difficult to assess.

At this point a wealth of data had been accumulated but their interpretation was still hindered by the fact that none of the investigated parameters (except temperature) had any influence on the observed rate of transmembrane reduction.

---

[c]The rate of reduction to V^0 is dependent on the alkyl chain length. Longer chain analogs reduce faster than shorter chains,e.g. methyl viologen does not fully reduce at all within the experimental time frame, while dioctyl viologen reduces very rapidly (< 2 sec.) to V^0.

Clarification was further obscured by the observation that the viologen was located inside the vesicle at the end of the reaction. Just like in the photochemical experiments, when the sample was oxygenated after all viologen had been reduced and dithionite was re-added, no viologen was immediately reducible. So again, the viologen appears not to have leaked out and the dithionite cannot penetrate into the vesicle, yet the viologen is reduced by the dithionite on a time scale much too fast to be accounted for by electron tunneling. To resolve this apparent paradox it was necessary to approach this problem from a different perspective and consider electrochemical principles.

3.4 Electrochemical Principles

Chemical and electrical potentials play an important role in energy-transducing membranes[16]. These gradients are often used to drive specific enzyme functions, e.g., ATP synthesis by the proton-translocating ATPase. Ca^{2+}, K^{+}, Na^{+}, and H^{+} are the ions most frequently used in these transmembrane processes. The metal ions are generally considered membrane impermeable so Nature uses specialized proteins to move them across the membrane. Active transport, i.e. transport against a concentration gradient, is accomplished with ion specific pumps, such as Ca^{2+}-ATPase, that are driven by other gradients or by ATP hydrolysis. Ion transport down a gradient is also possible with ionophores. These ionophores can be either mobile carriers, such as valinomycin, that transport ions by shuttling from one side of the membrane to the other accompanied by binding and releasing the ion at opposite membrane surfaces, or channel formers, such as gramicidin, that allow ion flow from one side to the other. In general, carriers have much higher selectivity for specific ions than channel-forming ionophores. Protons have a considerably higher membrane permeability than alkali metals. It is thought that proton transport through the membrane occurs via H-bond exchange with residual water molecules dissolved within the bilayer, similar to the H^{+} diffusion in liquid water and ice.

In many instances this ion transport is coupled to electron

transfer reactions between redox partners that are separated by the membrane. Electron transfer across the membrane is electrogenic. The resulting membrane polarization is often utilized as a driving force for ion-pumping in biological systems. Artificial membrane systems lack such pumps and if the charge gradient is not dissipated by ion movement, the electrical potential generated will prevent further reaction. For small vesicles this potential will become prohibitively large after only a few charges per vesicle have been translocated (Figure 17). Leakage of aqueous ions could provide a means for dissipating that potential.

These electrochemical principles apply to synthetic vesicle systems and may provide substantial information needed to understand transmembrane viologen reduction.

When the vesicles were eluted from the ion-exchange column nearly all $(C_7)_2V^{2+}$ had been removed from the external surface. This generates a $(C_7)_2V^{2+}$ concentration gradient outward that initially is very large (Scheme 4a). The premise for the following discussion is that the viologens are membrane permeable[a]. The viologen will start to diffuse down its concentration gradient. Because there are no other membrane diffusible ions in the system the rapidly developing

---

[a]This premise will be experimentally confirmed later (see Section 3.5). Diffusion of methylviologen across DHP vesicles has also been demonstrated by Patterson et al.[21].

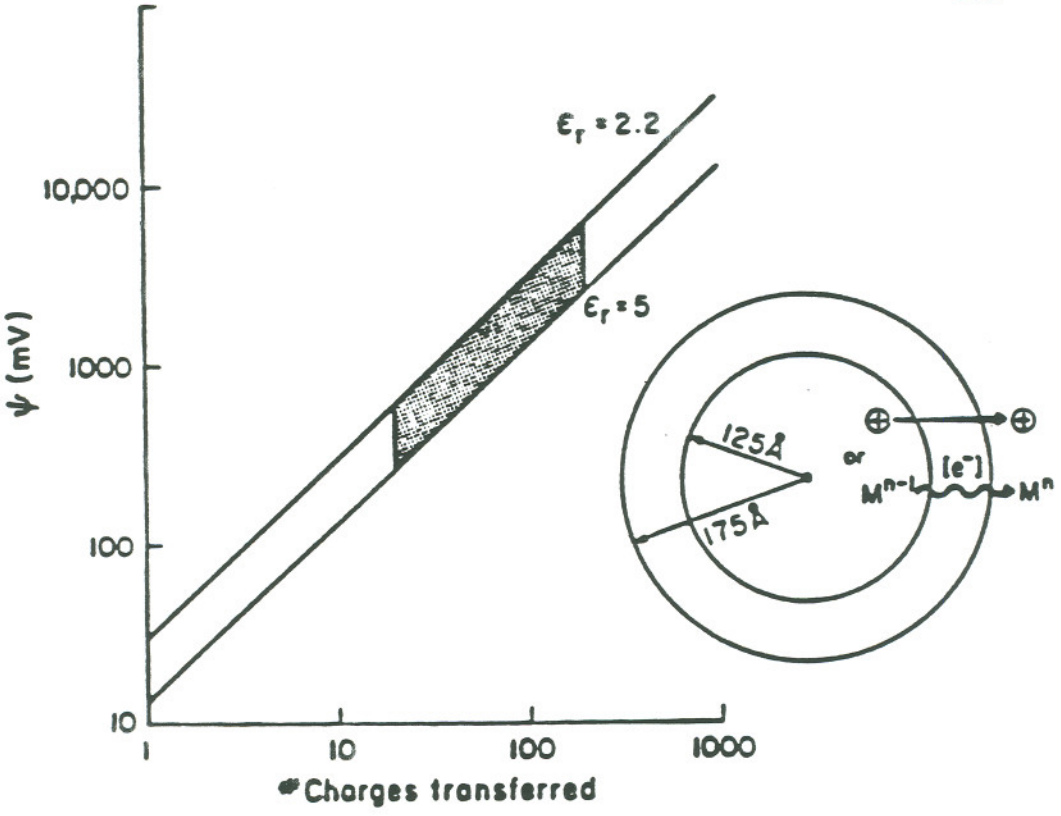

Figure 17: Membrane polarization scheme

Electric polarization of a concentric plate capacitor with dimensions of a small unilamellar vesicle; Er is the relative permittivity of the hydrocarbon phase, and psi is the transmembrane electrical potential generated by transfer of point charge across the bilayer (from James K. Hurst, in "Kinetics and Catalysis in Microheterogeneous Systems", M. Gratzel and K. Kalyanasundaram, eds., in preparation)

a)

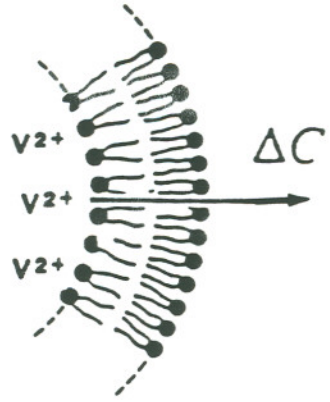

b)

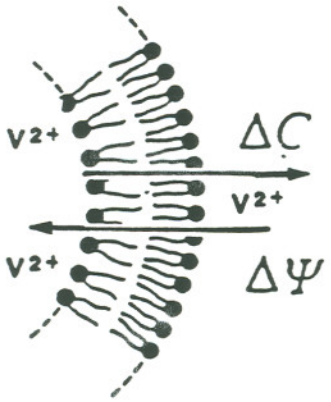

c) $$2{\cdot}3RT \log_{10} \frac{[X^{m+}]''}{[X^{m+}]'} = -mF\Delta\Psi$$

Scheme 4: Membrane Energetics

charge gradient will prevent further viologen leakage and a Donnan-type equilibrium[53] is established (Scheme 4b). At this point the free energies of the concentration and the electrical potentials are equal (Scheme 4c) and no further viologen leakage can occur in the absence of other ion movement.

Scheme 5 presents a postulated basic mechanism that can account for the observations. The viologen dication leaks out of the vesicle down its initially large concentration gradient. Once outside it is rapidly reduced by dithionite. If the dithionite is in excess and reduction is fast relative to diffusion, this concentration gradient will remain very large throughout the entire reaction. The radical cation migrates back into the vesicle in response to the developing transmembrane electrical potential. To complete charge compensation migration of aqueous ions has to occur, either by symport of anions or by antiport of cations. Under these circumstances, diffusion of aqueous ions can become rate-limiting, with the expectation that the reaction will be zero order in reactant concentration. The exact identity of this ion (or these ions - more than one ion may migrate) has not been clearly established in our studies. Although protons are more membrane permeable than alkali metal ions, the fact that the reduction rate is identical in phosphate buffer at pH 6.0 and 8.0, i.e. over a 100-fold change in H^+ concentration, suggests ion movement other than protons. This is further supported by the observation that no transmembrane reduction is observed when 75 mM

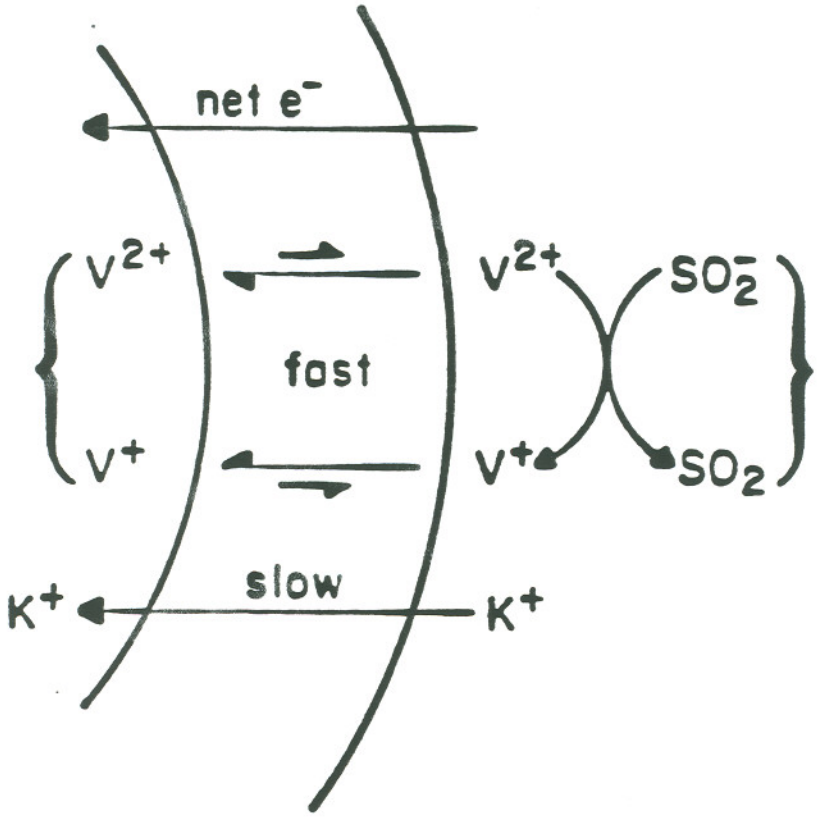

Scheme 5: Postulated basic mechanism

imidazole buffer at pH 8.0 is used instead of phosphate buffer. Addition of 0.1 M KNO_3 or 0.1M $NaClO_4$ (as 1 M aqueous solutions) to these preformed vesicles did not induce any transmembrane reduction, suggesting that alkali metal antiport is not the charge compensating step. Anions can compensate the charge gradient by diffusion in the same direction as the viologen. Since the anions (NO_3^- or ClO_4^-) are outside the vesicle and hence can only move in the direction opposite to that of viologen flow they are not able to balance the electrical gradient and increase the rate. Thus, anion cotransport might be the charge compensating step in the systems with anions on both sides of the bilayer, i.e. vesicles prepared in the presence of salts, such as phosphate buffer. However, the viologen counterion experiments seem to rule against anion symport, but their concentrations were low. Although low anion concentrations did not exhibit specific counterion effects, electrolyte leakage could be probed at high salt concentrations. Addition of high salt concentrations (0.32 M) to either 20 mM phosphate or 75 mM imidazole buffer showed a dependence of the rate upon the nature of the anion (Table 17). This dependence strongly resembled the Hofmeister series of anions, which "ranks" ions with respect to their effectiveness in precipitating proteins from aqueous solutions[43]. The following anions represent such a series: $SO_4^{2-} > HPO_4^{2-} > AcO^- > Cl^- > NO_3^- > I^- > ClO_4^- > SCN^-$ [53]. This order "holds for a great many physical, chemical, and biological effects of ions in water and is itself correlated with ion hydration energy"[44]. For instance, the surface tension of water shows a salt

Table 17: Anion dependence of the viologen reduction rate.

anion (X)	t_{98} ǂ (min)
I^-	< 0.5
CO_3^{2-}	2ǂ
NO_3^-	3
Br^-	9
F^-	22
OAc^-	26
Cl^-	33
SO_4^{2-}	42

ǂ time to reduce > 98% of viologen entrapped

4 mM pc, 80 uM $(C_7)_2V^{2+}$, 22° C,

20 mM phosphate buffer, pH 8.0 0.32 M KX

ǂ 0.1 M carbonate buffer, pH 10.8

dependence, and the order of anions that decrease the surface tension is very similar to the Hofmeister series. A similar order is found for other surface or interface related phenomena, including the transfer of ions between water and a non-polar organic liquid[45]. The rationale for these series is the difference in hydration energy of the different anions. More strongly hydrated anions, such as F^-, are less concentrated at the water surface and cause a high surface tension while weakly hydrated anions, such as ClO_4^-, concentrate at the surface and thus lower the surface tension.

When the anions that were studied were ordered by increasing transmembrane reduction rates their order was virtually the same as for decreasing the surface tension of water and for denaturing proteins (i.e. Hofmeister series). There are several possible explanations for this anion effect in vesicle systems.

A possible explanation for the observed salt effect relates to the degree of hydration of the anions. It is most likely that the ion will diffuse across the membrane unsolvated. Thus the ion has to lose its solvent shell before entering the bilayer. Anions to the left of the Hofmeister series are strongly hydrated while anions to the right are weakly hydrated. The rates from Table 1 are consistent with this hypothesis, i.e. the reduction rate is inversely proportional to the hydration energy of the anions.

Evidence from other experiments (see Section 3.1) suggests that the membrane surface has an outer layer of positive charges. Anions may therefore preferentially concentrate at the interface, an effect that can lead to increased diffusion rates. Anion binding to lipid headgroups was recently demonstrated using ^2H nmr spectroscopy[46]. It was found that the conformation of the choline headgroup is influenced by the charge density at the membrane surface. This is reflected in the quadrupole splitting from ^2H nmr spectra of phosphatidylcholines with deuterated headgroups[47]. The degree of binding appeared to be directly related to the strength of the hydration shell of the anion. When the anions that were measured are ordered according to the percent change in the quadrupole splitting relative to buffer alone their order is identical to the order in Table 17. The viologen reduction rate is therefore also proportional to the binding affinity of the anion.

Another possibility is ion-pairing between the anion and the viologen dication. Good evidence for ion-pairing is the fact that anions to the right of the Hofmeister series, e.g. ClO_4^- and SCN^-, precipitate viologens from aqueous solutions[b]. If tight ion-pairing occurs, the viologen salt could diffuse across the membrane as a neutral species and the rate would not be retarded by potential gradients. The rate would still be expected to be zero order because

---

[b]Because these anions precipitated $(C_7)_2V^{2+}$ form aqueous solution no rates could be measured for these anions.

the driving force - the viologen concentration gradient - would remain nearly constant[c]. However, the data do not provide good evidence that ion-pairing contributes significantly to transmembrane diffusion of viologens.

It is quite possible that all of the effects described above influence the transmembrane electron transfer rate in liposome systems. Although it appears that the symport of anions compensates for the developing charge gradient upon viologen diffusion, other electrophoretic ion movement cannot be ruled out. Regardless of the identity of the migrating electrolyte, its diffusion coefficient is expected to be much lower than that of viologen[14], hence it is rate limiting in all cases. Thus it is not necessary to know the exact identity of this ion to determine the mechanism of transmembrane viologen reduction.

The observation that charge translocation is controlled by potential and charge gradients is further illustrated by the following experiment where a pH gradient across the membrane was imposed and the viologen reduction rate was measured as a function of this potential . Vesicles with entrapped $(C_7)_2V^{2+}$ were prepared by extrusion as usual. The pH of the phosphate buffer at the time of

---

[c]because the viologen dication is reduced immediately on the outside its external concentration remains close to zero. Hence the concentration gradient remains very large.

liposome formation was 7.5. The sample was divided into 5 aliquots and the pH of each aliquot was changed by adding either HCl or NaOH, resulting in samples ranging from pH 5.1 to 12.7. The rate of transmembrane viologen reduction was then determined for each of the samples. The results are shown in Table 18. Since the vesicles were made at pH 7.5 the rate at this pH represents the reference rate. At this pH protons and hydroxide ions are at equilibrium across the membrane and "normal" reduction kinetics are expected and observed. When the pH of the bulk solution was lowered by adding HCl to the external phase a proton concentration gradient developed. This gradient caused influx of protons into the vesicle. This, in turn, led to a membrane charge polarization in which the internal vesicle surface was positive relative to the external surface. This will in effect force the viologen out of the vesicle since it is the most permeable ion in the system and its own concentration gradient is outward. Thus an increase in the reduction rate would be expected - and is indeed observed. Just the opposite effect is expected when the bulk pH is raised. The higher external pH will force protons out the vesicle, thus leaving the vesicle interior negatively polarized[d]. Viologen leakage would go against this potential gradient and is therefore expected to be retarded under those conditions. The experimental result again is consistent with the theoretical

---

[d]It is immaterial for these theoretical considerations whether a proton or a hydroxide ion moves in response to the pH change. They are kinetically indistinguishable and the resulting potential gradients would be identical.

Table 18: pH-gradient dependence of the $(C_7)_2V^{2+}$ reduction rate.

adjusted pH	rate ($x10^{-7}$ M s^{-1})
5.1	10
5.9	3.7
6.6	2.1
7.5	1.7
12.7	0.062

4 mM pc, 108 uM $(C_7)_2V^{2+}$,
0.1 M phosphate buffer, pH 7.5
dithionite in 5-7 fold excess

prediction. The magnitude of the transmembrane potential imposed by the pH gradient can be calculated with the following equation[16]:

$$\Delta u_H^+ = -2.3\ RT/F \quad \Delta\ pH$$

where Δu_H^+ is the proton electrochemical potential gradient and delta pH is the pH difference from one side of the membrane to the other. A plot of log (rate) vs. Δu_H^+ (Figure 18) shows that the rate is proportional to the proton gradient. This is still consistent with the independence of the reduction rate on pH (see Section 3.3) because the imposition of a pH gradient simply represents an additional force that influences membrane polarization and hence diffusion rates. Although proton diffusion in response to the pH gradient is expected, this process had reached equilibrium prior to adding dithionite[e].

Given that other electrolyte movement is rate limiting for transmembrane redox the only way to investigate the actual transmembrane electron transfer step is to accelerate the charge compensation step. In liposomal systems this can be accomplished by addition of other lipophilic ions (that are not redox active), e.g.

---

[e]pH-jump experiments with DHP vesicles showed that proton equilibration is reached after several minutes (B.C. Patterson, unpublished results). Thus, since the time from imposing the pH gradient to adding dithionite was at least 10 minutes in each case, it is expected that proton equilibration is achieved prior to adding dithionite.

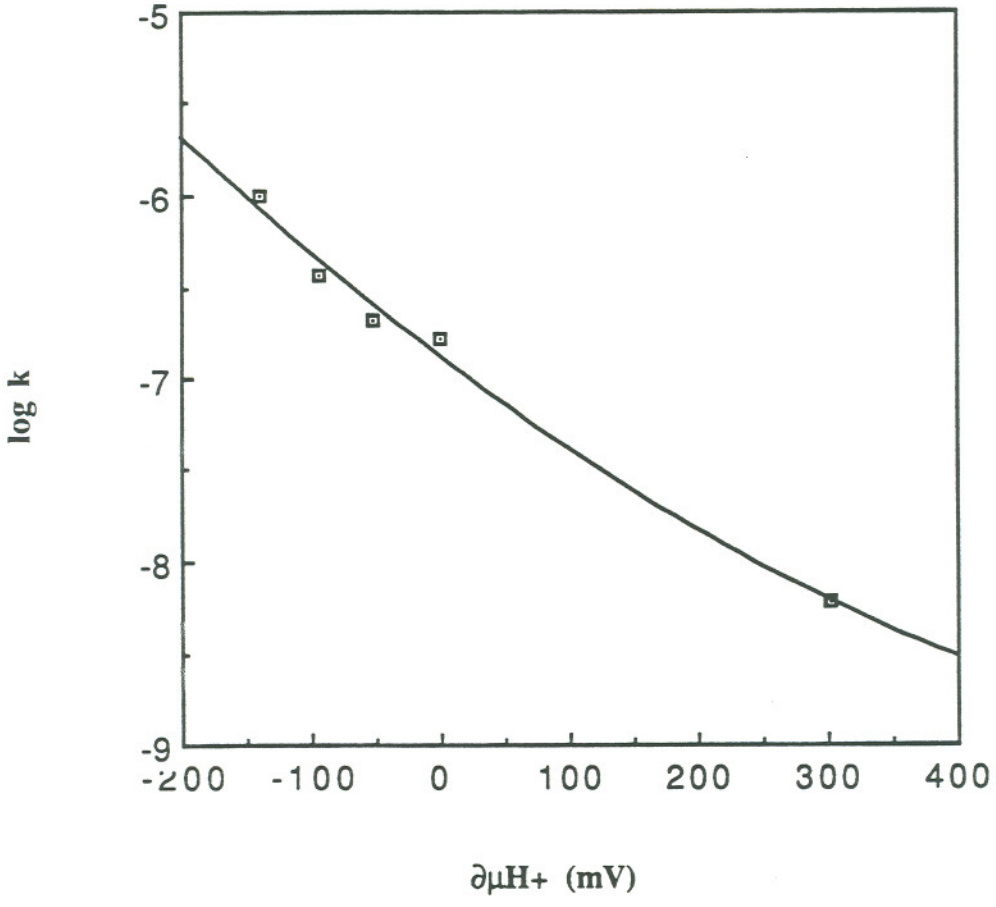

Figure 18: $(C_7)_2V^{2+}$ reduction rate dependence upon pH gradient

same conditions as in Table 18

tetraphenyl phosphonium, or by incorporating ionophores, such as valinomycin, into the membrane.

3.5 Ionophores

In the preceding section it was suggested that electrolyte movement in response to developing electrical gradients was rate limiting for transmembrane viologen reduction. The use of ionophores in biological systems to facilitate ion transport across membranes was also discussed. Thus, incorporation of ionophores into the vesicle bilayer should increase the rate of transmembrane viologen reduction. This rate enhancement was indeed observed with a number of different ionophores. Table 19 presents the $(C_7)_2V^{2+}$ reduction rates in the presence of lipophilic ions. In a typical experiment, the lipophilic ion was added to preformed vesicles containing $(C_7)_2V^{2+}$. The concentration of the added ionophore was in sufficient stoichiometric excess over $(C_7)_2V^{2+}$ to assure that complete charge balance could be achieved. The rate remained zero order in all cases. This suggests that ion migration is still rate limiting for transmembrane viologen reduction. It is conceivable that membrane permeability of a bulky molecule such as TPP is hindered by the large phenyl groups, and that its diffusion coefficient is lower than that of viologen. Although the transmembrane diffusion of monoalkyl bipyridines is expected to be at least as fast as $(C_7)_2V^{2+}$, there are other limiting factors. Because of their very low membrane binding, their effective surface concentration is relatively low so that the net flux is correspondingly diminished. It is worth noting that tetraphenylborate (TPB) had no effect on the rate. The other

Table 19: Transmembrane $(C_7)_2V^{2+}$ reduction rate in the presence of lipophilic ions.

ion	rate (x 10^{-7} M s^{-1})
-	0.92
TPP^+	5.8
TPB^-	0.89
Mebpy[#]	0.95
C_6bpy[$]	4.7

4 mM pc, 55 uM $(C_7)_2V^{2+}$, 22° C

0.1 M phosphate buffer, pH 7.5

[ion] = 1 mM

[#] Mebpy = monomethyl bipyridine

[$] C_6bpy = monohexyl bipyridine

ionophores all are cationic, hence their diffusion into the vesicle can electrically balance the outward diffusion of the viologen dication. Since the ionophores are initially located on the outside of the vesicle they can only migrate inward in response to a gradient. TPB, however, is anionic and hence cannot act as a charge compensator because its influx would further increase membrane polarization.

In order to gain further information about the mechanism of transmembrane redox, the rate of charge compensation had to be increased. The ionophores that can shuttle ions across the membrane fastest are channel-forming ionophores, such as gramicidin[16]. Because of the low solubility of gramicidin in water a 10 mM stock solution in methanol was prepared. Addition of 20 ul of this stock to 2 ml of 4 mM pc vesicles containing 45 uM $(C_7)_2V^{2+}$ in 0.1 M phosphate buffer, pH 8.0, gave a white precipitate. Therefore, the ionophore had to be incorporated during liposome formation. However, the presence of an ionophore during the ion-exchange step led to further complications. The physical basis for viologen dication entrapment inside a vesicle is the establishment of a Donnan-type equilibrium (see Section 3.4) which prevents leakage of viologen down its concentration gradient. In the presence of other membrane permeable ions or facilitators, such as ionophores, no such equilibrium can be established and viologen continues to leak out of the vesicle until it reaches an equilibrium concentration. At this

point most of the viologen will be outside the vesicle. When vesicles formed in the presence of gramicidin came off the ion-exchange column, entrapment was very low and that leakage continued until that equilibrium distribution was reached. This effect made it impossible to obtain quantitative data. Qualitatively, a significant increase in the transmembrane viologen reduction rate was observed. An approximate rate of 8×10^{-7} M s^{-1} could be estimated, which is greater than the rates measured in Table 19. To obtain good quantitative data it was necessary to use another ionophore. Valinomycin is a potassium-specific carrier that can rapidly shuttle K^+ ions across a membrane[16]. In mitochondrial membranes it is effective in submicromolar concentrations[59]. Like gramicidin, a methanol stock solution was prepared (10 mM) and small amounts (5-25 ul) were added to preformed vesicles with entrapped viologen. No visible disruption of the membrane occurred. Several tests were performed to assure that addition of small amounts of methanol did not affect membrane integrity (see Section 2.3). All tests showed that the methanol did not induce membrane leaks.

The addition of valinomycin drastically enhanced the rate of transmembrane viologen reduction. Furthermore, the rates were no longer zero order, but had the S-shaped appearance typical of an autocatalytic process (Figure 19). This kinetic curve indicates that after a small fraction of the viologen was reduced, a second pathway

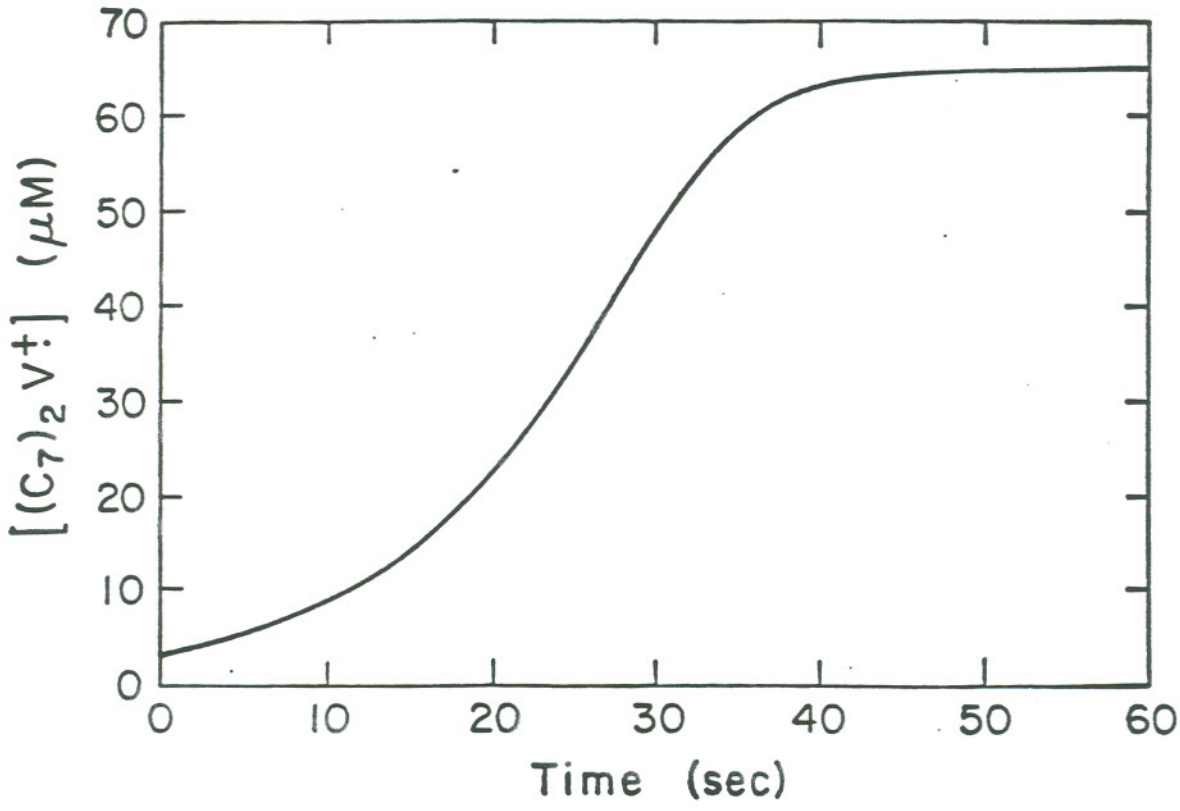

Figure 19: Transmembrane reduction of $(C_7)_2V^{2+}$ in the presence of valinomycin

4 mM pc, 22° C, 60 uM $(C_7)_2V^{2+}$, 75 uM valinomycin, 335 uM dithionite

0.1 M K^+ phosphate buffer, pH 8.0

for viologen reduction became available. Scheme 6 depicts a mechanism based on the results obtained from dithionite kinetics in the absence of ionophores (see Scheme 5) and the results shown in Figure 14. After adding dithionite and reducing the externally located viologen (k_2), net outward diffusion of entrapped viologen ensues k_1. The developing electrical potential is dissipated by K^+ antiport, facilitated by valinomycin (k_3). As the viologen radical accumulates on the outside, a second transmembrane redox pathway develops (k_4)[a]. This process, whose exact mechanism is still under investigation[21], involves electron transfer from a viologen on the outside to a viologen on the inside. As the viologen radical starts to accumulate on the inside it will diffuse outward (k_5), down its concentration gradient. Once outside, it can participate in the k_4 step, which, in part, accounts for the autocatalytic kinetics. The proposed outward diffusion of the viologen radical is experimentally confirmed by the observation that at the end of the reaction the viologen is found predominantly on the outside of the vesicle. This was determined as before by oxygenating the sample after completion of the reaction, degassing again and adding dithionite. The majority of the viologen was immediately reducible.

---

[a] The nature of the transmembrane redox step (k_4) is the subject of ongoing research[36]. It may involve electron tunneling, and also appears to have a significant diffusional component.

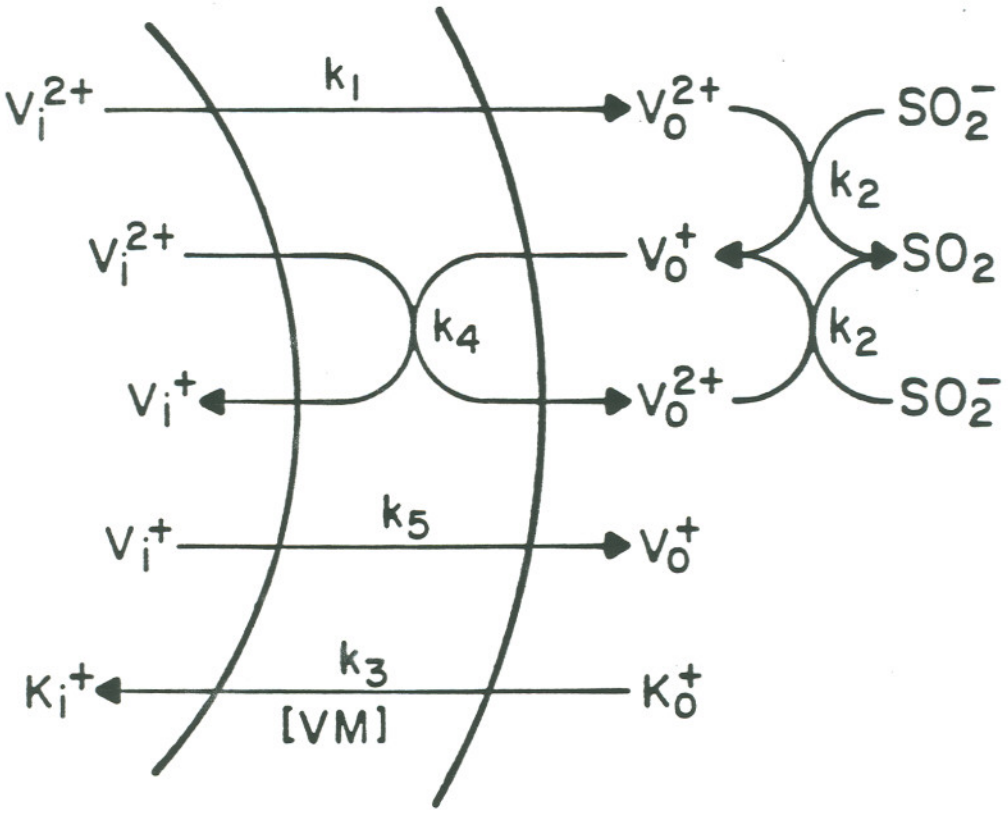

Scheme 6: Postulated Mechanism for transmembrane reduction of viologen

In order to determine the rate limiting step(s) for this mechanism it is necessary to measure the individual rate constants independently. The use of radiolabeled viologen allows the measurement of transmembrane diffusion of viologens at equilibrium. The experimental design was to entrap ^{14}C-labeled viologen inside the vesicle and add equal amounts of unlabeled viologen to the external phase and measure the rate of flip-flop type exchange between viologens bound to opposite sides of the membrane. However, the exchange rate was too fast to be measured with the designed experimental set-up. Several attempts were made to minimize the sampling time but in all cases the system had reached equilibrium before the first data point could be taken. The main problem was that the minimum amount of time required for the measurement from the moment that the cold viologen was added to the outside to the time the external viologen could be removed by ion-exchange filtration was about 20 seconds. During this short time period the labeled viologen that originally was inside only had reached its equilibrium distribution on both surfaces and, although exchange is still occurring at the same fast rate, no further redistribution of the ^{14}C could be observed. This rapid equilibration was observed for both viologens measured, ^{14}C-hexylmethylviologen and ^{14}C-diheptylviologen.

Although exact exchange rates could not be determined, one can estimate a lower limit for the diffusion of viologens across bilayer membranes from the data (Figure 20). Since complete equilibrium is

reached within 20 seconds, the diffusion rate has to be faster than 2.5×10^{-6} M s^{-1}. This corresponds to a lower limit for the first order rate constant of 0.15 s^{-1}. This confirms our earlier premise that viologens are capable of rapid diffusion through lipid bilayers. However, this rate was measured for viologen exchange, not for unidirectional diffusion of viologen. There are indications that binding of viologens induces structural changes in vesicle membranes[62]. These structural changes might facilitate transmembrane exchange of viologens. These changes are larger if viologens are bound juxtaposed on opposite surfaces rather than on one side only. Thus, the exchange rate determined above is likely to be faster than unidirectional viologen diffusion.

Diffusion of the viologen radical is expected to be even faster because of the reduced charge on the molecule. Although the exact diffusion rate of the radical could not be determined there is evidence from other experiments (vide infra) that its diffusion is indeed very fast.

Addition of increasing amounts of valinomycin (25-400 uM) to vesicles (4 mM pc) in 0.1 M potassium phosphate buffer, pH 7.5, with entrapped $(C_7)_2V^{2+}$ (65 uM) increased the rate of viologen reduction (Table 20). Rate saturation with respect to valinomycin concentration could not be achieved, even at the highest valinomycin:lipid ratio of 1:10. Literature reports of valinomycin

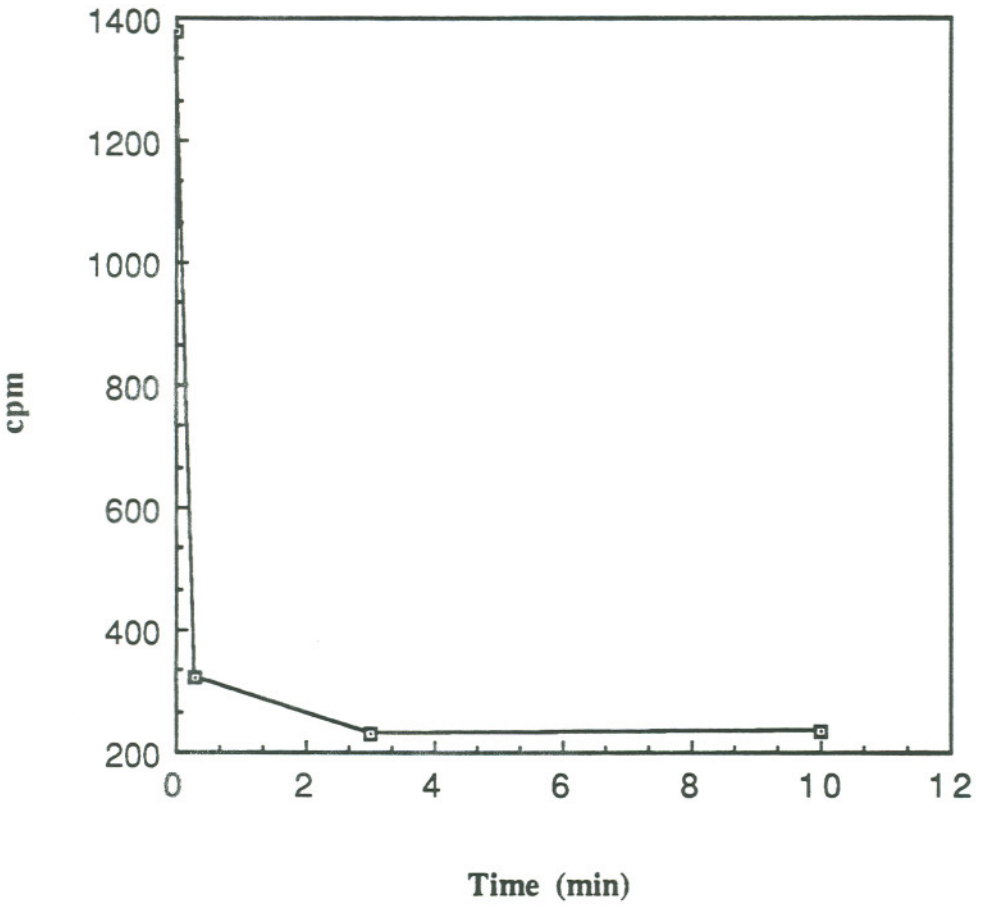

Figure 20: Transmembrane exchange of viologen

4 mM pc, 22° C, 15 uM $(C_7)_2V^{2+}$ on either side

of the bilayer, 0.1 M phosphate buffer, pH 8.0

Table 20: Valinomycin dependence of transmembrane $(C_7)_2V^{2+}$ reduction rates

[val.] (uM)	t_{98} (sec.)
25	105
50	70
75	40
100	18

4 mM pc, 22° C, 65 uM $(C_7)_2V^{2+}$

0.1 M K^+ phosphate buffer, pH 7.5

transport rates vary by several orders of magnitude[58], depending on the type of membrane. In mitochondrial membranes, the valinomycin turnover number is about 10^3 s^{-1} [59], while in erythrocytes, which more closely resemble vesicle bilayers, this rate is four orders of magnitude slower[57]. The rate of valinomycin diffusion in pc vesicles was measured with the following experiment: About 100 uM K^+ was entrapped inside pc vesicles by forming the liposomes in the presence of 20 mM K^+ and then replacing the external potassium ions with Na^+ ions by ion-exchange chromatography. The bulk concentration of K^+ was monitored with a potassium-ion specific electrode. From a calibration curve of measured voltage as a function of K^+ concentration, the bulk potassium concentration can be estimated from the voltage reading of the potentiometer. Before addition of valinomycin this reading corresponded to a $[K^+]$ of 10 uM. Addition of 10 uM valinomycin (as a 10 mM solution in methanol) decreased the voltage and the equilibrium K^+ concentration was calculated to be 90 uM. From the initial slope of the voltage vs. time curve a K^+ transfer rate of 0.1 s^{-1} was calculated. This number is consistent with the rates reported in the literature[58]. However, this rate was measured under conditions that were quite different from the viologen reduction systems. In the above experiment, there was a large K^+ concentration gradient, while in the viologen reduction system the K^+ concentration is equal on both sides of the membrane. In other words, in one system the valinomycin responded to a K^+ gradient while in the other system it responded to an electrical gradient. Thus,

the rate obtained above might be different from the rate in the viologen reduction system.

Both the reduction of externally located viologen by dithionite (k_2) and the transmembrane redox step (k_4) could be measured independently. Because the two reactions are temporally well separated they could be measured in a single experiment.

Recently, transmembrane electron transfer between methylviologen ions located on opposite sides of a DHP vesicle membrane was demonstrated in our laboratory[21]. It was observed that in a system with equimolar concentrations of viologen inside and out addition of dithionite rapidly reduced the external viologen followed by a slower reduction of the entrapped viologen. The stoichiometry of the transmembrane step suggests that electrogenic electron transfer is electrochemically balanced by comigration of a viologen radical. This inward viologen migration is supported by the observation that all viologen was located inside the vesicle after completion of the reduction.

The same reaction occurs in pc vesicles with entrapped $(C_7)_2V^{2+}$. Figure 21 shows a trace from stopped-flow kinetics of a system comprised of pc vesicles (4 mM pc) in 0.1 M phosphate buffer, pH 7.5, with 30 uM entrapped $(C_7)_2V^{2+}$ and equimolar concentration of $(C_7)_2V^{2+}$ on the outside of the vesicles. After flow mixing the concentration of

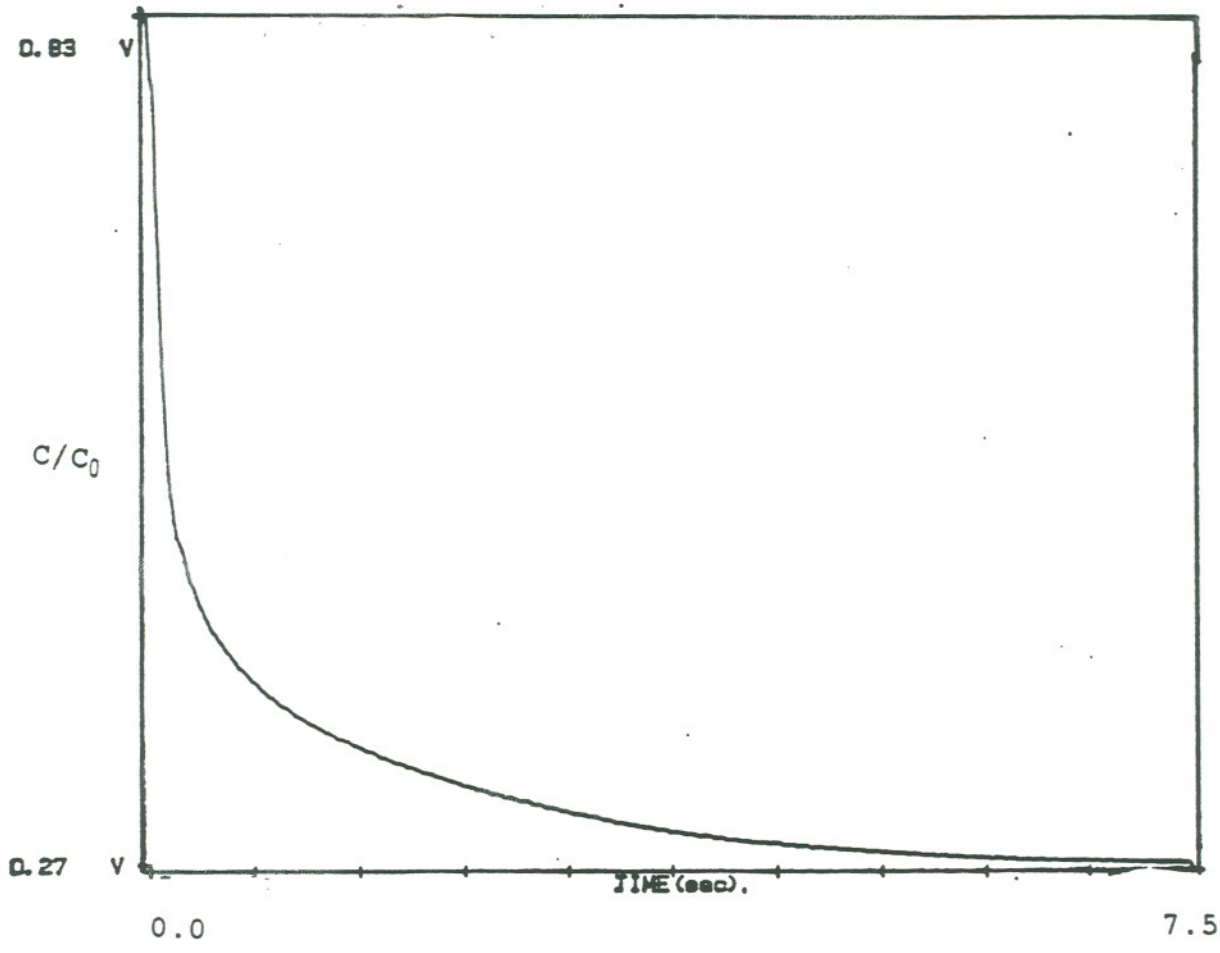

Figure 21: Transmembrane reduction with viologen
on either side of the membrane
4 mM pc, 22° C, 30 uM $(C_7)_2V^{2+}$ inside and out,
0.1 M phosphate buffer, pH 8.0,
180 uM dithionite

dithionite was 180 uM. The fast step, which represents the reduction of the external viologen, was analyzed as a pseudo first order reaction (Figure 22) and then converted to a second order rate constant with the following equations:

$$\frac{d\,[(C_7)_2V^{2+}]}{dt} = -k\,[SO_2^-]\,[(C_7)_2V^{2+}]$$

$$= -k_{observed}\,[(C_7)_2V^{2+}]$$

where $k_{observed} = k\,[SO_2^-]$ pseudo first order

$$S_2O_4^{2-} = 2\,SO_2^- \quad \text{with} \quad K = 1.4 \times 10^{-9}\ M \ [61]$$

$$k = \frac{k_{observed}}{\{\,[S_2O_4^{2-}]\,(1.4 \times 10^{-9})\,\}^{1/2}}$$

From this analysis, a second order rate constant for the reduction of externally bound $(C_7)_2V^{2+}$ of $k = 1.9\ (\pm\ 0.1) \times 10^7\ M^{-1}\ s^{-1}$ at 22° C was obtained. This number is consistent with the reduction rate of viologens by dithionite in homogeneous solution[60].

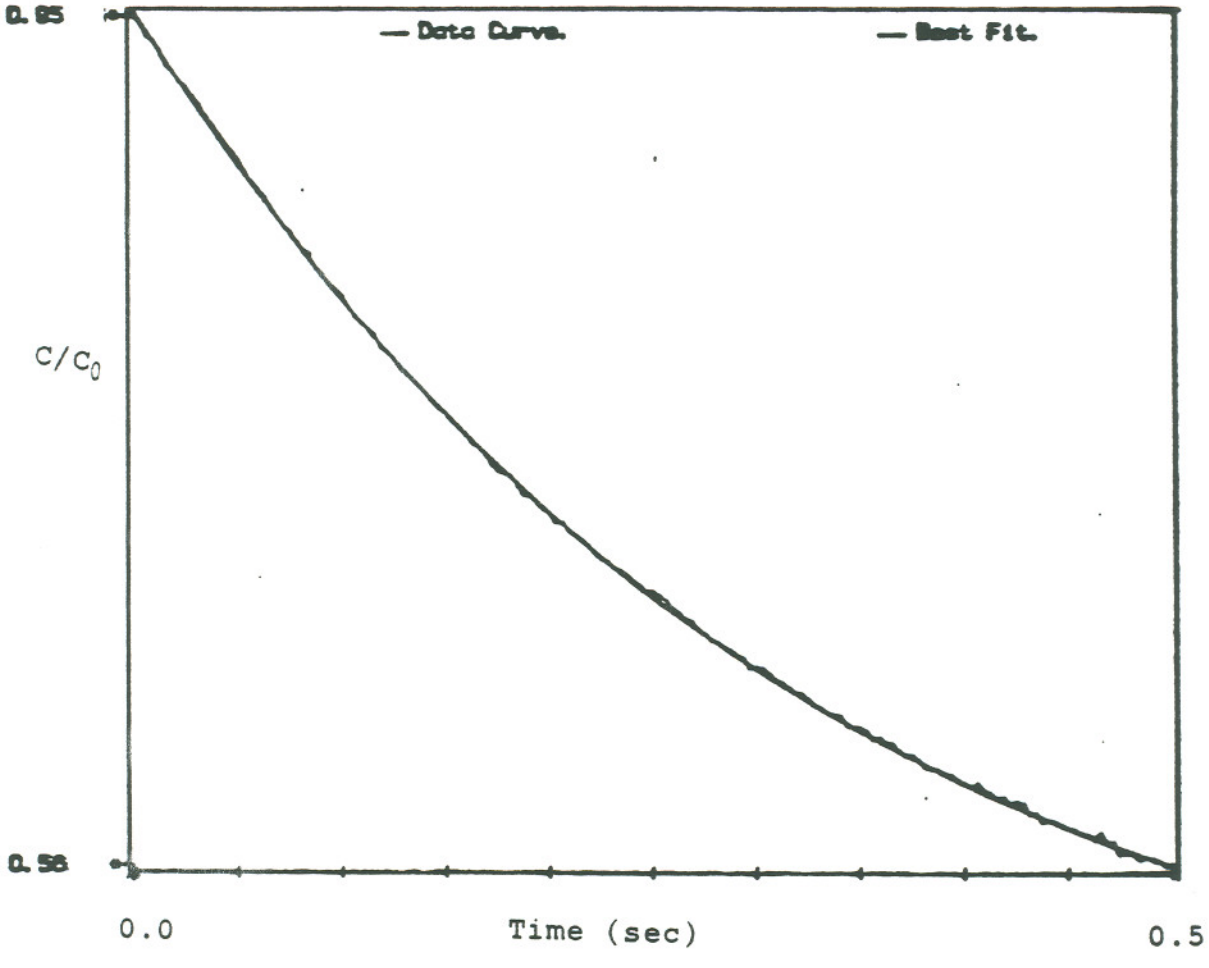

Figure 22: Reduction of externally bound $(C_7)_2V^{2+}$
by dithionite
same conditions as in Figure 21
(this is the fast step of Figure 21)

The transmembrane step could not be fitted with a single exponential, but second order analysis gave excellent results. Based on the postulated mechanism a first order fit would be expected if net, unidirectional viologen migration was rate-limiting while a second order fit suggests that the transmembrane redox step is rate-limiting. The calculated second order rate constant was 4.2 ($\pm$ 0.1) x 10^4 M^{-1} s^{-1} at 22° C.

These results indicate that transmembrane redox between viologens is indeed very fast and that diffusion of the viologen radical is even faster because its net diffusion in response to the electrical gradient is not rate-limiting. The rate equation for the transmembrane step is $-dV^{2+}/dt = k\,[V^{+}][V^{2+}]$. If viologen radical diffusion were rate-limiting the rate equation would be $-dV^{2+}/dt = k\,[V^{+}]$. From this equation and the rate determined above, a lower limit for the viologen diffusion rate constant of 0.84 s^{-1} was calculated. This rate constant is 6-times faster than the lower limit estimates for the $(C_7)_2V^{2+}$ dication, consistent with the expected higher permeability due to the reduced charge on the molecule.

Because the reaction mechanism for transmembrane reduction of $(C_7)_2V^{2+}$ by $S_2O_4^{2-}$ is complex (Scheme 6), the overall reaction could not be fitted to a simple rate law. To confirm the correctness of the proposed mechanism a computer simulation (see Appendix A) based on

that mechanism was compared to the actual data. Unlike other computer programs used in our kinetic analysis, this simulation is not a curve-fitting program. It simply computes and plots the results of a series of equations that keep track of the changes of the individual species during the reaction. In other words, the simulation calculates the concentration change of all species involved in the reaction and then plots their concentration as a function of time. Based on the mechanism in Scheme 6 the following equations were used:

$$V_i^{2+} = (V_i^{2+})_{initial} + d\,V_i^{2+}$$

$$V_o^{2+} = (V_o^{2+})_{initial} + d\,V_o^{2+} \qquad (2)$$

$$V_o^{+} = (V_o^{+})_{initial} + d\,V_o^{+} \qquad (3)$$

$$V_i^{+} = (V_i^{+})_{initial} + d\,V_i^{+} \qquad (4)$$

$$dV_i^{2+} = -(k_1\,V_i^{2+} + k_4\,V_i^{2+}\,V_o^{+})\,dt \qquad (1a)$$

$$dV_o^{2+} = (k_1\,V_i^{2+} - k_2\,V_o^{2+}\,SO_2^{-} + k_4\,V_i^{2+}\,V_o^{+})\,dt \qquad (2a)$$

$$dV_o^{+} = (k_2\,V_o^{2+}\,SO_2^{-} - k_4\,V_i^{2+}\,V_o^{+} + k_5\,V_i^{+})\,dt \qquad (3a)$$

$$dV_i^{+} = (k_4\,V_i^{2+}\,V_o^{+} - k_5\,V_i^{+})\,dt \qquad (4a)$$

Based on these equations a number of curves were obtained and compared to the data at different valinomycin loadings. The values for $k_{1\text{-}5}$ that were used for these graphs are presented in Table 21. Figure 23 shows a representative simulation graph with overlaid

Table 21: Rate constants for computer simulations

[val.] (uM)	k_1 (s^{-1})	k_2 ($M^{-1}s^{-1}$)	k_4 ($M^{-1}s^{-1}$)	k_5 (s^{-1})
25	2.0×10^{-5}	1.9×10^{7}	2.2×10^{4}	4.5×10^{-3}
50	5.0×10^{-5}	1.9×10^{7}	2.2×10^{4}	1.0×10^{-2}
75	1.0×10^{-4}	1.9×10^{7}	2.0×10^{4}	3.5×10^{-2}
100	1.6×10^{-3}	1.9×10^{7}	2.0×10^{4}	1.6×10^{-1}

4 mM pc, 22° C, 65 uM $(C_7)_2V^{2+}$, 0.1 M phosphate buffer, pH 7.5

180 uM dithionite

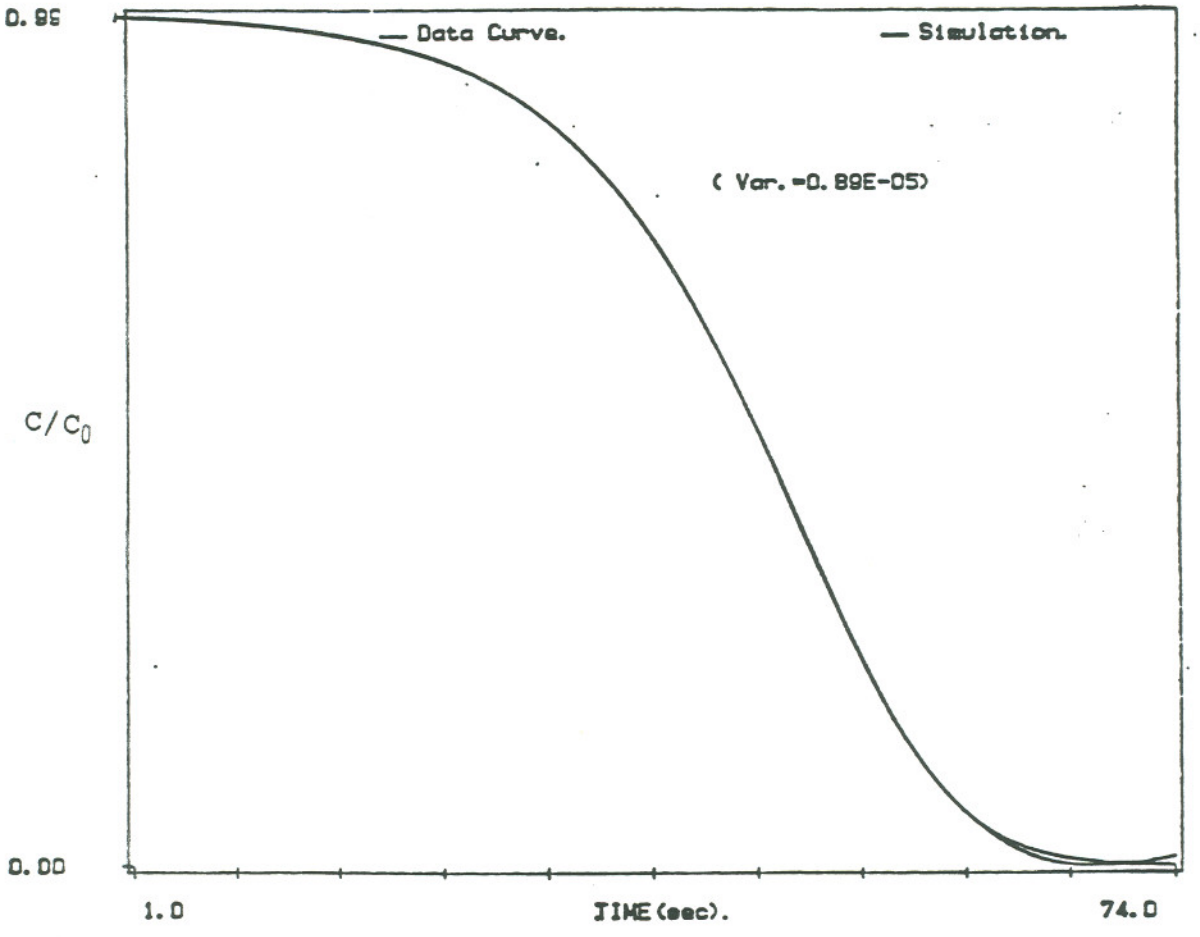

Figure 23: Computer simulation of transmembrane reduction of $(C_7)_2V^{2+}$

The simulation program is shown in Appendix A, the numbers used for the calculations are shown in Table 21

experimental curve[b]. Although the fits are quite good, the values for k_1 and k_3 used to obtain the simulation graphs do not compare well with the rate constants determined individually (Table 22). This indicates that some of the rate-limiting steps used in the simulation have not been identified correctly. This, of course, is not surprising since the simulation equations (1a-4a) do not take into account the possibility of rate limitation by the k_3 step. The analysis treats the reaction as if it were occurring in homogeneous solution with no other effects. The rate dependence on the valinomycin concentration on the other hand suggests that charge compensation is still (at least partially) rate-limiting. Thus, the k_1 and k_3 values used in the simulation are not representative of the actual rate constants, but are functions of k_3 and indicate coupling of viologen diffusion with potassium ion transport. Such coupling is supported by the dependence of these values on the concentration of valinomycin. Expressing mathematically the dependence of the individual rate constants on k_3 would be very difficult, although theoretically possible, and a simulation based on those expressions could be obtained. However, no new information about the other rate constants would be gained by such a procedure,

---

[b]The deviation of the simulation from the data curve at the end of the reduction is due to the reduction of $(C_7)_2V^+$ to $(C_7)_2V^0$. This reduction starts after all viologen has been reduced and does not interfere with the transmembrane kinetics. The simulation does not incorporate this reaction.

Table 22: Independently determined rate constants for Scheme 6

k_1	$> 0.15\ s^{-1}$
k_2	$1.9 \times 10^7\ M^{-1}\ s^{-1}$
k_3	$0.1\ s^{-1}$
k_4	$4.2 \times 10^4\ M^{-1}\ s^{-1}$
k_5	$> 0.8\ s^{-1}$

since the curve would now only be a function of k_3. It is worth noting that k_2 is identical to the independently determined value since it is not expected to be coupled with other steps. The value for k_4 is very close to the determined value and independent of the valinomycin concentration, indicating relatively weak coupling with the valinomycin step.

Qualitatively, the correctness of the postulated mechanism is confirmed by the good fit because simulations of alternative mechanisms did not yield any acceptable overlays. The alternative mechanisms included such variations as omitting the k_4 step and reversing the direction of the k_5 step. The problem of determining the rate-limiting steps in Scheme 6 arises from the complexity of the reaction, involving five individual reactions, of which four are coupled to each other. This strong interdependence makes it impossible to discern which step(s) is rate-limiting. Furthermore, because the reaction exhibits sigmoidal kinetics, the rate-limiting step is likely to change during the course of the reaction.

The following experiment confirms that the slow rate at the beginning of the autocatalytic kinetic trace is due to outward diffusion of entrapped viologen. 110 uM $(C_7)_2V^{2+}$ were entrapped inside pc vesicles (0.1 M phosphate buffer, pH 8.0) as usual, and 50 uM valinomycin and 350 uM dithionite were added. Figure 24a shows

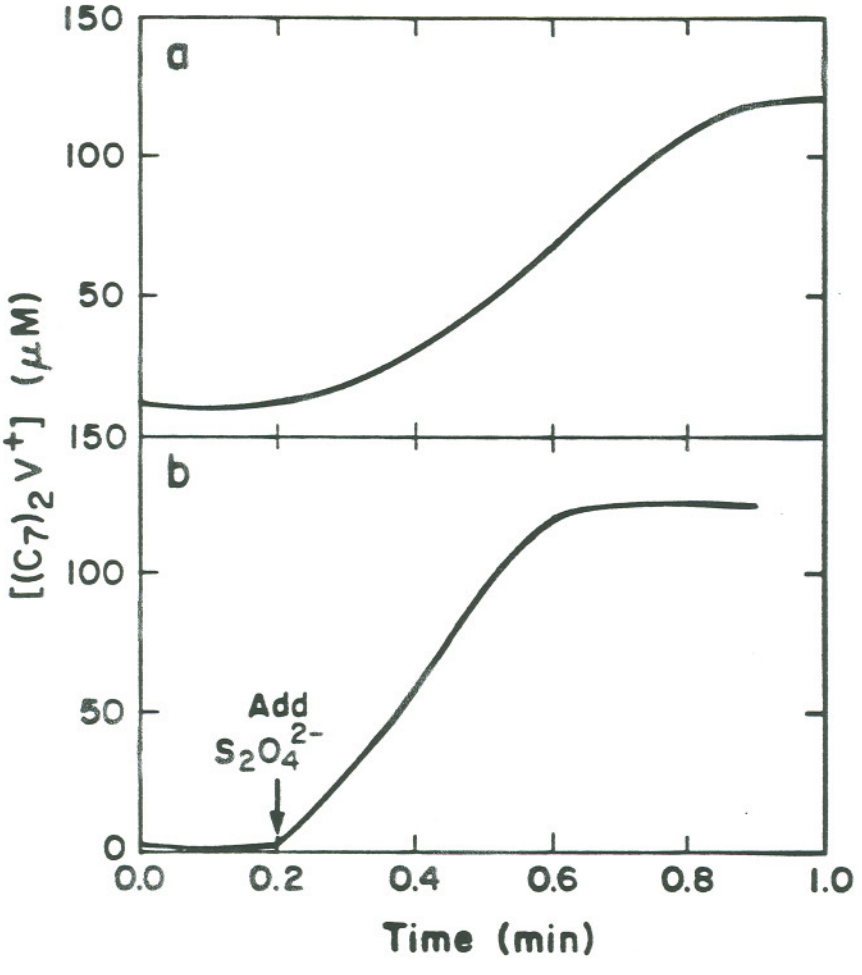

Figure 24: Transmembrane reduction of $(C_7)_2V^{2+}$ in the presence of external $(C_7)_2V^{2+}$

a: 4 mM pc, 22° C, 110 uM $(C_7)_2V^{2+}$

0.1 M phosphate buffer, pH 8.0

50 uM valinomycin, 350 uM dithionite

b: same as above, but 20 uM $(C_7)_2V^{2+}$ was added to bulk phase

the typical S-shaped appearance of the viologen radical. When 20 uM $(C_7)_2V^{2+}$ was added to the vesicle external surface prior to valinomycin and dithionite addition the reduction kinetics became nearly zero order (Figure 24b) and the slow induction period was eliminated (The zero order rate was 20 times faster than in the absence of valinomycin).

The following experiment disproved the possibility that valinomycin might induce pore formation within the membrane, which could account for the increased viologen leakage. ^{14}C-labeled sucrose was entrapped inside pc vesicles as usual. The sample was then divided into 4 aliquots to which various amounts of valinomycin were added. After 30 minutes the 4 samples were passed through Sephadex size exclusion columns to remove any sucrose that had leaked out of the vesicle. The results are presented in Table 23. It shows that valinomycin did not increase the amount of escaped sucrose. This indicates that valinomycin does not create pores in the membrane or otherwise induces leakiness. Because sucrose is a neutral molecule the charge compensating properties of valinomycin will not affect sucrose diffusion.

Other experiments indicated the possibility that viologen diffusion may be (at least partially) rate-limiting. The transmembrane viologen reduction rate was shown to be independent of the alkyl chains of the viologen. However, in the presence of

Table 23: Sucrose leakage in the presence of valinomycin

valinomycin (uM)	retained sucrose (cpm)
0	353
50	326
100	342
200	337

4 mM pc, 22° C, ^{14}C-sucrose 729 cpm, 0.1 M phosphate buffer, pH 8.0

valinomycin this is no longer true. The rate of transmembrane reduction of $(C_8)_2V^{2+}$ and $(C_{10})_2V^{2+}$, although still S-shaped, was considerably slower than that of $(C_7)_2V^{2+}$ at identical valinomycin concentrations (Table 24). Particularly the steep portion of the autocatalytic curve was slower. From Scheme 6, this section of the kinetic curve is sensitive primarily to the magnitude of the transmembrane redox step (k_4). Transmembrane redox shows a strong dependence on the alkyl tail in other systems[48], and the rate is inversely proportional to the chain length. Thus it is possible that the k_4 step and/or the viologen diffusion[c] might become partially rate-limiting for longer chain analogs. However, for $(C_8)_2V^{2+}$ a similar rate dependence on valinomycin concentration as for $(C_7)_2V^{2+}$ was found (Table 25), indicating that charge compensation is still (at least partially) rate-limiting for the overall process.

Taking into consideration all of the above results the following reaction sequence is proposed for the transmembrane reduction of viologen in the presence of valinomycin: Initially the viologen is distributed across the membrane according to a Donnan-type equilibrium, with most (> 95%) of the viologen entrapped inside the vesicle. Addition of dithionite and reduction of externally localized viologen shifts this equilibrium and the entrapped viologen

---

[c]It is expected that longer chain analogs diffuse slower through the bilayer, consistent with results from transmembrane redox in other systems (B.C. Patterson, unpublished results).

Table 24: Reduction rates of different viologens

viologen	conc. (uM)	t_{98} (s)
$(C_7)_2V^{2+}$	80	20
$(C_8)_2V^{2+}$	150	40
$(C_{10})_2V^{2+}$	207	120

4 mM pc, 22°C,

0.1 M K^+ phosphate buffer, pH 8.0

5-7 fold excess dithionite

Table 25: Valinomycin dependence of transmembrane $(C_8)_2V^{2+}$ reduction rates

[val.] (uM)	t_{98} (s)
50	70
100	40
200	14
400	6

4 mM pc, 22° C,
150 uM $(C_8)_2V^{2+}$
0.1 M K^+ phosphate buffer
pH 8.0

diffuses outward down its concentration gradient. This charge migration is balanced by the valinomycin-facilitated transport of potassium ions. Diffusing viologens are rapidly reduced at the outer vesicle surface. After a sufficient concentration of viologen radical has accumulated on the outside the transmembrane redox step (k_4) begins to operate and the overall rate of viologen reduction increases (steep portion of the S-shaped kinetic trace). The magnitude of the contribution of this step is strongly dependent on the concentration of external viologen radical. The concentration of external viologen radical in turn is strongly dependent on k_1 and k_5. The diffusion steps k_1 and k_5, however, are strongly dependent on k_3, the K^+ ion flow. After all viologen is reduced the radical will distribute to reach a concentration equilibrium. Because of the relatively low binding affinity of $(C_7)_2V^{2+}$ and the very small volume of the vesicle interior the viologen will predominantly be on the outside of the vesicle[d]. Thus, when the sample is oxygenated and reduced again all viologen is immediately reducible. This mechanism can account for all experimental observations and, although detailed interpretation is obscured by the complexity of the reaction, it is conceptually satisfying. It incorporates steps that have been

---

[d]As described earlier $(C_7)_2V^{2+}$ reduces to V^0 in bulk solution. After complete one-electron reduction of all viologen the viologen radical on the external membrane surface will partially distribute into bulk solution, where it is further reduced to zero-valent viologen. This reaction and the resulting gradient is also partially responsible for the observation that the viologen is located outside the vesicle after completion of the transmembrane reduction.

demonstrated independently and its overall rate is consistent with the individual rates (or their lower limits) that were measured independently. One inherent problem in analyzing transmembrane reactions is that conventional kinetic analysis does not strictly apply. Traditional kinetic laws were derived for and are strictly only valid in homogeneous solution. Transmembrane reactions are far more complicated[e] and other factors have to be incorporated in the rate laws. Thus the mathematics are more involved and good models have not yet been worked out.

The same rate-enhancing effect of valinomycin was observed in the photochemical non-reversible system with $Ru(bpy)_3^{2+}$ as the sensitizer, confirming the claim that the mechanism of photochemical and chemical transmembrane reduction are similar. Quantitative data for the photochemical system could not be obtained because of instrumental limitations. As described in the experimental section the amount of photoreduced viologen was determined by removing the optical cell periodically from the light beam and recording its optical spectrum. However, because the reaction is very fast in the presence of valinomycin, not enough data points could be collected to construct a kinetic curve.

---

[e]e.g. transmembrane redox in other systems shows a dependence on the lipid concentration (B.C. Patterson, unpublished results).

CHAPTER 4

CONCLUSIONS and SUMMARY

Several systems were studied in which apparent transmembrane electron transfer from reductants located on the outside of liposomes to entrapped viologen takes place. The mechanism of this electron transfer was shown to involve the diffusion of the acceptor to the reductant and subsequent reduction on the same membrane surface. Diffusion of the viologen dication is electrogenic and in all but one system electrolyte ion diffusion was rate-limiting. The single exception was the system with viologen on both surfaces, in which case electron transfer between juxtaposed viologens was rate-limiting. These results demonstrate that membrane dynamics are controlled by electrochemical potentials because the principles of electroneutrality cannot be violated. Increasing the rate of counterion flow by incorporating ionophores into the membrane allowed for a more detailed description of the mechanism and direct measurement of transmembrane redox rates. Determination of intrinsic membrane permeabilities of all ions of interest to rigorously test the proposed reaction mechanism proved very difficult. Ideally, these diffusion rates need to be measured at equilibrium. However,

addition of ions to only one side of the membrane provided a driving force in the form of a concentration gradient. Thus in most cases the measured rates are not intrinsic permeabilities, but the rates obtained in the presence of external driving forces. Even if such unperturbed diffusion coefficients could be determined, they would not apply to the investigated system because the chemical reactions in that system constantly perturb the equilibrium and therefore continuously provide a driving force for ion migration. And, since migration of one ion affects other ions in the system, imposed gradients and subsequent diffusion are interlinked. It is apparent that reactions across bilayer membranes are inherently complicated and, because every individual reaction step is coupled to one or more other steps, it is very difficult to determine quantitatively the relative contribution of each individual step to the overall reaction.

Photostimulated diffusion (i.e. viologen leakage caused by photochemically induced changes in membrane homogeneity) of $(C_7)_2V^{2+}$ does not occur in pc vesicles. Viologen diffusion was only observed in systems where the viologen was photochemically reduced, in which case the same electrochemical principles apply as for dithionite reduction and viologen migration is solely the result of an electrochemical gradient. The striking similarities of the observed kinetics for such photochemical systems and the systems with chemical reductants suggest that similar mechanisms are operative.

References:

1: S. S. Isied in "Progress in Inorganic Chemistry", Vol. 32, 1984, S. J. Lippard, editor.

2: C. R. Cantor, ed., "Biomembranes - Molecular Structure and Function", Springer-Verlag, New York, (1989)

3: F. M. Harold, "The Vital Force: A Study Of Bioenergetics", W. H. Freeman, New York, (1986)

4: J. S. Connolly, editor, "Photochemical Conversion and Storage of Solar Energy", Academic Press, New York, 1981

5: M. Calvin, Photochemistry and Photobiology, 37, 349-360, (1978)

6: M. Gratzel, "Energy Resources through Photochemistry and Catalysis", Academic Press, New York, (1983)

7: W. E. Ford, J. W. Otvos, and M. Calvin, Proc. Natl. Acad. Sci. USA, 76, 3590-3593, (1979)

8a: W. E. Ford and G. Tollin, Photochem. Photobiol. 35, 809-819, (1982)

8b: P. -A. Brugger, P. P. Infelta, A. M. Braun, and M. Gratzel, J. Am. Chem. Soc. 103, 320-326, (1981)

9: K. -P. Seefeld, D. Mobius, and H. Kuhn, Helv. Chim. Acta 60, 2608-2632, (1977)

10a: H. Kuhn, Pure Appl. Chem. 51, 341-352, (1979)

10b: T. Guarr and G. McLendon, Coord. Chem. Rev. 68, 1, (1985) and references therein.

10c: N. S. Hush, M. N. Paddon-Row, E. Cotsaris, H. Oevering, J. W. Verhoeven, and M. Heppener, Chem. Phys. Lett. 117, 8, (1985)

10d: C. A. Stein, N. A. Lewis, and G. Seitz, J. Am. Chem. Soc. 104 2596 (1982)

11a: M. S. Tunuli and J. H. Fendler, J. Am. Chem. Soc. 103, 2507-2513, (1981)

11b: L. Y. C. Lee, J. K. Hurst, M. Politi, K. Kurihara, J. H. Fendler, J. Am. Chem. Soc. 105, 370-373, (1983)

12: A. D. Bangham, M. M. Standish, and J. C. Watkins, J. Mol. Biol. 13, 238-252, (1965)

13: D. Papahadjopoulos, Biochim. Biophys. Acta 241, 254-259, (1971)

14: H. Hauser, D. Oldani, and M. C. Phillips, Biochemistry 12, 4507-4517, (1973)

15: A.L. Lehninger, "Principles of Biochemistry", Worth Publishing Inc., New York, 1982

16: D. G. Nicholls, "Bioenergetics", Academic Press, 1982

17: a) N. R. Clement and J. M. Gould, Biochemistry 20, 1539-1543, (1981)

b) C. M. Biegel and J. M. Gould, Biochemistry 20, 3474-3479, (1981)

18: B. R. Lentz, T. J. Carpenter, and D. R. Alford, Biochemistry 26, 5386-5397, (1987)

19: M. I. Khramov, S. V. Lymar, V. N. Parmon, and K. I. Zamaraev, Doklady Phys. Chem. 289, 598-601, (1987)

20: K. I. Zamaraev, S. V. Lymar, M. I. Khramov, and V. N. Parmon, Pure Appl. Chem. 60, 1039-1046, (1988)

21: B. C. Patterson, D. H. Thompson, and J. K. Hurst, J. Am. Chem. Soc. 110, 3656-3657, (1988)

22: W. S. Singleton, M. S. Gray, M. L. Brown, and J. L. White, J. Amer. Oil Chem. Soc., 42, 53-56, (1965)

23: W. E. Ford and M. Calvin, Chem. Phys. Lett. 76, 105-108, (1980)

24: G. Sprintschnik, H. W. Sprintschnik, P. K. Kirsch, and D. G. Whitten, J. Am. Chem. Soc. 99, 4947-4954, (1977)

25: A. Laukanis, P. A. Lay, A. W. -H. Mau, A. M. Sargeson, and W. H. F. Sasse, Austr. J. Chem. 39, 1053-1058, (1986)

26: L. A. Summers, "The Bipyridine Herbicides", Academic Press, New York, 1980, and references therein

27: P. -A. Brugger, M. Gratzel, T. Guarr, and G. McLendon, J. Phys. Chem. 86, 944-946, (1982)

28: J. H. Ross and R. I. Krieger, J. Agric. Food Chem. 28, 1026-1031, (1980)

29: M.Krieg, M. -P. Pileni, A. M. Braun, and M. Gratzel, J. Coll. Interf. Sci. 83, 209-213, (1981)

30: Y. Barenholz, D. Gibbes, B. J. Litman, J. Goll, T. E. Thompson, and F. D. Carlson, Biochemistry 16, 2806-2810, (1977)

31: L. D. Mayer, M. J. Hope, and P. R. Cullis, Biochem. Biophys. Acta 858, 161-168, (1986)

32a: T. Watanabe and K. Honda, J. Phys. Chem. 86, 2617-2619, (1982)

32b: D. Meisel, W. A. Mulac, and M. S. Matheson, J. Phys. Chem. 85, 179-187, (1981)

33: B. C. Patterson, unpublished results

34a: K. A. Norton and J. K. Hurst, J. Am. Chem. Soc. 100, 7237-7242, (1978)

34b: P. R. Bevington, "Data Reduction and Error Analysis for the Physical Sciences", McGraw-Hill, New York, 1969

35: E. E. Wegner and A. W. Adamson, J. Am. Chem. Soc. 88, 394-403, (1966)

36: Brian C. Patterson, Ph.D. dissertation, Oregon Graduate Institute of Science and Technology, 1990

37: J. H. Fendler, "Membrane Mimetic Chemistry", Wiley Interscience, 1982

38: A. W. Adamson, "Physical Chemistry of Surfaces", Wiley Interscience, New York, 1982

39: K. Kalyanasundaram, Coord. Chem. Rev. 46, 159-244, (1982)

40: See e.g., M. Gratzel, "Heterogeneous Photochemical Electron Transfer", CRC Press, Boca Raton, (1988) and references therein

41: W. E. Ford, J. W. Otvos, and M. Calvin, Nature 274, 507-508, (1978)

42: I. Tabushi and S. Kugimiya, J. Am. Chem. Soc. 107, 1859-1863, (1985); and references therein

43: F. Hofmeister, Arch. Exptl. Pathol. Pharmakol. 24, 247, (1888)

44: W. P. Jencks, "Catalysis in Chemistry and Enzymology", McGraw-Hill, New York, (1969), p. 372

45: A. W. Evans, Trans. Farad. Soc. 33, 794, (1937)

46: P. M. Macdonald and J. Seelig, Biochemistry 27, 6769-6775, (1988)

47: J. Seelig, P. M. Macdonald, and P. G. Scherer, Biochemistry 26, 7535-7541, (1987)

48a: J. K. Hurst and D. H. P. Thompson, J. Membr. Sci., 28, 3-29, (1986)

48b: D. H. P. Thompson and J. K. Hurst, Molecular Electronic Devices 413-425, (1988)

49: J. W. Nichols and D. W. Deamer, Proc. Nat. Acad. Sci. 77, 2038-2042, (1980)

50: M. Eigen and L. DeMayer, Proc. R. Soc. London Ser. A 247, 505-533, (1958)

51: A. W. -H. Mau, J. M. Overbeck, J. W. Loder, and W. H. F. Sasse, J. Chem. Soc. Farad. Trans. 2, 82 (5), 869-876, (1986)

52: K. J. Laidler and J. H. Meiser, "Physical Chemistry", The Benjamin/Cummings Publishing Company, Inc. (1982), pp.299

53: T. E. Creighton, "Proteins - Structures and Molecular Principles", W. H. Freeman & Co., New York, (1984), p.150

54: I. Tinoco, K. Sauer, and J. C. Wang, "Physical Chemistry - Principles and Applications in Biological Sciences", Prentice-Hall, Inc. Englewood Cliffs, (1978), pp.156

55: S. McLaughlin

56: C. Tanford, "The Hydrophobic Effect: Formation of Micelles and Biological Membranes", Wiley-Interscience, New York, (1980), pp.70

57: D. C. Tosteson, P. Cook, T. Androli, and M. Tiefenberg, J. Gen. Physiol. 50, 2513-2525, (1967)

58: P. J. F. Henderson, Ann. Rev. Microbiol. 25, 393-428 (1971) and references therein.

59: D. H. Haynes, T. Wiens, and B. C. Pressman, J. Membr. Biol. 18, 23-38, (1974)

60: K. Tsukahara and R. G. Wilkins, J. Am. Chem. Soc. 107, 2632-2635, (1985)

61: D. O. Lambeth and G. Palmer, J. Biol. Chem. 248, 6095, (1973)

Appendix A:

The following program was used to obtain computer simulations of Scheme 5. It was incorporated into another program that allowed for plotting and overlays of stopped-flow data. The entire program was developed by Brian C. Patterson and will be published in its entirety in his Ph.D. dissertation[36].

```
C       SUBROUTINE SIMUL(RATE,VARS,START,ISTOP,SIM)
C
        BYTE VAR(5),DECIDE
        REAL K(5),VARS(10)
        VIRTUAL SIM(3968)
C
        OPEN(UNIT=10,NAME='CONST.DAT',TYPE='OLD')
        READ(10,102)(K(I),I=1,5)
102     FORMAT(5(E10.3,2X))
        READ(10,104)V2T,PEROUT,S2O4,VM
104     FORMAT(E10.3,2X,F5.3,2X,E10.3,2X,E10.3)
        CLOSE(UNIT=10)
C
C            ***** SIMULATION *****
C
122     WRITE(5,*)
        DO 130 I=1,5
          WRITE(5,125)I,K(I)                                    !RATE CONSTS.
125       FORMAT(1X,'k',I1,'=',E10.3)
130     CONTINUE
        WRITE(5,*)
        WRITE(5,132)V2T                                         !TOTAL VIOL.
132     FORMAT(1X,'Total viologen conc.(TOT) =',E10.3)
        WRITE(5,134)PEROUT                                      !% VIOL. OUT
134     FORMAT(1X,'Fraction of viologen outside(PERO) =',F5.3)
        WRITE(5,136)S2O4                                        !DITHIONITE
136     FORMAT(1X,'Dithionite conc.(DIT) =',E10.3)
        WRITE(5,137)VM                                          !VALINOMYCIN
137     FORMAT(1X,'Valinomycin concentration(VM) =',E10.3)
        WRITE(5,*)
C
140     WRITE(5,*)'Do you wish to change a variable? (Y/N)'
        READ(5,145)DECIDE
145     FORMAT(A1)
        IF(DECIDE.EQ.'N')GO TO 200
        IF(DECIDE.NE.'Y')GO TO 140
C
C           ***** CHANGE VARIABLE *****
C
        WRITE(5,*)'Enter variable name'
        READ(5,150)(VAR(I),I=1,5)
150     FORMAT(5A1)
        WRITE(5,*)'Enter value'
        READ(5,160)TEMP
160     FORMAT(E10.3)
```

```
      IF(VAR(2).EQ.'2')K(2)=TEMP
      IF(VAR(2).EQ.'3')K(3)=TEMP
      IF(VAR(2).EQ.'4')K(4)=TEMP
      IF(VAR(2).EQ.'5')K(5)=TEMP
      IF(VAR(2).EQ.'O')V2T=TEMP
      IF(VAR(2).EQ.'E')PEROUT=TEMP
      IF(VAR(2).EQ.'I')S204=TEMP
      IF(VAR(2).EQ.'M')VM=TEMP
      GO TO 122
C
C        ****** START SIMULATION CALCULATIONS ******
C
200   DT=RATE/5.0
      EQK=1.4E-09
      SO2=(EQK*S204)**0.5
      V2I=V2T*(1-PERO)
      V2O=V2T*PERO
      VO=0.0
      VI=0.0
C
      DO 210 I=1,(ISTOP+1)*5
        J=I
        DV2I=-(K(1)*V2I+K(4)*V2I*VO)*DT
        DV2O=(K(1)*V2I-K(2)*V2O*SO2+K(4)*V2I*VO)*DT
        DVO=(K(2)*V2O*SO2-K(4)*V2I*VO+K(5)*VI)*DT
        DVI=(K(4)*V2I*VO-K(5)*VI)*DT
         V2I=V2I+DV2I
         V2O=V2O+DV2O
         VO=VO+DVO
         VI=VI+DVI
        IF(MOD(J,5).NE.0)GO TO 210
        SIM(J/5)=START*((V2T-(VO+VI))/V2T)
      IF(MOD(J,500).EQ.0)WRITE(5,205)J*DT,SIM(J/5)
205   FORMAT(1X,F5.1,' sec.  C/Co=',F5.3)
210   CONTINUE
C
      OPEN(UNIT=10,NAME='CONST.DAT',TYPE='NEW')
      WRITE(10,510)(K(I),I=1,5)
510   FORMAT(1X,5(E10.3,2X))
      WRITE(10,520)V2T,PEROUT,S204,VM
520   FORMAT(1X,E10.3,2X,F5.3,2X,E10.3,2X,E10.3)
      CLOSE(UNIT=10)
C
      DO 530 I=1,5
        VARS(I)=K(I)
530   CONTINUE
      VARS(6)=V2T
      VARS(7)=PEROUT
      VARS(8)=S204
      VARS(9)=FAST
      VARS(10)=VM
C
      RETURN
      END
```

APPENDIX B:

In early studies vesicle prepared by ultrasonic dispersion exhibited a short "lag period" before the onset of transmembrane viologen reduction. Although no viologen was reduced during this induction period there was extensive oxidation of the external reductant, dithionite, as observed by ultraviolet spectroscopy. This indicated a redox active impurity in the system. Because the reaction of dithionite with this impurity was relatively slow ($t_{1/2}$ = several minutes) it was unlikely that the impurity was in the bulk solution, but rather must be localized within the membrane. This impurity could be quantitatively determined by titration with dithionite, and for any given vesicle preparation its concentration was constant through several titrations. This lack of variation ruled against O_2 as the contaminant, since adventitious oxygen should vary from one degassed aliquot to the next. To further prove that residual O_2 was not the redox active impurity an oxygen scrubbing enzyme system was added to the vesicles to assure complete removal of O_2. The enzyme system consisted of glucose, glucose oxidase and catalase and it converts any oxygen to water via the following reactions:

glucose oxidase: glucose + O_2 = glutamic acid + H_2O_2

catalase: 2 H_2O_2 = 2 H_2O + O_2

---

2 glucose + O_2 = 2 gluconic acid + 2 H_2O

When this enzyme system was added to the vesicles and allowed to scavenge all oxygen the amount of titratable impurity was unchanged. This shows that O_2 is not the impurity in question, a result that is consistent with the further observation that this induction period was never observed with extruded vesicles.

Since extruded vesicles never showed these side effects it is likely that their origins were associated with the sonication process. It is well known and documented that ultrasound can disrupt chemical bonds, e.g. cleavage of H_2O to form H_2 and H_2O_2[a] . It is therefore conceivable that there is modification of some bonds of the surfactant, particularly the lipid double bonds would be susceptible to such chemistry. Also, any residual $CHCl_3$ that was not completely

---

[a]The possibility that H_2O_2 was the redox impurity was discounted because both species are expected to be in bulk solution and thus oxidation of dithionite due to reaction with H_2O_2 would be rapid. This was confirmed by addition of various amounts of H_2O_2 to preformed vesicles followed by addition of dithionite. Oxidation due to H_2O_2 was complete before the first optical spectrum could be recorded, while the subsequent slow reaction of dithionite with the impurity was not affected by H_2O_2 at all.

removed prior to vesicle formation could exhibit significant sonochemistry. It is well known that dichlorocarbenes add readily to olefins to form dichlorocyclopropanes. Thus the ultrasonic formation of dichlorocarbenes from chloroform and the subsequent addition of this highly reactive species to the double bonds of the lipid alkyl chains could form such dichlorocyclopropanes which could react with dithionite. Indeed, when special attention was paid to assure complete removal of chloroform the impurity related reactions were not observed. This hypothesis was further supported by the observation that synthetic lipids that do not have any double bonds, such as DMPC and DPPC, did not produce any redox active contaminants upon sonication.

During the course of this investigation it was found that viologen itself undergoes some changes due to sonochemistry. Prolonged sonication of viologen produced small amounts of material whose fluorescence spectrum resembled that of pyridones (Figure B1). This formation showed a strong pH dependence (Figure B2), with increasing formation at higher pH (Scheme B1). These contaminants appeared to be noninterfering, however. Addition of dipyridone[b] to extruded vesicles containing viologen did not alter the subsequent kinetics of transmembrane reduction by dithionite. A product with the same fluorescent properties was formed when viologen was added to

---

[b]The dipyridone was synthesized and kindly provided by Dr. David H. Thompson.

vesicles made by ultrasonication (with incomplete removal of chloroform) and then reduced with dithionite. Initially all viologen was rapidly reduced to the radical cation. The radical was then slowly decomposed to a product that could not be reoxidized to the viologen dication. Its spectral properties were very similar to those of the dipyridone.

These "side effects" illustrate that small impurities can have large effects in liposome systems and that ultrasonication gives rise to numerous chemical reactions that can be interfering.

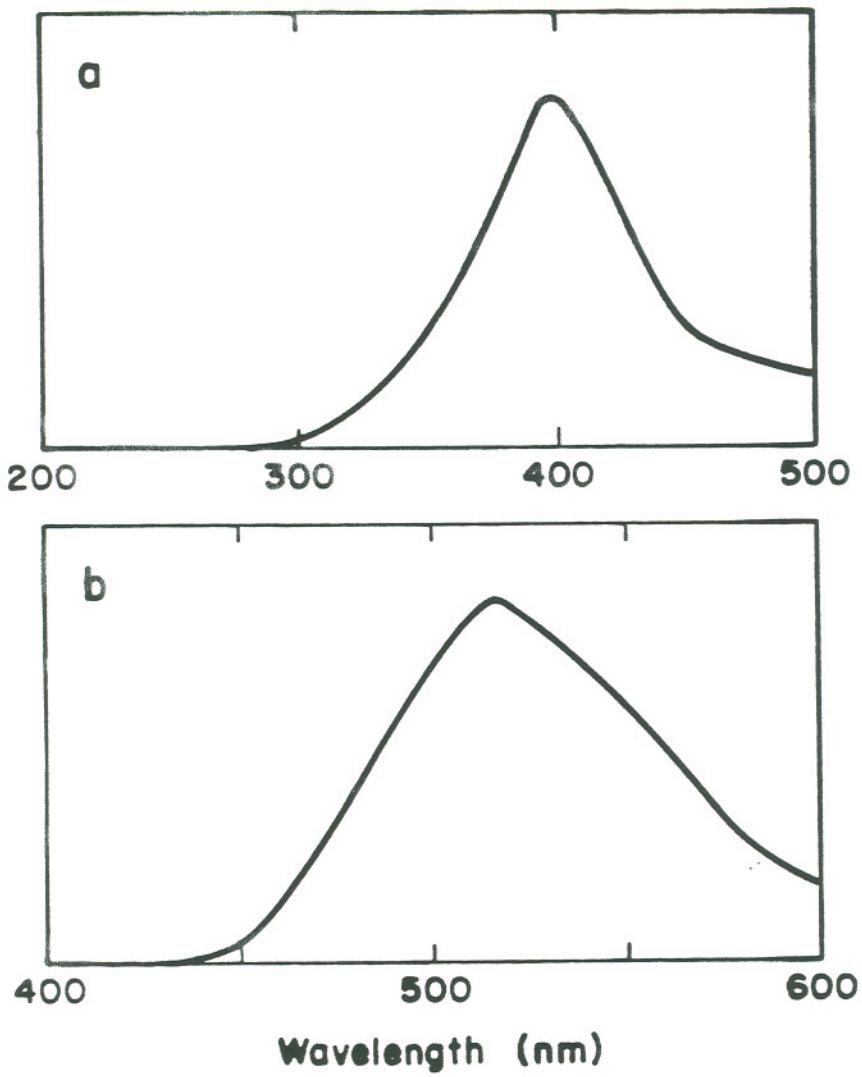

Figure B1: Fluorescence spectra of $(C_7)_2V^{2+}$ degradation product

250 uM $(C_7)_2V^{2+}$ sonicated for 10 min,

0.1 M phosphate buffer, pH 8.0

a: Excitation spectrum, emiss. wavelength = 520nm

b: Emission spectrum, excit. wavelength = 380nm

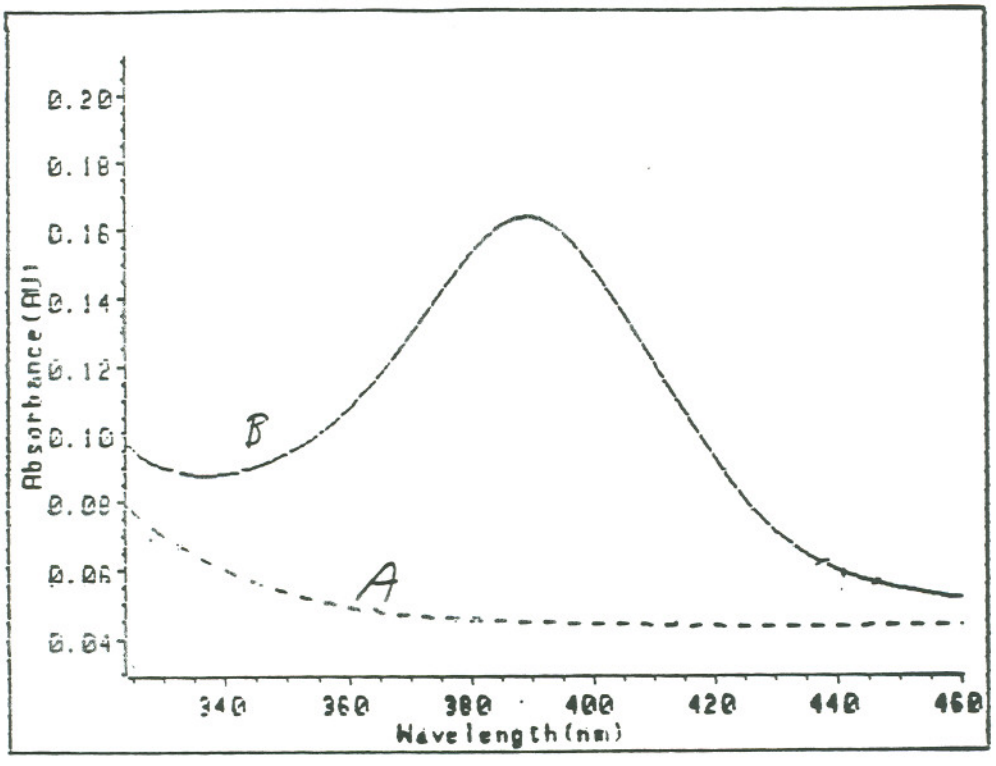

Figure B2: Optical spectrum of $(C_7)_2V^{2+}$ degradation product

250 uM $(C_7)_2V^{2+}$ sonicated for 10 min.

a: at pH 2.5

b: at pH 11

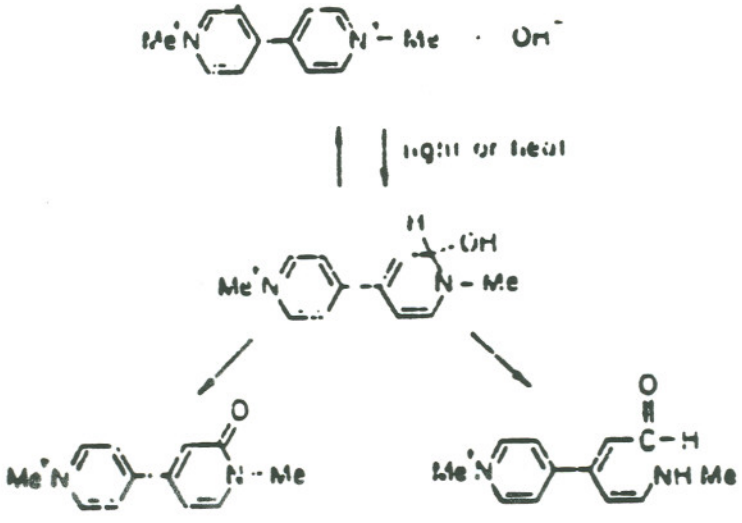

Scheme B1: Pathways for viologen degradation

(from reference 51)

BIOGRAPHICAL NOTE

The author was born in 1958 in Reutlingen, West-Germany. In 1978 he began to study chemistry at the Eberhard-Karls Universitat in Tubingen where he completed his Vor-Diplom in 1981. He then participated in an academic exchange program that brought him to the University of Oregon in Eugene, Oregon. Although originally intended for only one year he stayed on to complete his M.S. degree in Organic Chemistry in the spring of 1984. A change in research interests lead the author to the Oregon Graduate Center where he did his dissertation research under the direction of Dr. James K. Hurst in the fall of 1984. Upon completion of his studies the author joined the R & D section of the Chemical Division of Bio-Rad in Richmond, California, as a research chemist.